BUCKET BRIGADE DEVICES CIRCA 1977

OUTLINE

Part I

General Discussion of Bucket Brigade Technology--what it is and how it works.

A. A philosophical review of the BBD

   1. Born 1968

   2. Suffered major setback 1970

   3. Reborn 1976.

B. Comparison of BBD and CCD

   1. Ease of fabrication

   2. Ease of operation

   3. Packing density

   4. I/O.

C. Design considerations for the modern BBD

   1. Tetrode

   2. Doping--signal handling capability

   3. Channel length.

D. Performance of the Modern Bucket Brigade Device

   1. Dynamic range

   2. Noise

   3. Sampling rate.

BUCKET BRIGADE DEVICES CIRCA 1977

OUTLINE

Part II

Examples and Performance of Bucket Brigade Devices.

A. Simple audio delays

1. SAD-1024 -- SAD-512D
2. Ways of operating delays--Differential time multiplex
3. Typical applications
    a. Reverberation
    b. Chorus
    c. Flanging
    d. Simple comb filters
    e. Fault monitoring

B. High speed BBD delays

1. Unmultiplexed
2. Multiplexed.

C. Tapped Delay Line

1. Basic building blocks for signal processing
2. Examples
    a. Parallel multipliers
    b. Vector/matrix operator
    c. Correlator
    d. Matched filter
    e. FIR filter.

BUCKET BRIGADE DEVICES CIRCA 1977

OUTLINE

Part III

Signal Processors

A. Binary-Analog Correlator

   1. High speed multiplex-demultiplex

   2. Various architectures

   3. Applications.

B. Analog-Analog Convolver

   1. Structure

   2. Performance

   3. Applications

C. Transversal Filters.

   1. Structure

   2. Performance

   3. Advantages of FIR filters.

D. Miscellaneous

   1. Parallel-in Serial-out

   2. Analog averager.

BUCKET BRIGADE DEVICES CIRCA 1977

Gene P. Weckler
Robert R. Buss
Reticon Corporation
910 Benicia Avenue
Sunnyvale, California 94086

PART I

ABSTRACT

The bucket brigade was a development of the late 60's at which time it was quite extensively studied. The major shortcoming was found to be inadequate transfer efficiency, thus relegating its usage only to audio applications. Before the problem could be solved, along came charge-coupled devices which showed promise of improved transfer efficiency, higher clocking frequencies and higher density; therefore, most of the work switched from bucket-brigade devices to charge-coupled devices. New processes were developed in order to make charge-coupled devices that could truly realize their predicted potential; however, with these new processes and with charge-coupled devices working fairly well, nobody ever asked what improvement could be realized in a BBD if both modern technology and modern understanding were applied.

In this paper we will describe the modern bucket-brigade device. Transfer efficiencies of 0.9998 have been obtained at 5MHz sampling rates while at lower rates an efficiency of 0.99995 is not uncommon. Bucket-brigade technology is such as to permit simple adaptation to tapped delay-line configurations, with easy and precise control of tap weights. This capability is of great importance as it permits BBD's to transcend simple delay applications and enter the very broad field of discrete-time filtering. Interfaces with other MOS devices on the same chip likewise are easy to implement. The modern BBD thus leads to the efficient realization of simple delays, tapped delays, and programmable tapped delays--both real time and erasable-- as well as to correlators and transversal filters. In many cases a BBD offers a simpler and more effective solution than would a corresponding CCD or the much-more-complex fully digital system.

INTRODUCTION

The basic structure of the bucket brigade is shown in Figure 1. This device in its integrated form was invented by Sangster (ref. 1, 2) at Phillips in 1968. There was much interest in this device since it offered a first glimpse of a practical way of implementing an analog delay. However, the initial device had many shortcomings, with the major one being very poor transfer efficiency. Potential variations during the charge-transfer period introduced excessive channel-length and barrier-height modulation and consequent transfer inefficiency. As a result, the device was limited to few stages and to low-frequency applications.

The first major advance made in improving the transfer efficiency was also made by Sangster (ref. 3, 4) and his co-workers at Phillips. It came from the introduction of an isolation or tetrode structure with a d-c biased gate separating each clock element from its neighbor, as in Figure 2. The performance was greatly improved, but still limited to audio frequencies and to a relatively small number of transfers. At about this time the charge-coupled device (CCD) was invented at Bell Telephone Laboratories (ref. 5). CCD showed the promise of making possible charge-transfer devices without the shortcomings which appeared inherent in the bucket-brigade device. In a BBD, the charge must be transferred from capacitance to capacitance under the control of the separating MOS transistors. In the switching process, there is an uncertainty or noise in the capacitive charge transfer over the intervening barrier that is proportional to kTC and somewhat analogous to thermal noise in a resistance. k is Boltzmann's constant, T is absolute temperature, and C is the capacitance being charged. The CCD arrangement did not have discrete capacitances separated by barriers, so this noise source appeared to be absent, and, further, clock-line capacitances to be driven were smaller so that driving problems should be less severe. The CCD in concept was a very simple structure requiring only simple processing. In short, CCD looked to have all the potential advantages at first associated with the bucket-brigade. Nonetheless, performance fell far short of expectations. It took five years and many millions of dollars to develop the understanding and technology to the point which allowed these postulated advantages to be truly realized. It was then that a re-examination of bucket-brigade technology was initiated. Devices fabricated using some of the modern techniques and employing a tetrode structure were found to perform reasonably well (ref. 4), but transfer efficiencies were still less than one could wish; furthermore, stability was erratic and the devices were sensitive to clock shapes, particularly the transition edges.

DEVELOPMENT OF THE MODERN BBD

It was at this point in the development of charge-transfer devices generally that a closer look was taken at the underlying BBD structure, the technology, and the processing techniques. The basic bucket-brigade structures of Figures 1 and 2 employ idealized transistors and capacitors; the physical realization suffers from parasitic effects. The MOS control gates overlap the junctions which are conveniently represented in the figures as nodal points. Any overlap beyond that required to ensure a continuous channel results in unwanted capacitance, particularly capacitance to the prior node. Each nodal diffusion has (depletion) capacitance to the substrate. These capacitances divert charge and increase the difficulty of efficiently providing the desired transfer-clock waveforms. Further, the depletion capacitance is voltage-dependent and so leads to nonlinearities in the transfer characteristic. One method to minimize parasitic capacitance is to use self-aligned structures, that is, a processing method whereby one masking step controls the openings for a channel and also the subsequent formation of a control gate which is automatically self-aligned.

The non-linear depletion capacitance would be minimized by a high substrate resistivity, but uniformly high resistivity would lead to excessive sensitivity to the problems of channel-length (conductivity) modulation; and further, high channel resistance leads to poorer high-frequency performance.

CONSTRUCTION FEATURES

Modern technology permits selective control of resistivity by selective ion implantation. One can thus make resistivity high where wished and low where wished. The bucket-brigade could have the advantage of a high-resistivity basic substrate for minimum junction capacitance but without its deleterious effects on conductivity modulation, etc. The desired low-resistivity areas could be selectively controlled, as shown in Figure 3. Further, the ion implantation can be used to control thresholds so that N-channel devices become eminently feasible, with all the consequent advantages of higher speed, better transfer efficiency, etc., which follow from the higher mobility of the carriers.

Figure 3a is a plan view of the semiconductor surface showing in linear fashion the organization of the bucket brigade. An equivalent cross-section view is as in Figure 3b. These sketches are exaggerated to show details. The substrate material is p^- material which is then implanted to a p^+ state everywhere except the regions intended to underly the diffusion between successive clock and tetrode gates (and certain other input and output regions), as shown. The tetrode-gate and clock-gate regions are

then masked off and n^+ material diffused to form the bulk of the signal path. Note that these masked-off regions later receive the polycrystalline silicon control gates in automatic self-alignment with the underlying undiffused channel region; however, the channel region under the gates has been implanted to p^+ concentration so that low-resistivity and positive thresholds is the desired result. In the intervening diffused area, the nodal area of the schematic circuit of Figure 2, there was no ion implant and substrate resistivity is high. The result is that depletion width under the diffusion is relatively large and parasitic capacitance to the substrate small. In a later step, a second-layer poly is applied above the diffused area and connected to the clock gate to the left to form the desired signal-storage capacitance.

Devices have been made using the structures and processes described. Transfer efficiency as high as 0.99997 has been obtained at low sample rates while values as high as 0.9998 at 5MHz have been measured.

PERFORMANCE FEATURES

Transfer efficiency is one of the important factors in any charge-transfer device since it affects the number of transfers possible (and hence the delay) before serious degradation of bandwidth occurs. Quantitatively, it is easier to use the accumulated inefficiency, the product $N\varepsilon$ of the number of transfers N and the inefficiency ε(=1 - transfer efficiency) in considering the effects. The bucket-brigade is a sampled-data system, with the associated restriction that the signal band must be restricted to a range somewhat smaller than the Nyquist limit of $f_c/2$, where f_c is the sample frequency (equal to the clock frequency for the examples given). In this signal band there are two factors causing the high-frequency response (modulation transfer factor) to be less than the corresponding value at low frequencies. The first factor is inherent in the sampled nature, in the fact that the output signal is only a stair-step approximation of the desired analog signal (assuming full-wave output). That is, the output is a sequence of pulses whose successive amplitudes carry samples of the analog values. The representation is good for low frequencies, where many samples per cycle occur, but becomes increasingly poor as the signal frequency rises toward the Nyquist frequency; that is, the signal-frequency component in the stair-step representation is less than the stair-step amplitude by a factor $\sin(\pi f/f_c)/(\pi f/f_c)$. This factor introduces a loss of $\sim$4dB for $f=f_c/2$.

The second factor is the loss resulting from accumulated transfer inefficiency, which contributes a loss expressible as $R_{dB} = -17.4N\varepsilon \sin^2(\pi f/f_c)$ where R_{dB} is the reduction, expressed in decibels, relative to the response at low frequencies, f is the signal frequency, and f_c is the sample frequency for the BBD. This expression reaches a maximum value of 17.4 $N\varepsilon$ dB at $f = f_c/2$. Thus, for 5000 transfers and $\varepsilon = 10^{-4}$ (efficiency = 0.9999), the

loss is 8.7dB at $f_c/2$ and 4.35dB at $f_c/4$. Measured values of transfer inefficiency ε, are shown in Figure 4, and its effects on delay-bandwidth product is shown in Figure 5.

The dynamic range is limited at the upper end by signals so large that distortion becomes excessive, and at the lower end by signals too small to be distinguishable from noise. If one ignores all effects from overlap and depletion capacitances, barriers, etc., the maximum peak-to-peak input swing is $\Delta V = (V_{bb} - V_T)C_1/C_s$ where V_{bb} is the tetrode gate voltage, V_T is the threshold voltage (assumed constant at the value of body bias present), and C_1/C_s is the ratio of driving capacitance at an interior node to the initial storage capacitance C_s. Consider Figure 2. When ϕ_2 is at zero, ϕ_1 is at maximum and node 1 charges through transistor 2 and the tetrode transistor to $V_{bb} - V_T$. Meanwhile, C_s is charged via the input to some potential which is ΔV below $(V_{bb} - V_T)$. When ϕ_1 falls and ϕ_2 rises, the potential on C_s rises by the amount ΔV to $V_{bb} - V_T$ at the expense of the potential at node 1, which falls from $\phi_2 + V_{bb} - V_T$ by an amount $\Delta V(C_s/C_1)$. At the next clock transition, the potential at node 1 instantaneously falls back by the magnitude of ϕ_2 to a value $\Delta V(C_s/C_1)$ below its initial terminal value of $V_{bb} - V_T$, and then rises again to $V_{bb} - V_T$ at the expense of node 2. But the minimum potential cannot be less than the substrate potential (assumed zero), so that within the above constraints $\Delta V_{max} \leq (V_{bb} - V_T)(C_1/C_s)$. Parasitic capacitances and other effects in general act to reduce the maximum ΔV (ref. 6).

Noise generated in the bucket-brigade limits low-level signals. Ref. 7 shows the variance per stage in the number of charges transferred at each transfer is proportional to kTC, as stated earlier, with the result that the noise spectral density has two principal factors. The first factor is proportional to kTC times the number of stages and inversely proportional to clock frequency, meaning that noise increases directly with the number of stages and decreases as clock frequency increases. This latter effect is important as it degrades performance at low clock frequencies. Qualitatively, the kTC noise is spread over a very broad frequency range, just as is thermal noise, and hence folds about each harmonic of the clock frequency. As clock frequency is reduced, there are more sections of the spectrum folded down into the useful band lying between 0 and $f_c/2$. The second factor is a frequency variable nominally proportional to $\sin^2 \pi f/f_c$ but substantially reduced by transfer inefficiency at the upper end. Figure 6 taken from ref. 7 illustrates this latter effect. $M\varepsilon$ is the accumulated transfer inefficiency. Note that the curves are normalized to show only the second factor; the important $MkTC/f_c$ factor has been removed.

These noise effects limit the dynamic range of a modern BBD to the range 50-80dB, with the actual range obviously dependent on capacitance, bandwidth, the number of stages, the clock frequency, and, to a lesser

extent, on the transfer efficiency. Figure 7 shows a transfer curve for a typical BBD showing, for a 1KHz bandwidth, a dynamic range in excess of 75dB (or 65dB for a 10KHz bandwidth) while Figure 5 shows the shrinkage of delay-bandwidth product as accumulated transfer inefficiency, $N\varepsilon$, increases.

INTERACTION BETWEEN CONSTRUCTION AND PERFORMANCE

The input structure to the bucket-brigade is very simple. It is basically an NMOS transistor analog switch connecting the input to a capacitor, as in Figure 2, which allows one to run a given amount of charge onto the input capacitance and then, via the bucket-brigade, transfer that charge on into the first and later buckets. The size of the input structure can be varied to tailor the voltage sensitivity at the input. As shown earlier, each node potential, including that at the input, has an upper limit of $V_{bb} - V_T$ while being charged from a succeeding capacitor. The change ΔV from this upper limit is controlled at C_S by the input circuit, and the resulting change at the next and later interior nodes is $\Delta V(C_S/C)$ where C is the interior node capacitance. Interior signal voltage swing is limited in magnitude to less than $V_{bb} - V_T$, so input capacitance relative to C controls the input sensitivity. Also, since $V_{bb} - V_T$ is the upper limit for the input, the ratio C_S/C affects the input bias level, along with the ion implant level.

The output structure is equally simple. It can consist of a source follower connected to one of the buckets of a stage (note that a "stage" encompasses two buckets). The source follower adds some small amount of capacitance to that bucket. Thus, the output stage's capacitance likewise controls the output sensitivity, and thus affects the system's overall gain; that is, the signal voltage variation is $\Delta V(C_S/C)$ at an interior node, and at the output this variation becomes $[\Delta V(C_S/C)](C/C_{out}) = \Delta V(C_S/C_{out})$ where C_{out} is the capacitance of the output node. Note that this result follows because charge is conserved. This "gain" is then modified by the transfer factor of the source follower, which may have a value of the order of 1/2. A single source follower will produce a half-wave output signal; each time the appropriate clock goes high an output will be produced from the source follower. Two source followers may be used, one connected to a bucket driven by phase one of a stage and the other connected to an adjacent bucket driven by phase two of the stage, as illustrated in Figure 8. Then a full-wave output will result. A full-wave output is much easier to handle, requiring only simple filtering to reduce any clock glitches or sampling glitches, and it does not require an external sample and hold. It also allows one to work much closer to the Nyquist frequency without as severe filtering requirements. With half-wave output, the desired signal is superposed on the more positive half cycles, but its peak-to-peak

magnitude is constrained to be less than the peak-to-peak clock amplitude. One must thus filter out the full clock amplitude, as well as the unwanted sidebands. With full-wave output (or a sampled-and-held output) the clock amplitude component is reduced by 40 to 60dB, simplifying the filtering. The clocking requirements of the bucket brigade are also quite simple; it requires two-phase complementary square-wave clocks. The timing is not critical, the edges are not particularly critical. The device is basically very forgiving. Charges are mostly stored on discrete capacitors, so that a storage site does not disappear when the clock potential goes to zero. Thus, while not recommended, completely non-overlapping clocks still provide bucket-brigade operation. Again, the relative times spent in each clock state are relatively unimportant. Non-overlapping clocks with "on" states differing by 10 to 1 have provided nearly normal BBD operation. The conditions to be avoided are excessively overlapping clocks (which can turn all transistors on simultaneously) and undershoot spikes which can inject unwanted charge from the substrate via forward-biased diodes. Suitable clock waveforms are square waves generated from complementary outputs of CMOS flip flops. Tetrode gate voltage does have an effect on transfer efficiency; it preferably is set to operate at a voltage very nearly equal to the clock, or less than but within a volt of the clock maximum.

Another very nice feature of the bucket-brigade device is the ease with which buckets may be tapped to obtain output, as mentioned above. A tap may easily be implemented by connecting a source follower to an intermediate bucket. Note that this tap is to a physical diffusion so that it is easily implemented. The physical size and separation of stages is not a significant problem. Capacitance perturbations can be minimized by considering the tap's capacitance as an integral part of the total node capacitance. It is possible to connect source followers to every bucket along a device, as shown in the diagram of Figure 8, and not seriously affect the transfer efficiency. This is in part due to the fact that we are looking at real capacitances and not trying to tap in on "phantom capacitances". Another way of implementing taps is by capacitive divider pickoff, as shown schematically in Figure 9, which allows one to build transversal filters with taps which can be capacitively weighted, with on-chip electrode structures, just as is done with charge-coupled devices; however, in the BBD it is possible to separate the sensing-electrode pattern from the clocking-electrode pattern without causing any serious degradation of transfer efficiency. Furthermore, it is possible to cancel clocking transients because coupling from ϕ_1 through C_a cancels that from ϕ_2 through C'_a, etc. In Figure 9, the relative tap weight is given by

$$w = \frac{C_a - C_b}{C_a + C_b}$$

It is evident that the weight, w, may be controlled over the range +1 (when $C_b = 0$) to -1 (when $C_a = 0$). One thus realizes simplicity of signal extraction, without having to bother with coordination with clocks multiplexed on the same lines as the signals. An example of such design is shown in Figure 10. These are but a few of the unique advantages of the bucket brigade which, with suitable modern technology, make it a device quite adequate for a goodly number of signal-processing applications.

WHY USE BUCKET-BRIGADE DEVICES?

We have all known that charge-transfer devices are very suitable for analog signal processing. However, most people immediately conclude that using charge-coupled devices is the only way to do the job. If you say that you are going to use a bucket-brigade device, immediately they ask: "Why not use charge-coupled?" The answer is itself a question: "Why not use the device most suited to the task? Why restrict the technology regardless of its suitability?" Bucket-brigade devices have a distinct range of applicability, with many favorable factors such as those discussed:

1. With proper design, transfer efficiency is so high that it is not an important factor for many applications.

2. Processing is by standard MOS processing, with high yield and compatibility with other MOS devices, so that flip-flops, clock drivers, shift registers, output buffers, etc., may be designed onto the same chip.

3. One or many taps are easily and precisely implemented, with simple output circuitry.

4. Clocking and other interface requirements are simple and non-critical. There are no tricky multiphase clocks with requirements on precise control of rise and fall times--a simple two-phase complementary square wave clock is all that is required. CMOS clock generators usually are adequate.

5. Output circuitry is equally simple, allowing one to do either capacitive nondestructive sampling of the bucket such as in a tapped delay line (Figure 9), or to use source-followers which are directly (nondestructively) driven by the buckets and which in turn act as current sources to the outside world. The output circuitry on-chip often dominates the real estate so that packing density of the delay elements themselves becomes of secondary importance.

6. The bucket brigade is capable of sampling to 5MHz or more. This situation is also compatible with peripheral circuitry, which usually is capable of operating to 5MHz or more.

SUMMARY

In summary, then, bucket-brigade devices should be used for audio and other low-frequency applications, in some video-delay applications, and in signal processing generally, where the bucket brigade is a natural. It is exceedingly flexible and noncritical in delay applications. With modern technology, it exhibits high transfer efficiency, moderate speed, and simplified interface requirements. It allows you to make transversal filters using split-electrode structures; however, the split electrodes are strictly sensing structures and are not part of the clocking circuit, nor do the structures suffer from overlap capacitance as is typical in CCD split-electrode structures. The sense electrodes are separate from (and balanced to) the clocking electrode structure. Furthermore, in a transversal filter, a processing gain is available because of the summed signals from multiple taps; thus, the device is not as sensitive to noise as would be a simple long delay used, for instance, in audio or video type applications.

CCD is needed when extremely long delays are desired, such as an 8000-stage audio delay line where wide dynamic range is also desired. Properly designed CCD's have higher transfer efficiency, and a noise limit that does not increase as rapidly as in a BBD when the number of stages is increased. CCD's also should be used when sampling rates significantly in excess of 10MHz are desirable, or when packing density is of prime importance, and where the penalty of extra complexity is permissible.

Operation at elevated temperatures limits storage lifetimes, and hence forces a practical limit to the amount of delay possible, or alternatively, to the number of taps possible. Further, in most signal processing applications such as correlators or transversal filters, one finds a limitation imposed by the time required to do the calculation and the number of points in the calculation. Therefore, a time-complexity compromise must be made. For instance, at 1MHz sample rate, it would take 32ms to compute a 32-point calculation, and 64ms for a 64-point calculation. A compromise must be made between the total number of taps in the device and the speed of the computation. It has been found that, for the accuracy that is possible in today's charge transfer devices and the speeds at which they are capable of operating, 32 to 64 stages are about the optimum number of stages in signal processing. This is not to say that units could not be cascaded or extended to increase the number of points in the computation; however, it takes time to make the application to additional points. Therefore, if processing requires less than 100 stages, it is much better to use a bucket-brigade and have all the advantages of today's technology and the advantages of available peripheral circuitry, rather than have all of the processing and application problems of charge-coupled devices.

REFERENCES

1. F. L. J. Sangster and K. Teer, "Bucket-Brigade Electronics - New Possibilities for Delay, Time-axis Conversion, and Scanning," IEEE Journal Solid-State Circuits, Volume SC-4, pp. 131-136, June, 1969.

2. F. L. J. Sangster, "The Bucket-Brigade Delay Line, a Shift Register for Analogue Signals," Phillips Technical Review, Volume 31, pp. 97-110.

3. F. L. J. Sangster, "Integrated Bucket-Brigade Delay Line Using MOS Tetrodes," Phillips Technical Review, Volume 31, p. 266.

4. L. Boostra and F. L. J. Sangster, "Progress on Bucket-Brigade Charge-Transfer Devices," presented at the IEEE International Solid-State Circuits Conference, Philadelphia, Pennsylvania, February, 1972.

5. W. S. Boyle and G. E. Smith, "Charge-Coupled Semiconductor Devices," B. S. T. J., Volume 49, pp. 587-593.

6. W. J. Butler, M. B. Barron, and C. M. Puckette IV, "Practical Considerations for Operation of Bucket-Brigade Circuits," IEEE Journal Solid-State Circuits, Volume SC-8, No. 2, pp. 157-168, April, 1973.

7. D. D. Buss, W. H. Bailey, and W. T. Eversole, "Noise in Bucket-Brigade Devices," IEEE Transactions on Electron Devices, ED-22, No. 11, pp. 977-981, November, 1975.

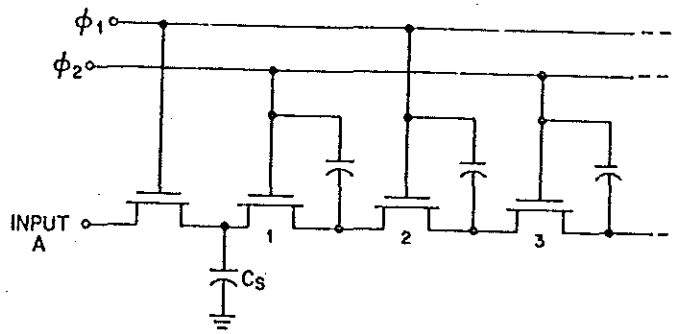

Fig. 1 Basic bucket-brigade structure.

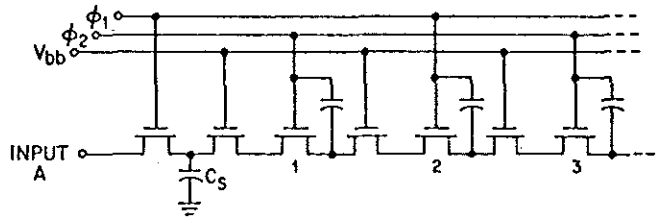

Fig. 2 Improved bucket-brigade structure with tetrode isolation.

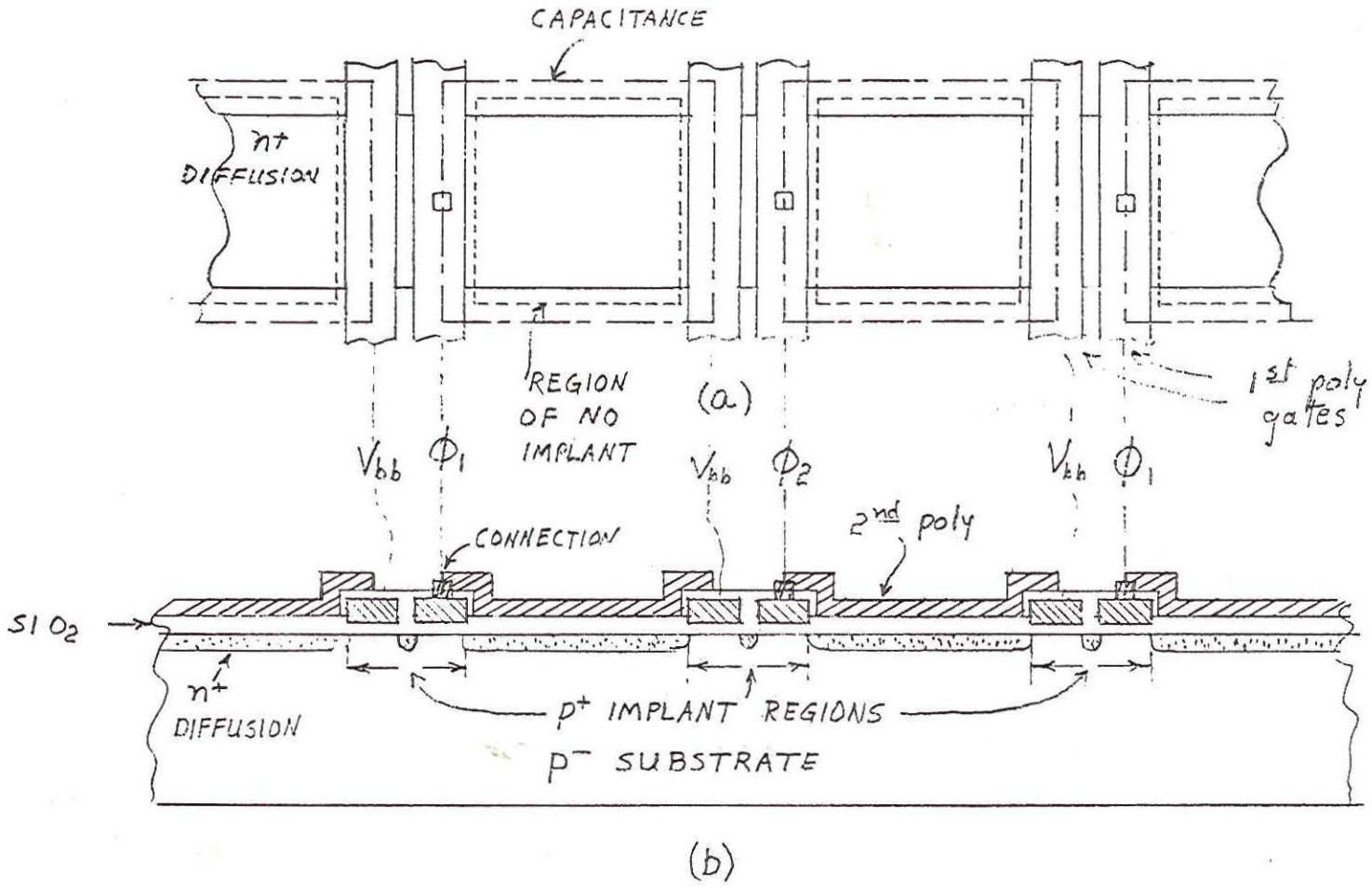

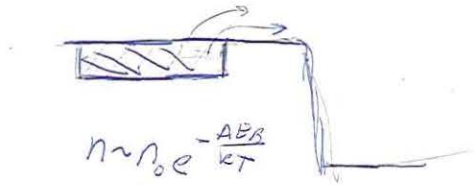

Comment re low sampling rates giving big transients.

Fig. 3. Sketch of BBD Layout

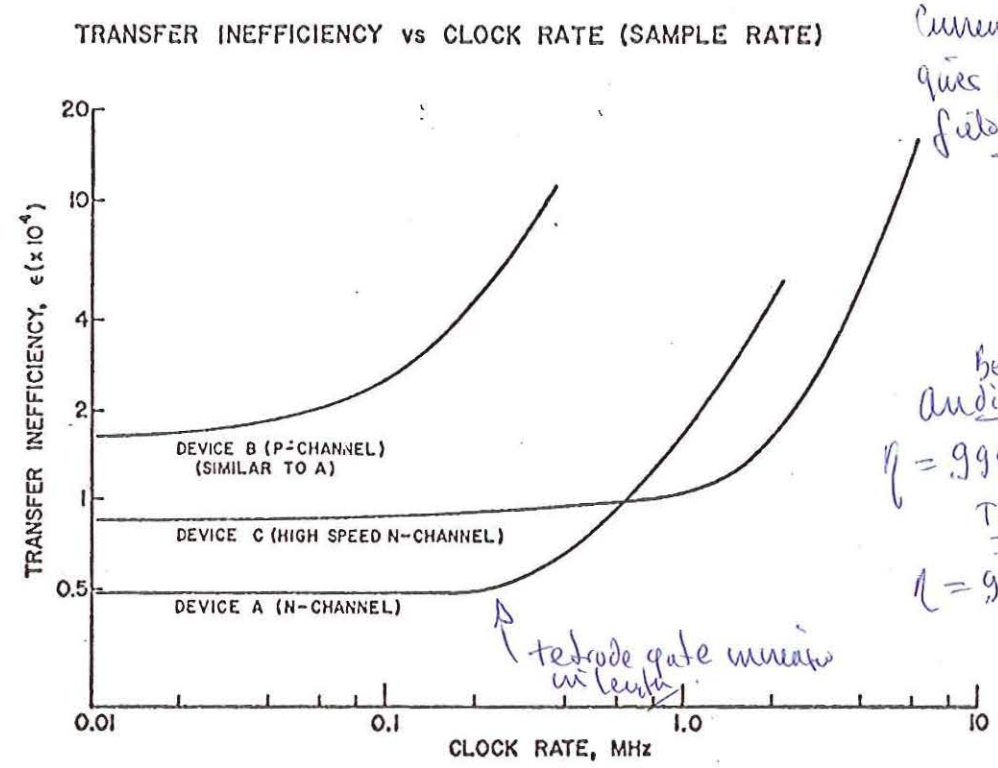

Fig. 4 Transfer efficiency vs. sample rate for two commercial audio devices and one high-speed device.

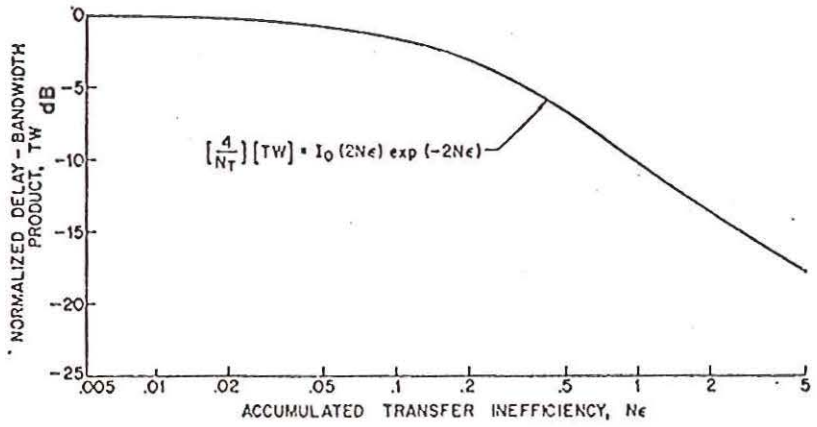

Fig. 5 Normalized delay-bandwidth product vs. accumulated transfer inefficiency $N\varepsilon$.

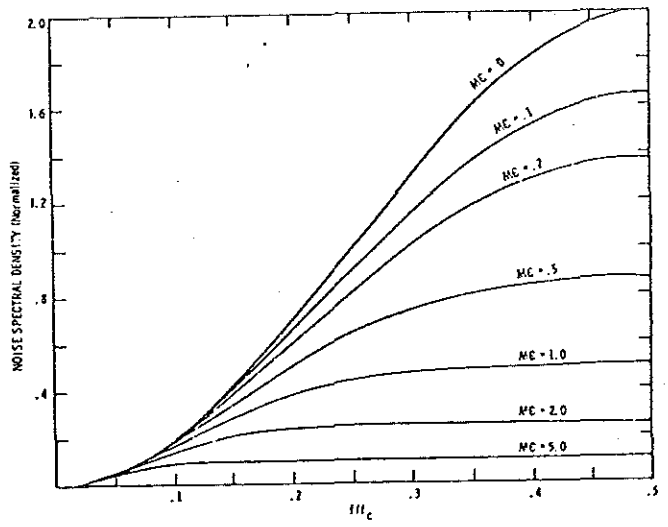

Fig. 6. Normalized noise power spectral density as a function of normalized frequency. Imperfect charge transfer severely attenuates the high frequency noise components.

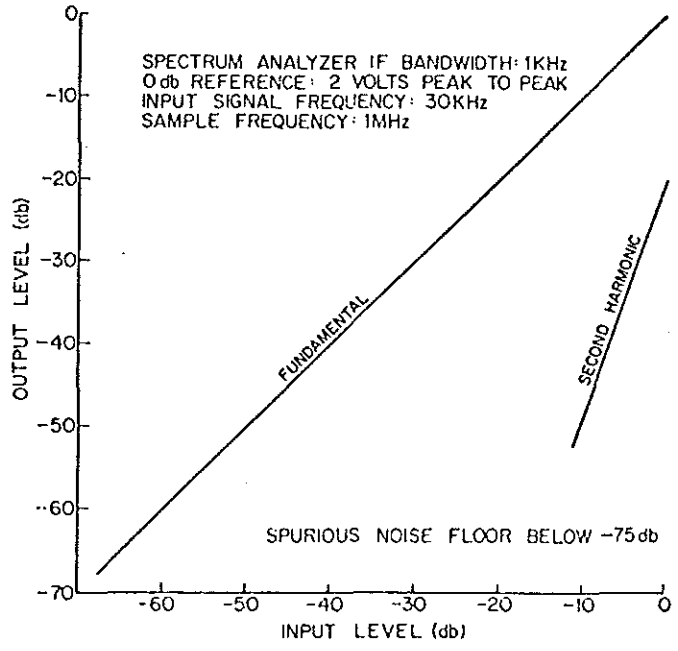

Fig. 7 Dynamic range and linearity for tetrode BBD.

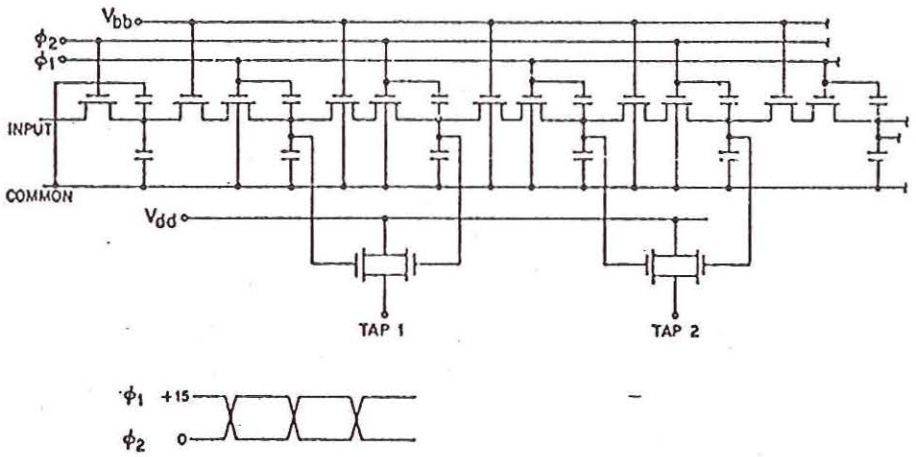

Fig. 8 Equivalent schematic circuit for tapped BBD.

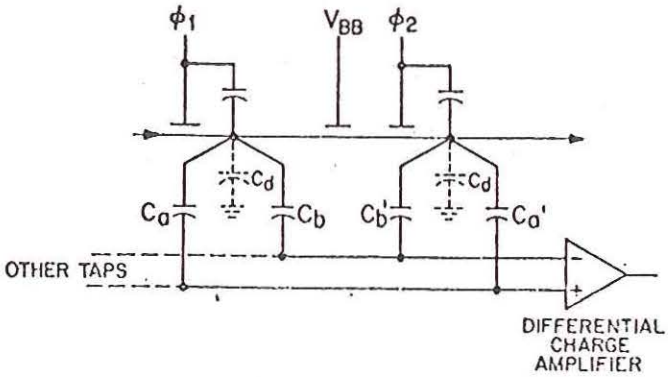

Fig. 9 Capacitive divider taps for BBD.

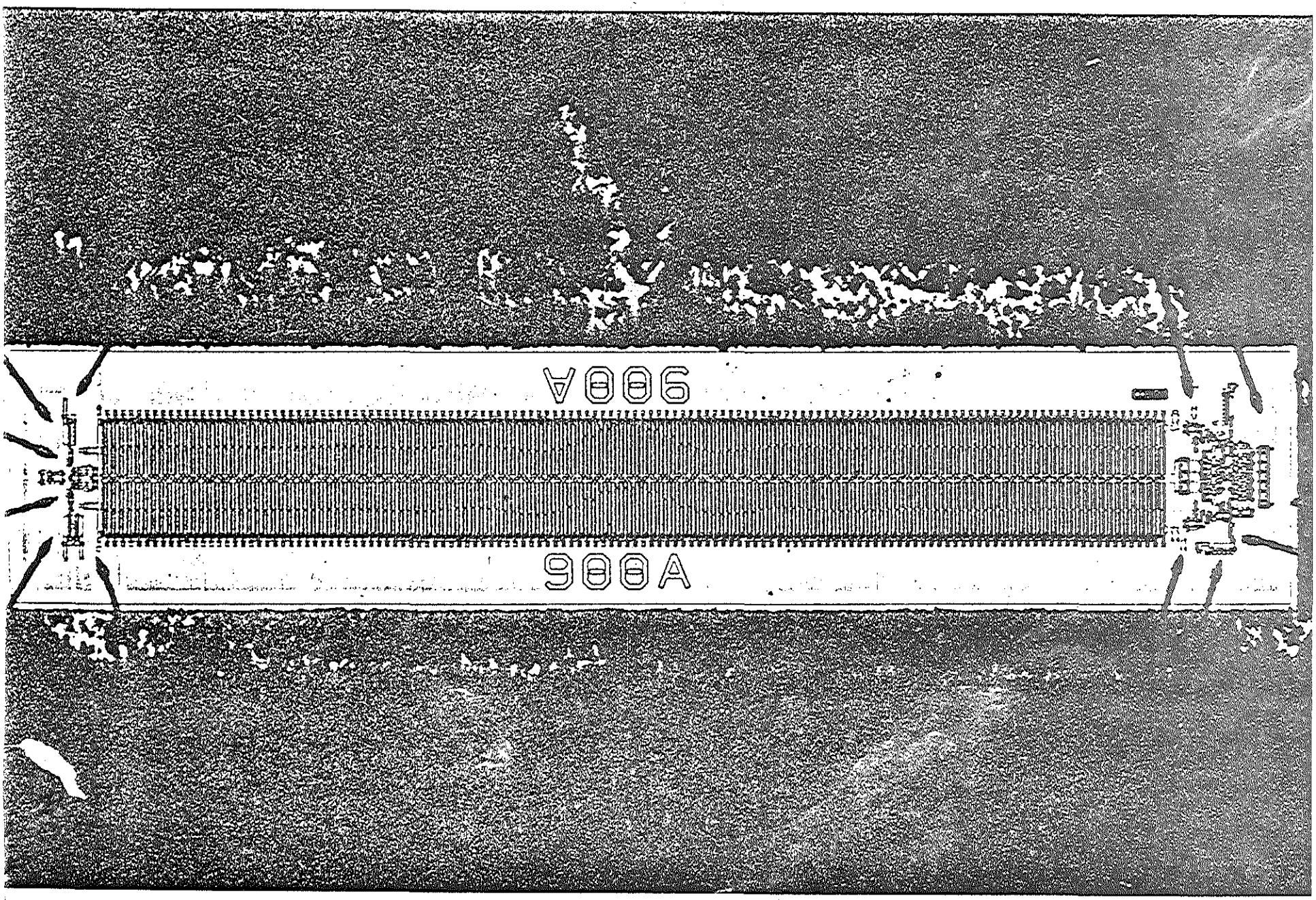

Figure 10. R5171 -- 64 Stage Split Electrode Filter.

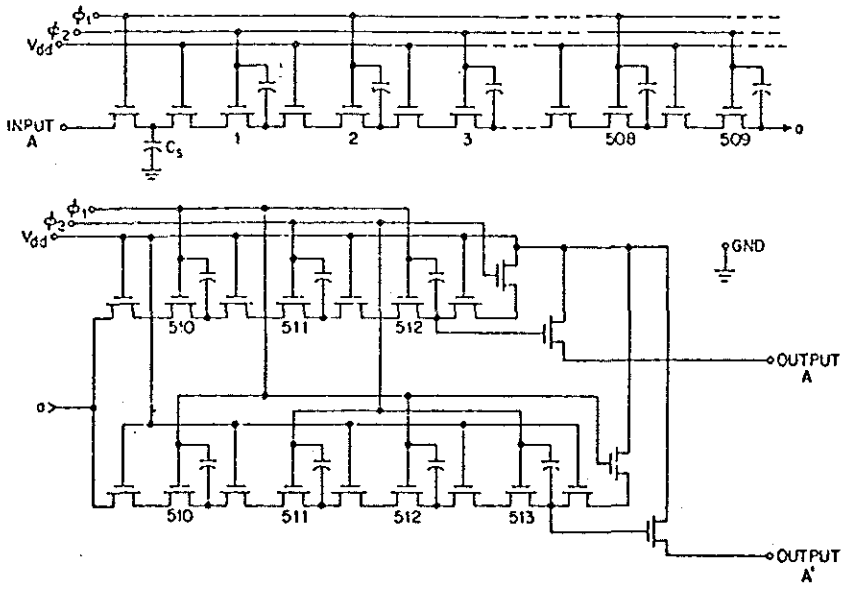

Fig. 11 Equivalent circuit diagram for an audio-frequency BBD, the SAD-1024.

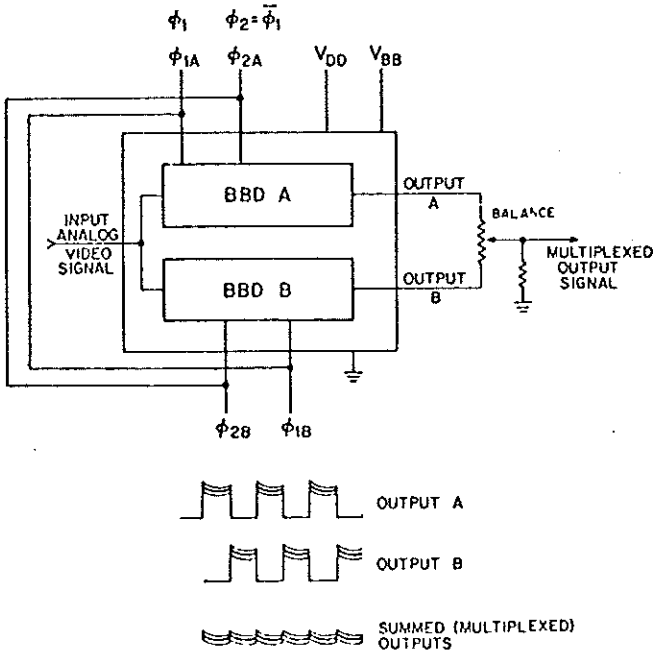

Fig. 12 Method of multiplexing delay lines to obtain wide-band high-frequency operation (SAD-341).

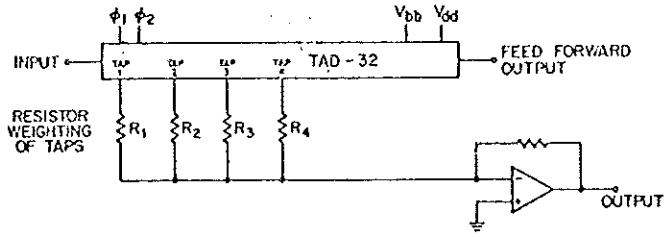

Fig. 13 The TAD-32, a Tapped Analog Delay device.

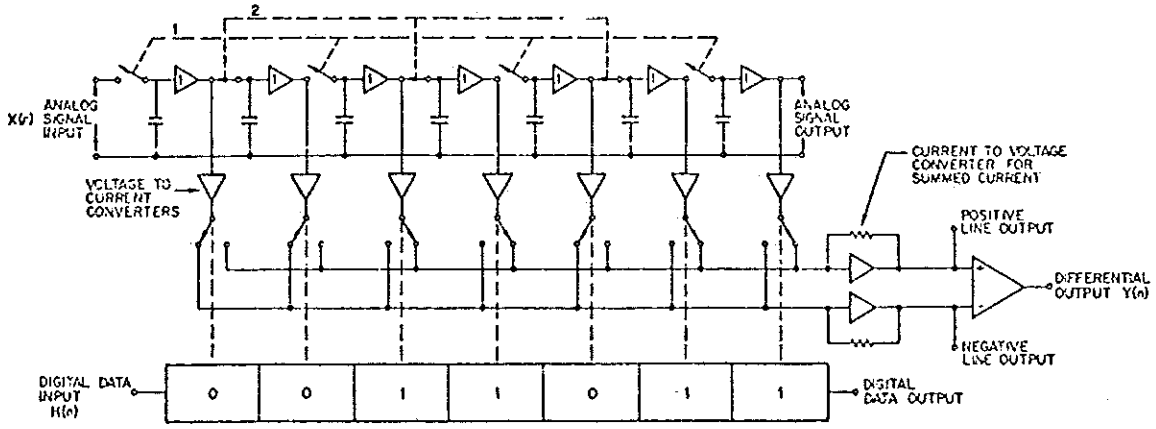

Fig. 14 An example of a BBD Binary-Analog Correlator (BAC-32).

PART IIA

ABSTRACT

What is a charge-transfer device and how can it be used to make electronic music?

Charge transfer devices represent a rapidly developing area of semiconductor technology which allows one to controllably delay analog signals. The ability to controllably delay an analog signal permits the realization of filters whose characteristics are also controllable. A "flanger" is a typical example of an electronically variable "comb filter". When applied to percussive instruments it produces a hollow swishy sound akin to that of a jet plane but without the rumble and roar. The flanger, as well as several other applications of analog delays, will be described in more detail later.

Let us first review the fundamentals of charge-transfer devices. The realization of an analog delay, its principles of operation, and its basic characteristics will be reviewed.

FUNDAMENTALS OF CHARGE-TRANSFER DEVICES

"Charge-transfer device" is a generic term which is applied to a family of solid-state electronic components, which under the application of a proper sequence of clock pulses moves packets of charge in a controlled manner. These packets of charge can represent discrete-time samples of an analog signal. They can be moved at a controlled rate from an input terminal to an output terminal. The signal appearing at the output terminal is a time delayed replica of the input signals. The delay which can be realized depends on the number of samples of the input that exist in memory between the input and the output terminals, and the rate at which these samples are moved from input to output. The number of samples that can be stored between the input and the output terminal depends on the basic design of the device; however, the rate at which the samples are moved depends on the rate of the clock pulses which is under the control of the user. It is, therefore, possible for the user to control the resulting delay in any manner he so desires within the limits of the particular device and those imposed by the sampling theorem.

For those who watch old movies either at the pizza parlor or on TV, one might envision a long line of firemen passing buckets of water from the cistern to the fire. Such a line is usually referred to as a bucket brigade. It is not surprising that one commonly used charge-transfer device is called a Bucket Brigade Device, BBD.

The bucket brigade concept of sampling and delaying an analog signal has been of interest for many decades. It was not until the development of MOS integrated circuits that a practical method of implementation became available.

The basic structure of the MOS bucket brigade is shown in Figure 1. This device in its integrated form was invented by Sangster (Ref. 1, 2) at Phillips in 1968. There was much interest in this device since it offered a first glimpse of a practical way of implementing an analog delay. However, the initial device had many shortcomings, with the major one being very poor transfer efficiency, i. e. transfer inefficiency is a measure of the amount of charge left behind at each transfer. As a result, the device was limited to but a few stages and to low-frequency applications since the amount of charge left behind depended in these early devices on the amount of time allotted for the transfer.

The first major advance made in improving the transfer efficiency was also made by Sangster (Ref. 3, 4) and his co-workers at Phillips. It came from the introduction of an isolation or tetrode structure with a d-c biased gate separating each clocked element from its neighbor, as in Figure 2. This tetrode structure in effect reduced the Miller capacitance between the output and the input of each individual stage similar to the function performed by the tetrode grid in a tube. The performance was

greatly improved, but still limited to audio frequencies and to a relatively small number of transfers. At about this time the charge-coupled device (CCD) was invented at Bell Telephone Laboratories (Ref. 5). CCD showed the promise of making possible charge-transfer devices without the shortcomings which appeared inherent in the bucket-brigade device. In short, CCD looked to have all the potential advantages that were at first associated with the bucket brigade. The CCD appeared to be a very simple structure requiring only simple processing. However, despite the theoretical improvement, the simple structure with the simple process produced devices not much better in performance than the bucket-brigade devices on which there was supposed to be improvement. It took five years and many millions of dollars to develop the understanding and technology to the point which allowed these advantages to be truly realized.

It was at this point in the development of charge-transfer devices generally that a closer look was taken by Reticon at the underlying BBD structure, the technology and the processing techniques. Self-aligned structures would reduce parasitic capacitance and improve efficiency. A decrease in substrate resistivity would help to reduce the sensitivity to voltage and to clock wave shape. It would also reduce the conductivity modulation of the region under the transfer gate, which should improve transfer efficiency. However, junction capacitance effects would be adversely affected. It was then determined that, using modern technology, one could selectively control resistivity and its effects by ion implantation--conductivity could be high where wished, and low where wished. The bucket brigade could have the advantages of a high-resistivity basic substrate for minimum junction capacitance but without its deleterious effects on modulation, etc. The desired low-resistivity areas could be selectively controlled. Further, the ion implantation could be used to control thresholds so that N-channel devices became eminently feasible, with all the consequent advantages of higher speed, better transfer efficiency, etc., which follow from the higher mobility of the carriers. Figure 3 shows a comparison of transfer efficiency for both N and P channel audio delay. The superiority of the N channel device is obvious.

APPLICATIONS OF BBD TO ELECTRONIC MUSIC

Having developed an efficient, high performance, externally controlled analog delay device such as the Reticon SAD-1024, the question arises how can it be applied to the electronic enhancement of sound. Many desirable, as well as interesting, acoustical effects may be synthesized with an analog delay device. A partial list of these effects include enhancement and control of reverberation, generation of chorus, flanging, vibrato, as well as the reduction or cancellation of undesirable effects such as wow and flutter introduced by some tape machines. At this point let us discuss a few of these applications. We will begin by discussing chorus and phasing effects.

Chorus (Multiple Voice) and Phasing Effects (Flanging)

If a solo voice or instrument is joined by the same sound delayed by approximately one to five milliseconds, the resultant is a very popular "spacey" sound. The phenomenon sounds as if there were two voices or instruments present. This is particularly true if the pitch of one is varied slightly (i.e., the two are not exact replicas). If the resultant signal is again delayed and added as before, the effect is that of four voices, etc., until delay becomes so large as to cause blurring. Delay can thus be used to enhance or modify the apparent size of a group of musicians (or speakers, etc.,). The SAD-1024 is readily adapted to such use. Figure 4a shows two delay elements in a stable, nonfeedback arrangement of this application. Additional delay elements can be added, as desired, without loss of stability.

Chorus produced by simple delay alone (without modifying pitch or other characteristics) is likely to sound thin and lifeless because each reproduction

is an exact counterpart of the previous signal. The effect of slightly different sources can be produced by varying the clock rates by a small amount as in vibrato (and as indicated in Figure 4a). The amount of variation is much less than with vibrato, because the pitch change should not be evident. What is wanted is just enough difference between the direct and delayed signal to make them appear to come from separate sources, i.e., in "chorus".

When the desired effect is that of several different voices added together, it is possible to vary the clock rate slightly but in a random rather than regular manner. Such a clock rate might be derived from noise passed through a narrow-band filter. The output frequency is changed as in vibrato, but the randomness simulates the slight differences in sources, rather than conventional vibrato with one or more deterministic sources. The exact combination desired is subject to artistic interpretation; no rules can be given.

Use of the circuit of Figure 5, but with appropriately small delays, might be thought equivalent to Figure 4a; however, the effect then would be reverberation more like that of "singing in the shower". Sounds build and decay over a period of time; there is not the abrupt start and stop of the ensemble, but rather an exponential rise and decay of sound. The circuit of Figure 4b thus is more realistic for chorus, but either circuit can give subtle or noticeable effects to the extent desired.

Flanging is a sound effect somewhat similar to chorus. It can be obtained with a circuit similar to that of Figure 4b. Variables at the control of the operator are the balance between the direct and delayed signal and the amount of delay. Delay is controlled very simply by control of the clock frequency.

Delay is given by

$$T_D = N/2f_c$$

where N = number of delay elements
f_c = sampling clock frequency

For example, for $N = 1024$, a range of f_c from 50KHz to 500KHz gives a range of delay, T_D, from 10msec to 1msec. Qualitatively, the frequency response is comb-like with peaks spaced 100Hz at 10msec delay and spaced 1000Hz at 1msec delay.

Vibrato and Other Effects

Vibrato is defined as a slight pitch variation at a cyclic rate, usually of the order of 5 to 10Hz, such as that produced by the rapid oscillatory movement of the figering hand of a violinist. It is customarily used to add a richness to the sound. The result of vibrato is the combinations of sounds from various paths to give a slight chorusing effect. Such pitch variations can be synthesized by changing the delay element's clock rate is a slow cyclical manner (see Figure 6). Changing the clock rate alternately increases and decreases the delay through the device and hence the pitch in a fashion analogous to the Doppler effect. If the clock-rate changes slowly, we can consider the transit time of the delay element to be constant for any particular instant of the input waveform. Delay is thus given by

$$T_D = N/2f_c \text{ seconds}$$

where T_D = the transit time (delay) through the device
N = the number of storage sites in the bucket brigade
f_c = the sampling clock frequency.

The factor 2 in the expression for T_D appears because the signal sample moves from cell to cell on each clock transition (i. e., two cells per complete clock cycle).

Now suppose f_c is varied cyclically by a small amount such that

$$f_c = f_{co}(1+k\cos\omega_v t)$$

where f_{co} is the average sampling frequency
$\omega_v = 2\pi f_v$ is the vibrato angular frequency,
k is the per-unit peak frequency deviation of the clock frequency.

The transit time is then

$$T_D = N/[2f_{co}(1+k\cos\omega_v t)]$$

Usually, $k \ll 1$, and T_D can be approximated by

$$T_D \simeq \frac{N}{2f_{co}}(1-k\cos\omega_v t)$$

This expression demonstrates the fact that when clock frequency is high, delay time is low, and vice versa.

To find the frequency variation, we use the definition that angular frequency is the rate-of-change of phase and note that the phase of the output is delayed relative to that at the input by the product of the input frequency, ω_s, and the transit-time delay, T_D. Thus the output phase, ϕ_{out}, and frequency, ω_{out}, are given by

$$\phi_{out} = \phi_s - \omega_s T_D = \omega_s t - \omega_s T_D$$
$$\omega_{out} = d\phi_{out}/dt = \omega_s\left[1 + \frac{Nk\omega_v}{2f_{co}}\sin\omega_v t\right]$$

where: ϕ_s is increasing at the angular rate $\omega_s t$ (linear if ω_s is constant as assumed for this discussion), f_{co} is the average clock frequency, as before.

As expected, if the time delay is momentarily decreasing, the output frequency is momentarily increasing and vice versa. The magnitude of the peak frequency change is not great, and is controlled by the magnitude of the change in clock frequency in the factor k.

As an example, let

N = 1024 (i. e., 1024 elements of delay)

f_{co} = 50KHz

k = 0.05 (i. e., 5% peak change in clock frequency)

$\omega_v = 7 \times (2\pi)$ (i. e., a vibrato rate of 7Hz)

Then: $\left|\omega_{out}/\omega_s\right|_{max} = \left|f_{out}/f_s\right|_{max}$

$$= 1 + \frac{1024 \times 0.05 \times 2\pi \times 7}{2 \times 50 \times 10^3}$$

$$= 1 + 0.0225$$

That is, the output vibrato peak to peak frequency change is seen to be 4.5 percent of a steady-state input frequency. As a comparison, a musical half-step of total change is slightly less than 6 percent.

Chorus and vibrato applications are similar to reverberation applications: high performance of the device is required. Here again the superior performance of N-channel devices is important, because of their stability and simplified circuit requirements. It is also desirable that neither the d-c bias point nor the a-c gain vary with clocking frequency. This is another characteristic of the N-channel devices which make them super' for high quality low-cost audio applications.

Reverberation

Acoustic reverberation is caused by the build-up of sound in an enclosed space. The build-up occurs because of the addition of sound components from simply-reflected and multiply-reflected pencils or rays of sound returned from internal reflecting surfaces. Similarly, the sound field present when sound from the source is suddenly terminated does not die away immediately but decays in an exponential manner as the reflected sounds diminish by acoustic absorption.

Reverberation can thus be synthesized as in Figure 5. Each delay element represents the time of travel in some possible path from the source S to the observer at O. Feedback adds the effect of multiple-reflection paths. Differing path lengths are represented by differing delays. A single delay element can produce reverberant effects, but would be excessively frequency sensitive with the reverberant sound having distinct flutter. Several different path lengths (delays) are desirable. Attenuation in a path represents its acoustic absorption loss; therefore, the adjustment of loss allows the control of reverberation time.

In an actual room, the direct sound is received first, followed by simple reflections, and then by an increasingly complex mix of multiple reflections. Thus an equivalent synthetic reverberator must be equipped to generate and handle a similarly complex combination of signals. Let us first consider the general situation.

Reverberation time is defined as the time (after cessation of the signal at the source) for the sound to decay to one-millionth of its initial energy level (to a level 60 dB down). Let us consider a simple case with only one closed-loop path active. The relationship is

$$T \text{ (reverberation time)} = 60(t/\alpha) \text{ seconds}$$

where: α (dB) = the attenuation, and t = time delay in seconds for one passage.

For example: if t = 100 milliseconds and α = 3 dB, then T = 2 seconds. Notice that shorter reverberation times can be produced by introducing greater attenuation or shorter delay; longer reverberation requires longer path delay or less attenuation or both. Also notice that a 10-millisecond delay corresponds to a room path length of less than 10 feet for one trip; as a result delays longer than 10msec are usually used. Round-trip attenuations of less than 3 dB lead to narrow peaks in the comb-like frequency response and thus present more difficulty in maintaining stability; so it is preferable to use a mix of relatively long delays with higher values of attenuation. If short delays are used (e. g., 10msec), then small values of loop attenuation are required to keep the effect, due to short delay, from dying away rapidly. Stability of gain is most necessary.

If, as may be done, we add the output signals from the various delay elements (see Figure 5), the output power is increased approximately in proportion to the number of paths, N. The result is an overall system gain of 10 log N dB. As a result, increased loss should be introduced in the individual path attenuators, as additional paths are added, if the same total reverberation time is to be maintained.

Feedback around a single delay element gives rise to a comb-filter type of response of amplitude vs. frequency. Schroeder[6] has developed methods of reducing the frequency sensitivity of the resulting filter and shows various combinations of filters to achieve reverberation characteristics comparable to that of actual rooms. Schroeder further states that some improvement is obtained by converting a comb-filter type of reverberator to an all-pass type of filter. Details may be found in the listed publications. In essence, the number of paths to be summed, the delays which are selected, and their

manner of combination during implementation depend on the particular application and the cost/performance tradeoffs of the system under consideration. Ideally, many parallel delay paths are required to simulate acoustics of a desirably reverberant room; practically, at least four, and preferably more, parallel paths are required if undesirable flutter is to be minimized. Adding all outputs into a single feedback path simulates actual room conditions more closely than a group of parallel paths, each with separate feedback; however, adjustable gain. Individual preference as to feedback path should rule.

The frequency response of the delay device is of particular importance in this reverberation application because: (a) long delays are desirable and (b) multiple passages through the device result in amplification of gain variations. The high-frequency loss in gain of a bucket-brigade device tends to be a fixed amount at a fixed fraction of the clock frequency, with the -3 dB point between one-third and one-half the clock frequency. To obtain a long delay calls for the minimum allowable clock frequency and hence the forcing of high-frequency attenuation in the desired pass band. The N-channel SAD-1024 is substantially better than comparable P-channel devices in control of this high-frequency attenuation, since the product of the maximum delay and the usable bandwidth is in the order of two times that attainable with a P-channel device.

The loop transmission factor in reverberation applications must be nearly unity. The SAD-1024 with its near-unity gain is substantially easier to use than comparable P-channel devices with 8 to 10 dB insertion loss. To achieve effects comparable to room reverberation requires that a large number of modes be present. These modes must be spread over time in the time domain (i. e., spread in frequency in the frequency domain). The mode spread must also take into account the acoustical responses of the ear. That is, low frequencies and high frequencies must die away more gradually than middle frequencies to compensate for the ear's variation in frequency sensitivity at different sound levels. The ultimate requirements are that the ear be unable to distinguish different rates of decay (i. e., of the different modes), and that the number of modes be great enough that objectionable flutter is avoided.

CONCLUSION

The availability of high performance analog delay devices has resulted in a whole new array of products that electronically enhance sound.

The performance necessary to make these products possible could only be realized by applying modern technology to the design of the analog delay. Only the N-channel BBD can offer the high transfer efficiency, high sampling frequency, wide bandwidth and large dynamic range at a cost-effective price necessary to realize high performance audio components.

REFERENCES

1. F. L. J. Sangster and K. Teer, "Bucket-Brigade Electronics - New Possibilities for Delay, Time-axis Conversion, and Scanning", IEEE Journal, Solid-State Circuits, Volume SC-4, pp. 131-136, June, 1969.

2. F. L. J. Sangster, "The Bucket-Brigade Delay Line, A Shift Register for Analogue Signals", Phillips Technical Review, Volume 31, pp. 97-110.

3. F. L. J. Sangster, "Integrated Bucket-Brigade Delay Line Using MOS Tetrodes", Phillips Technical Review, Volume 31, p. 266.

4. L. Boonstra and F. L. J. Sangster, "Progress on Bucket-Brigade Charge-Transfer Devices", presented at the IEEE International Solid-State Circuits Conference, Philadelphia, Pennsylvania, February, 1972.

5. W. S. Boyle and G. E. Smith, "Charge-Coupled Semiconductor Devices", B. S. T. J., Volume 49, pp. 587-593.

6. M. R. Schroeder, "Natural-Sounding Artificial Reverberation", Journal of the Audio Engineering Society, V. 10, No. 3, pp. 219-223, July, 1962.

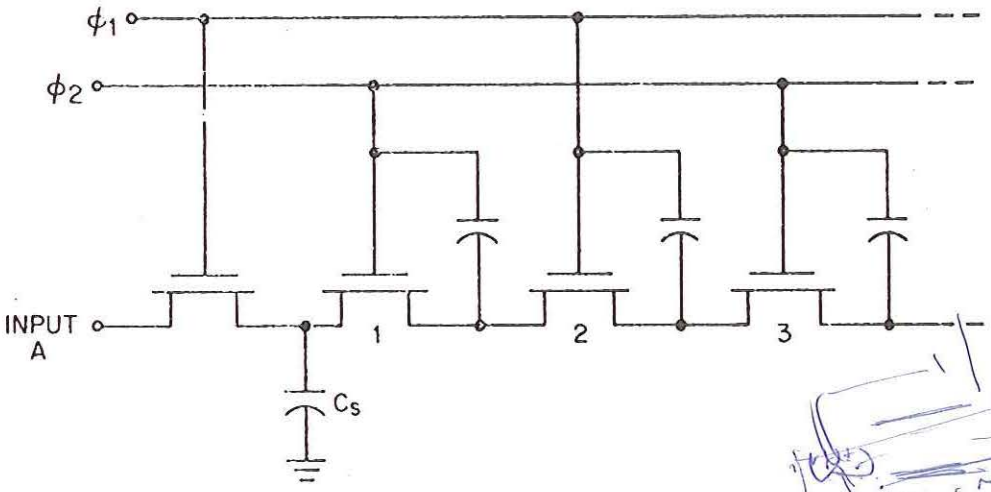

Figure 1. Basic Bucket-brigade Structure

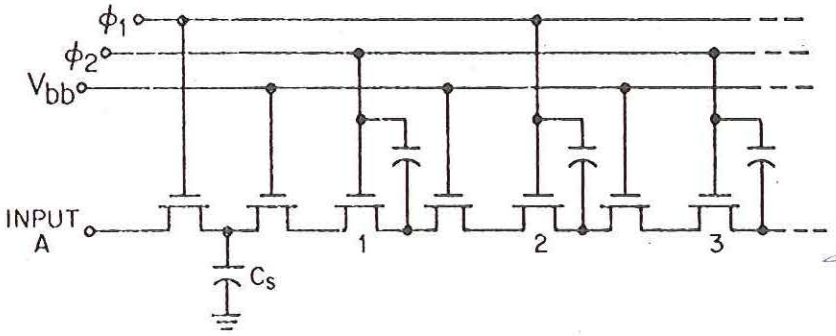

Figure 2. Improved Bucket-brigade Structure With Tetrode Isolation

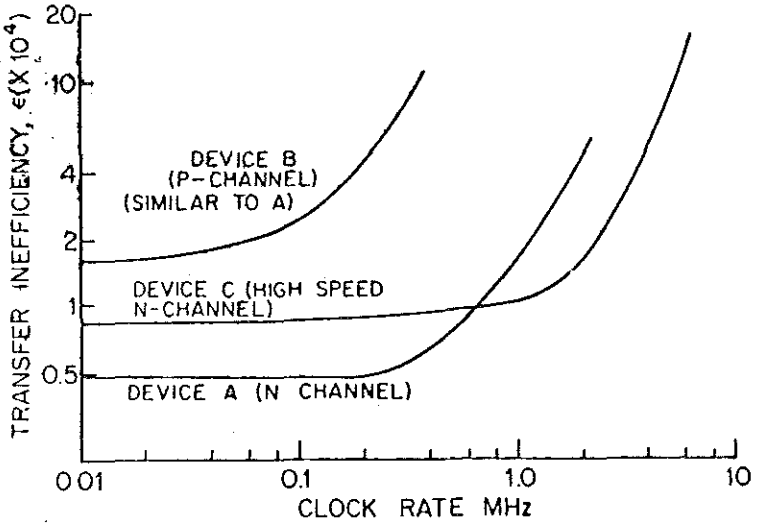

Figure 3. Transfer inefficiency vs. sample rate for two commercial audio devices and one high-speed device.

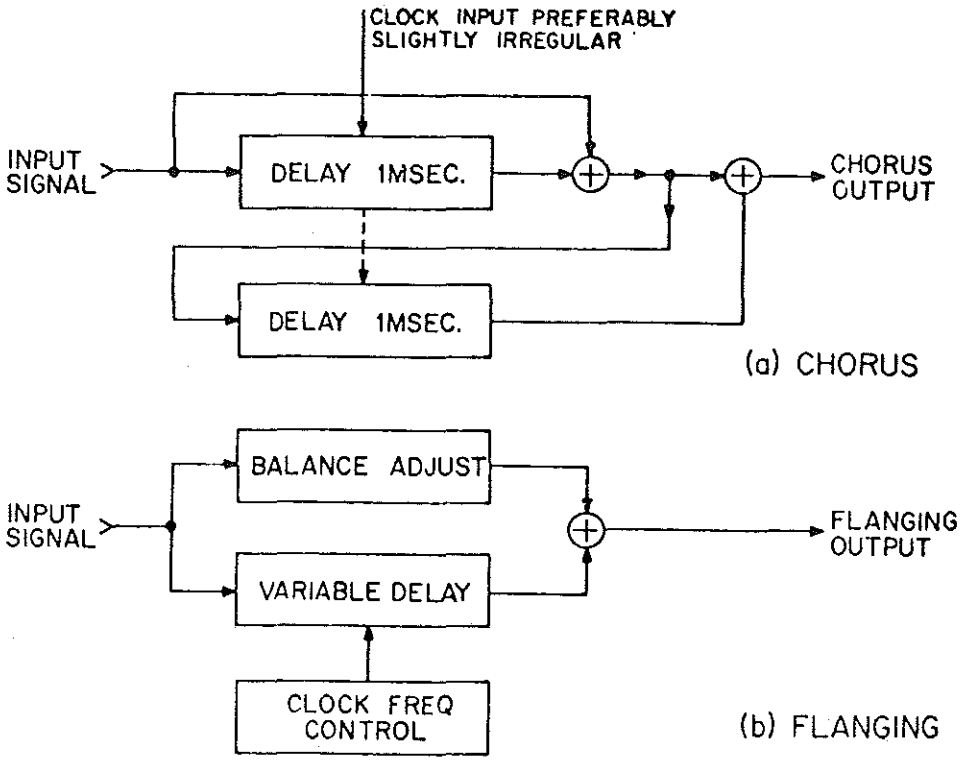

Figure 4. Circuits for Production of Chorus and Flanging Effects

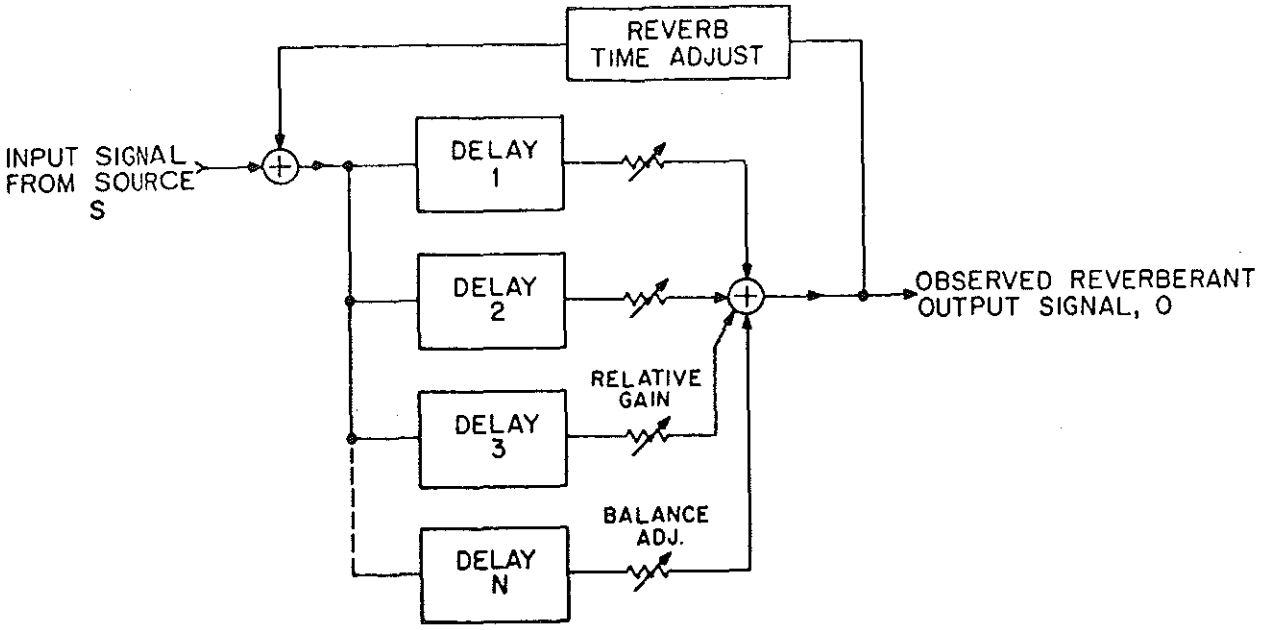

Figure 5. Production of Synthetic Reverberation

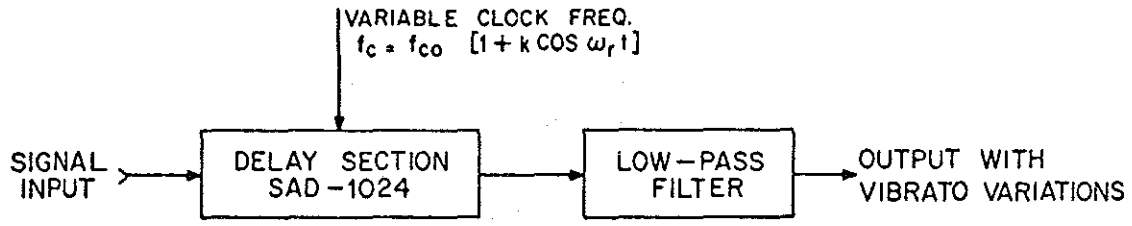

Figure 6. Block Diagram of Circuit for Producing Vibrato Effects

PART II B

A TAPPED ANALOG DELAY FOR SAMPLED DATA SIGNAL PROCESSING

Gene P. Weckler

Abstract

A new dimension in analog signal processing is now available to the engineer. A 32-tap sampled-analog delay line offers a cost-effective way of implementing linear phase filters, performing correlation, realizing adaptive phase equalizers and many other functions heretofore accomplished by digital techniques.

1. INTRODUCTION

The Tapped Analog Delay (TAD) is a 32-stage charge-transfer device. Each stage is tapped and these taps are brought to the outside through buffer amplifiers. Each buffer amplifier output appears as a source follower, thus permitting variable loading of the taps in order to create various tap-weight functions. The TAD-32 permits the storage of analog signals which can be non-destructively sensed at successive delay times. The taps are spaced one sample time apart along the delay. An additional special feed-forward output tap is provided so that devices may be connected in cascade without causing a discontinuity in the spacing of the taps from one device to the next. With this arrangement, timing integrity is maintained. The ability to cascade devices permits the user to build processors (such as transversal filters) with more than 32 taps.

2. GENERAL DESCRIPTION

The Tapped Analog Delay is a new silicon integrated circuit which provides the design engineer with a whole new bag of tricks. The delay line characteristic of this device can be modeled by the series of sample-and-hold (S/H) circuits shown in Figure 1. Two-phase sampling is shown where the even numbered S/H's sample ϕ_2 switches are closed and the odd numbered S/N's sample when the ϕ_1 switches are closed. As a result, each input sample is sequentially moved from a given S/H to the adjacent S/H on each clock transition. For a particular input sample to reach the output of the fifth S/H requires five clock transitions, and for that same sample to reach the eleventh S/H requires six more clock transitions. In CTD terminology, each S/H is called a stage, and a given sample of information remains in a stage for one sample time. If desired, any stage could be non-destructively read out to obtain delayed replica of the input signal. In sampled-data systems the delay between the taps is inversely proportional to the sampling frequency, thus providing flexibility and stability not available with a continuous time system, as will become more evident later when filters are discussed. The sampled-data system has the flexibility of a digital system without the complexity, cost or power consumption.

The equivalent circuit of the TAD-32 is shown in Figure 2. Samples are set up on the initial storage node during the period while the ϕ_1 clock wave-form is at its high (positive) level. When ϕ_1 drops, the sample value is frozen and the simultaneous rise of ϕ_2 permits exchange of charge with the tap-1 node, similarly for other nodes. The sample values thus first appear at the various nodes when ϕ_2 rises. When ϕ_2 falls and ϕ_1 rises, the charge state is transferred to the second node for each tap, thus maintaining

the output value for both halves of the clock period. The resulting output is designated full-wave (or full-period) output. Futher, there is one sample time delay between the samples as they appear at successive output taps. The last node supplies a feed-forward tap at the proper time to provide the set-up signal for another, series-connected TAD-32, so that multiple-section processors with more than 32 taps can be implemented. Clocking of the second device must be synchronous with the first, i.e., $\phi_{1A}=\phi_{1B}$.

The device is capable of sampling at rates from 100 Hz to more than 5 MHz. This capability permits the translation in frequency of a given filter characteristic over a range of more than four orders of magnitude simply by varying the clock rate. A two-phase clock is required to drive the device with complementary square waves with amplitude in the range of 12 to 15 volts. These are positive square waves, as sketched in Figure 2, thus providing a positive output with reference to ground at each tap. The output from each tap is a full-wave or boxcar output, as discussed above; no additional filtering is necessary before summing the desired weights. The summing amplifiers can combine the summing and filtering functions.

Figure 3 shows the performance of a TAD-32 operated as a low-pass filter. The impulse response of this filter is very nearly a Hamming window; therefore, one would expect the peak side lobes to be suppressed by -43 dB relative to the center lobe or passband. The experimental results of Figure 3 for a sample rate of 120 KHz indicate that -41 dB was achieved. The width of the main lobe at -20 dB is 12 KHz, which compares favorably with theory. It is apparent that band edge rates in excess of 80 dB/octave are possible. Furthermore, this characteristic can be realized over a 50 dB range of input signal as is apparent from the spectrum analyzer photograph of Figure 3.

This picture shows the spectral response or filter characteristic obtained for two inputs differing by 40 dB. The background response is for an input level 20 dB below the maximum level, thus from this picture one must conclude that nearly 60 dB of dynamic range is possible while still realizing a -40 dB stopband to passband ratio. From this we must agree that the performance attainable from the TAD-32 exceeds by far most other approaches. We will now discuss the realization of this performance in useful filter responses.

3. THE TAD AS A TRANSVERSAL FILTER

The Tapped Analog Delay is the basic building block of the transversal filter. The transversal filter represents the most effective application of charge transfer devices to sampled-data signal processing. The signals that appear at each tap of the TAD are weighted and summed by the technique shown in Figure 4. The ability to externally control the weight on each tap allows the user to design a wide variety of filter functions all based on the same basic component, and by switching in different tap weight functions it becomes possible to program in a predetermined way a desired set of filters. For example, a time-multiplexed filter bank could be realized using one TAD and multiplexing the taps to several tap weight functions, each derived with resistors.

The output of a transversal filter or finite impulse response (FIR) filter depends on a finite number of past values of the input. This type of realization does not require feedback and as a result coefficient accuracy, lack of signal-to-noise, or non-linearities are much less critical than in recursive or infinite impulse response (IIR) filters, where feedback is employed. An FIR with a non-recursive implementation has all its poles at the origin in the Z-plane and, therefore, is always stable. And finally, one of the most advantageous properties of a finite impulse response filter is that it may be designed to have an ideal linear phase characteristic.

With the introduction of data communication systems, phase characteristics of filters have become as important as their amplitude characteristics. In general, when a signal is passed through a filter, which has a non-linear phase characteristic, the signal waveform undergoes an asymmetrical distortion, which severely degrades a digital communication system. The transversal filter offers two approaches to remedy the ills of phase distortion. First of all, if only finite impulse response filters with linear phase were employed, there is no phase distortion. On the other hand, should phase distortion already be present, the transversal filter offers one of the most straightforward cost effective ways of performing phase equalization. Equalizers can be designed that will flatten the amplitude response while correcting the phase distortion. Special filters synthesized for communication systems can substantially improve the overall system performance. The use of a low-pass filter with linear phase to prevent anti-aliasing in data acquisition systems is a typical example of an

application which can best be accomplished with a transversal filter. The alternative to the transversal filter is an analog filter with its characteristic limitations of stability and accuracy.

The transversal filter does not excel in just one or two of these areas. It offers the best obtainable performance in every one of the aforementioned areas. To some, this may sound over-zealous; however, those who have had the opportunity to actually implement a transversal filter will fully appreciate the performance potential now within easy reach.

4. PRINCIPLES OF TRANSVERSAL FILTERING

4.1 THE TAD AS A BI-POLAR CORRELATOR

Probably one of the simplest functions that can be performed with a TAD is that of bi-phase correlation. Let us first consider the correlation of two valued (bi-phase) sequences as depicted in Figure 5. As shown in the figure, each tap has a switch in series with it. Sequence A is used as a program word for the switches, i.e., a "1" in the sequence represents a closed switch, while a "0" represents an open switch. Sequence B is sampled into the charge transfer delay line. The sample rate must, of course, be selected so that the delay through the line equals the period of the sequence, i.e., the sample rate must equal the data rate in the sequence. The output signal is a measure of similarity between the two sequences and reaches a maximum when two identical sequences are in perfect alignment.

Let us now consider replacing sequence B by an analog signal as shown in Figure 6. Since the analog signal has both positive and negative values, it is desirable to add a second pole to the switch so that, as shown in the figure, each tap may take on either a plus "1" or a minus "1" value depending on the switch position, thus controlling which input of the differential amplifier is selected. Sequence $\alpha(n)$, which is the tap weight function, is now represented by a p-n sequence, i.e., positive-negative values. As in the previous example, the amplitude of the output is a measure of similarity between the analog input signal and the p-n sequence represented by the tap weight function.

Let us now ask how we would mathematically represent the relationship between the input signal X (k) and the output Y (k), where k represents the k^{th} sample time. Let the tap-weight function be represented by $\alpha(n)$ where n is the tap position with n = 0 being the input, n = N-1 being the last tap furthest from the input, and for the case of the two pole switch shown in Figure 6, $\alpha(n) = \pm 1$. The k^{th} output, i.e., the value of the output Y for the k^{th} sample period, corresponds to the values of the input for the period between the (k-n) and the k^{th} sample times. This is merely a statement of what samples of the input exist in the delay line at the time just following the acquisition of the k^{th} sample. The N pervious samples are present in the line with the $(k-n)^{th}$ sample residing at the n^{th} tap. Therefore, the signal at any given tap is given by the (k-n) value of the input times the value of the n^{th} tap weight. The output for any given sample time is given by the summation of outputs from all the individual taps, which yields the following expression relating the output, the input, and the tap-weight function:

$$Y(k) = \sum_{n=0}^{N-1} \alpha(n)\, X(k-n) \qquad (1)$$

This expression is referred to as the convolutional summation and can be shown to be the discrete-time or sampled-data equivalent to the convolution integral of linear system theory.

A further analogy to linear systems theory can be made by identifying the tap weight function as the impuse response of our sampled-data system. This may be demonstrated by entering a single non-zero sample into the TAD and observing the output. Referring to the mathematical expression for the output, it is apparent that for each value of k an output appears from only one tap, since only a single non-zero sample exists in the line. Therefore, as this single sample is clocked through the line the output will be a sequence representing the tap-weight function, hence the impulse response of the sampled-data system.

So far it has been shown that the tapped analog delay can perform the function of correlation and that its system function is in reality a discrete-time convolution of a sequence representing a repetitive sampling of a continuous-time input signal and a sequence represented by the tap-weight function. This is consistent since for even functions correlation and convolution are equivalent.

The tap weight functions discussed so far have been simple bivalued functions so that an intuitive feel could be developed for the actual processes that were taking place in the system. Although binary sequence and p-n sequence correlators are often employed, their realization by digital hardware becomes prohibitive when

increased accuracy is desired, due to the power and size requirements. The tapped analog delay line in a single device allows analog accuracies in excess of seven bits of binary accuracy to be obtained with simple resistive loading of the taps. This capability immediately suggests the realization of an analog correlator with impulse response matched to a given signal; this realization is normally referred to as a matched filter.

4.2 THE TAD AS A MATCHED FILTER

The matched filter is a concept that finds extensive applications in all signal processing, in particular in the area of spread spectrum communications and radar. A filter is said to be matched to a particular desired signal if its impulse response is a time reversed replica of that signal. We have previously discussed this type of operation when deriving the mathematical expression for the output from the tapped analog delay. The above definition of a matched filter was for the time-domain and since it is a convolutional process, we know that in the frequency domain a multiplication is taking place between the two frequency functions, i.e., the spectrum of the input signal times the spectrum of the tap-weight function. Therefore, one would expect the real value to be a maximum when the two frequency functions are conjugate functions. This then says that the impulse response should be the Fourier Transform of the conjugate spectrum of the frequency function being sought. This is analogous to the familiar property that maximum power transfer occurs for a conjugate matched load.

To further appreciate the matched filter, let us consider the example depicted in Figure 7. The input to the TAD is a linear frequency chirp. As depicted in Part A, Figure 7, the chirp starts with a low frequency and ends with a high frequency. Part B shows the successive samples of the chirp which exist in the TAD at the time just following the acquisition of the last sample. We see that the first sample exists in the N^{th} stage of the TAD and the second sample exists in the N-1 stage, etc. It is obvious from the description that in order to match the chirp of the input signal it would require the tap weight function to be the time reversal of the input function.

Much more could be said about matched filters, their design, and their application, but the concept of matching the time reversed impulse response to obtain an ideal correlation is the important concept to remember.

Another important concept that should be remembered with respect to transversal filters is that the frequency domain representation is the Fourier Transform of the impulse response. This suggests the possibility of realizing a variety of filter responses by simply tailoring a tap weight function appropriately. This, in fact, is true and leads to the discussion of the realization of what is referred to as finite-impulse response filters.

4.3 THE TAD AS A FINITE IMPULSE RESPONSE FILTER

The next question to be addressed is, what techniques are used to select a tap weight function that will result in a desired filter characteristic. There are numerous detailed treatments of this subject in the literature. The discussion to be presented here will be heuristic rather than rigorous. The objective is to help the potential user of the TAD-32 develop an insight to the performance of finite impulse response transversal filters.

One excellent way to develop insight into the interaction of tap weights on filter performance is to implement a TAD-32 with a potentiometer for each tap. It is possible to simultaneously observe both the impulse response and the spectral response while varying the tap weights.

Let us begin the discussion of how to select a tap weight function by examining the responses obtained from several rather simple tap weight functions. Figure 8 shows three tap weight functions: a. all taps given the same value, b. an alternating sequence of plus and minus values, each value separated by a zero and, c. an alternating sequence of pairs, each pair separated by a pair of zeros. The tap weight function shown in Figure 8 is a rectangle of width N/f_s, where N is the number of taps, f_s is the sampling frequency, and $1/f_s$ is the time between taps. A rectangular pulse has a familiar Fourier Transfer as shown in Part D of the figure. As one might have anticipated, this rather simple tap-weight function leaves much to be desired as a filter. This will be rectified in a later section. For the time being, let us try to develop an appreciation for the overall concept before tackling the details.

Let us now look at the alternating sequences of Parts B and C. The dotted lines show the sinusoidal inputs that would most nearly correlate with these tap weight functions. As one might have anticipated, these latter two tap weight functions have each produced a bandpass characteristic, however, at different frequencies. These are shown in Parts E and F. The resulting filter responses, however, maintain the

sin x/x characteristic obtained from Part A, where all taps had the same value.

Let us assume that Sequence B was obtained from Sequence A by the multiplication of Sequence A by Sequence B, i.e., tap 1_a X 1_b, tap 2_a X tap 2_b, etc. Multiplication in the time domain infers convolution of frequency functions. We know that the frequency function for the rectangular window of A is a sin x/x function and we saw that a definite correlation exists for a particular frequency for Sequence B.

A single frequency in time domain appears as a delta function at that frequency in the frequency domain, hence a convolution between a delta function at f_0 and any other function is a shifted version of that function centered at f_0. We should, therefore, not be surprised that both of the band-pass responses have the same shape as the low pass translated to a higher center frequency.

Let us recall from the above discussion of matched filters that the impulse response of the filter, i.e., the tap-weight function, is the Fourier transform of the spectral response of the filter. Suppose we wish to design a low pass filter. Figure 9a shows the desired frequency response. The Fourier transform is shown in Figure 9b. Since we have only a finite number of taps it is necessary that we truncate the time function, choosing (N-1)/2 values on each side of zero. Choosing the tap weight functions to be an even function assures that the filter will be linear phase. It is, therefore, necessary for the tap weight function to be symmetrical around the center tap. The bandwidth of the filter is the reciprocal of the equivalent time separation between the center of the tap weight function and the first zero crossing of the tap weight function. It is usually desirable to try to make the impulse duration as long as possible. This infers that the sample rate for a filter should be as near the Nyquist rate, i.e., the maximum information frequency, as is possible and still be able to realize the desired filter shape. For example, if the choice is between using three zero crossings and four zero crossings of the sin x/x to realize the same bandwidth filter, one would realize a longer impulse duration using four zero crossings, thus giving the best ratio of stopband to passband rejection, even though the size of the taps between the third and fourth zero crossing are quite small and contribute little to the resulting output. This results because for the same cutoff frequency, it would necessitate different sampling rates; therefore, four ze ro crossings would have the lower sampling rate, thus a longer impulse duration for the same number of taps. The tap weights for a 31-tap low pass filter are obtained from the following expression:

$$\alpha(n) = \frac{\operatorname{Sin} \frac{\pi}{A}\left(n - \frac{N-1}{2}\right)}{\frac{\pi}{A}\left(n - \frac{N-1}{2}\right)} \qquad (2)$$

where: n is the tap number starting at the tap nearest the input and progressing to the output end.
N is the total number of taps being used.
A is the number of zero crossings each side of center.

Figure 10 shows the resulting frequency response for the unwindowed filter. This is not exactly what we had in mind.

It is apparent that to improve the characteristics of these filters it is necessary to somehow disguise the fact that tap-weight function is finite. The effects of truncation are a result of approximating a function which exists for all time, by a finite number of terms. For example, the Fourier series of a square wave has an infinite number of terms; however, a square wave may be approximated quite closely using only a finite number of these terms. However, when only a finite number of frequency terms are used, oscillations will occur at discontinuities in the time function. The converse is also true, i.e., if only a finite number of time samples are used to approximate a frequency response. This phenomena leads directly to the discussion of window functions.

The process of terminating a series after a finite number of terms can be thought of a multiplying the finite length impulse response by a finite width window function. In a sense, the window function determines how much of the original impulse response is actually seen, so the term window is quite descriptive. In the case where the series is abruptly terminated without modification of coefficients, the window function is said to be rectangular. The rectangular window function can be considered as a source of the oscillations as demonstrated in the previous example. Since it is necessary to terminate the series with a finite number of terms, the question arises whether there might be a better window function for this purpose. It is possible to gain some insight into this concept by considering again the terminated series to be represented as a product of an infinite length impulse response and a window function. Since multiplication in the time domain corresponds to convolution in the frequency domain, the actual frequency response may be considered as a convolution of the desired frequency response and the frequency response of the window function. It has already been seen that a rectangular window function produces a rather

poor filter. There exist numerous other possible window functions that minimize some of the difficulties encountered with the rectangular function. In order for the spectrum of the window function to have minimal effect on the desired amplitude response when the two functions are convolved, it is necessary that the window spectrum approximate an impulse response. Obviously, an ideal impulse spectrum is impossible since this would require an infinitely long window. In general, the spectrum of a window function consists of a main lobe representing the middle of the spectrum and various side lobes located on either side of the main lobe. It is desired that the window functions satisfy the two criteria: that the main lobe should be as narrow as possible, and that the maximum side lobes should be as small as possible relative to the main lobe. It turns out that both of these criteria cannot be simultaneously optimized, so that most usable window functions represent a compromise between these two factors. A window function in which minimization of side lobe width is the primary objective would tend to have a sharper cutoff but might suffer from some oscillations in the passband and significant ripple in the stopband. Conversely, a window function in which minimization of the side lobe level is the primary objective would tend to have a smooth amplitude response and very low ripple in the stopband. The sharpness of the cutoff might not be as great. Table 1 shows a comparison of some of the more generally used window functions. For work with the TAD-32, it has been found that the Hamming window function is one of the easiest to apply and gives very good results. If we now return to our previous example, where we chose the sin x/x impulse response, and we multiply that impulse response by a Hamming window. The resulting spectral response is shown in Figure 10as the windowed filter response. A marked improvement in the side lobe rejection is quite apparent as well as a very steep fall-off. Cut-off edges in the neighborhood of 80-100 dB per octave are not uncommon with a 32-tap transversal filter. This same characteristic may be translated to a higher frequency by multiplying the terms by the appropriate sequence, as shown in the previous example of Figure 8, thus forming bandpass filters at whatever frequency one wishes to center the filter. Futhermore, since the characteristics are all dependent on the clock or the sample rate, it is possible to shift characteristics, shifting either the band edge or the center frequency of a bandpass merely by changing the sampling frequency. This provides flexibility not normally available from a filter.

5. CONSLUSION

The TAD-32 offers a means by which the theory that has been developed for digital filters and digital processing can be implemented directly in analog form without the need for analog to digital conversion. Thus, the advantages of digital signal processing can be combined with the speed and simplicity of analog circuitry.

It is especially well suited for realization of a wide variety of filters including low pass, band pass, matched, linear phase, as well as programmable and time multiplexed filters. In addition to its technical advantages it offers a cost effective way of implementing these functions.

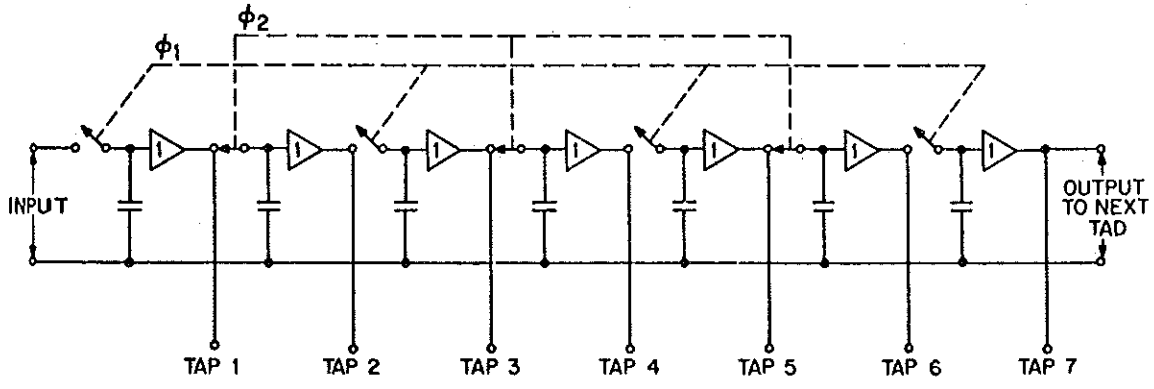

Figure 1: A Tapped Analog Delay Line Made with Sample and Holds.

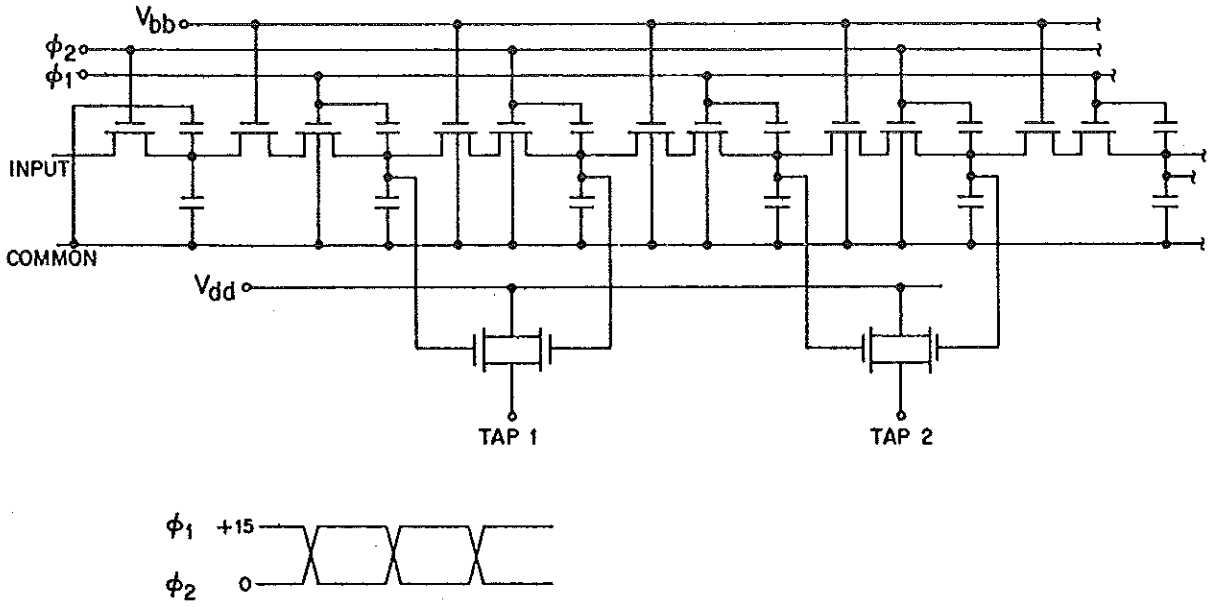

Figure 2. A Tapped Analog Delay Line Made Using Metal-Oxide-Silicon Integrated Circuit Technology

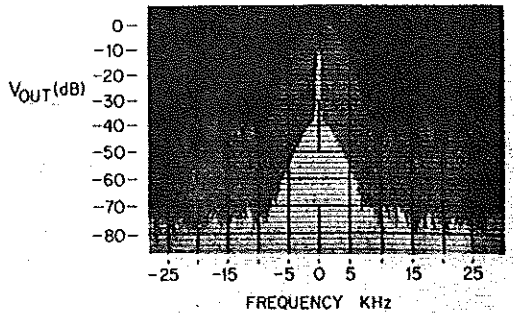

Figure 3. Photo of Spectrum Analyser Output with Hamming Window

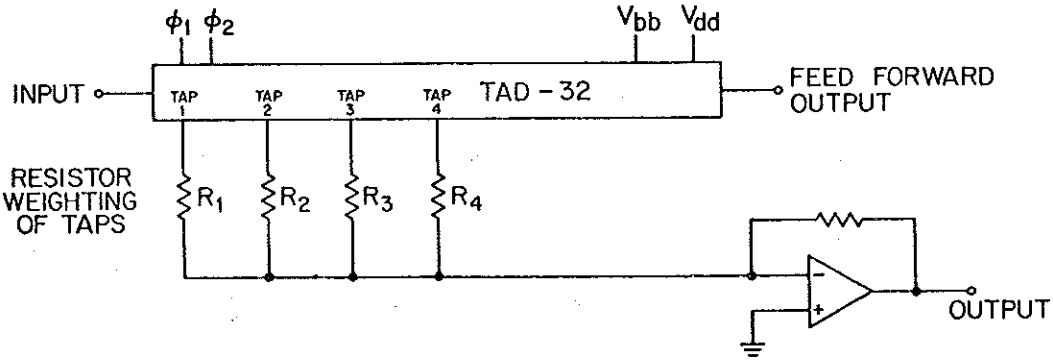

Figure 4. Schematic Representation Showing Resistor Loading of Taps for the Realization of a Desired Filter Function.

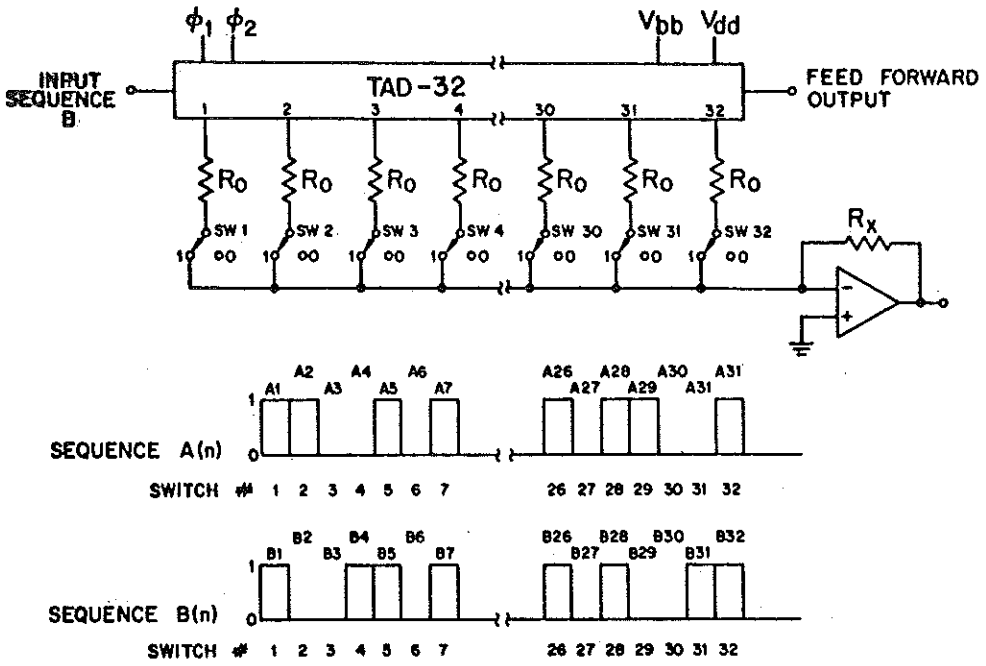

Figure 5. Schematic Showing Tapped Analog Delay Performing Binary Correlation.

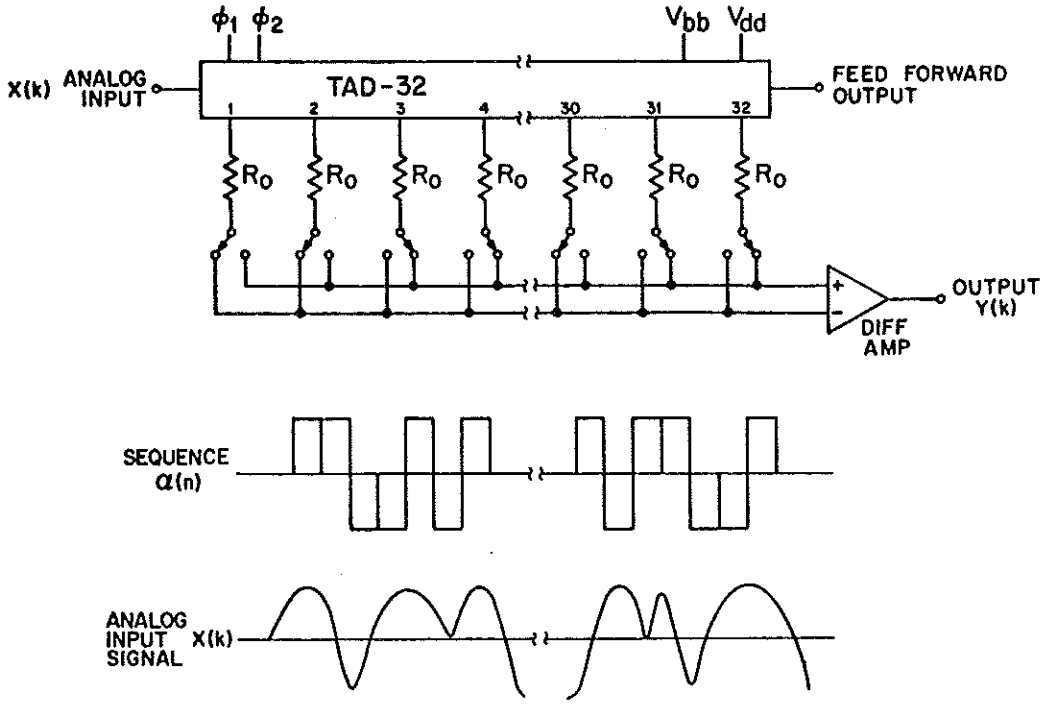

Figure 6. Schematic Showing the Tapped Analog Delay as a Bivalued Analog Correlator.

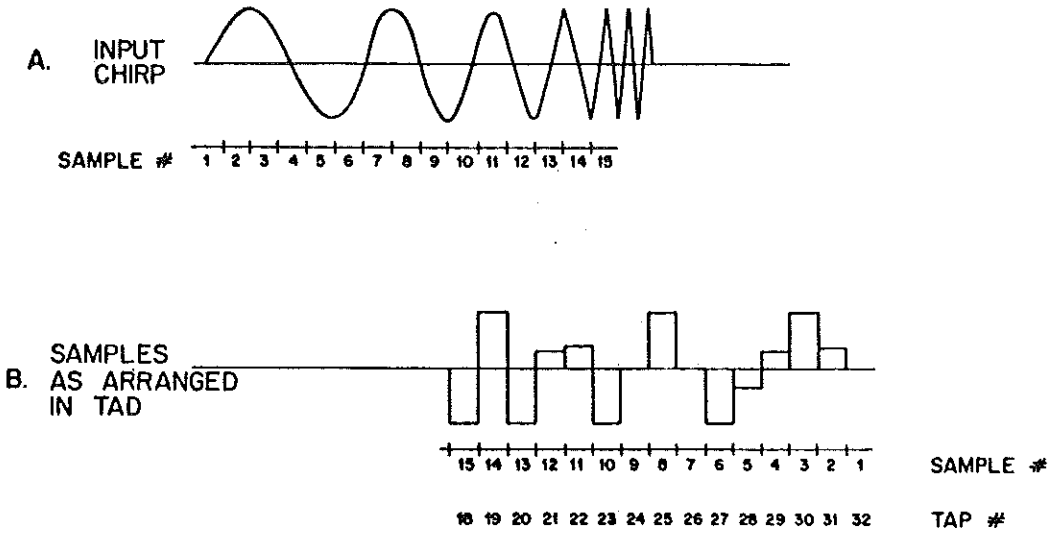

Figure 7. Arrangement of Samples of Input Chirp Along the Length of a Tapped Analog Delay.

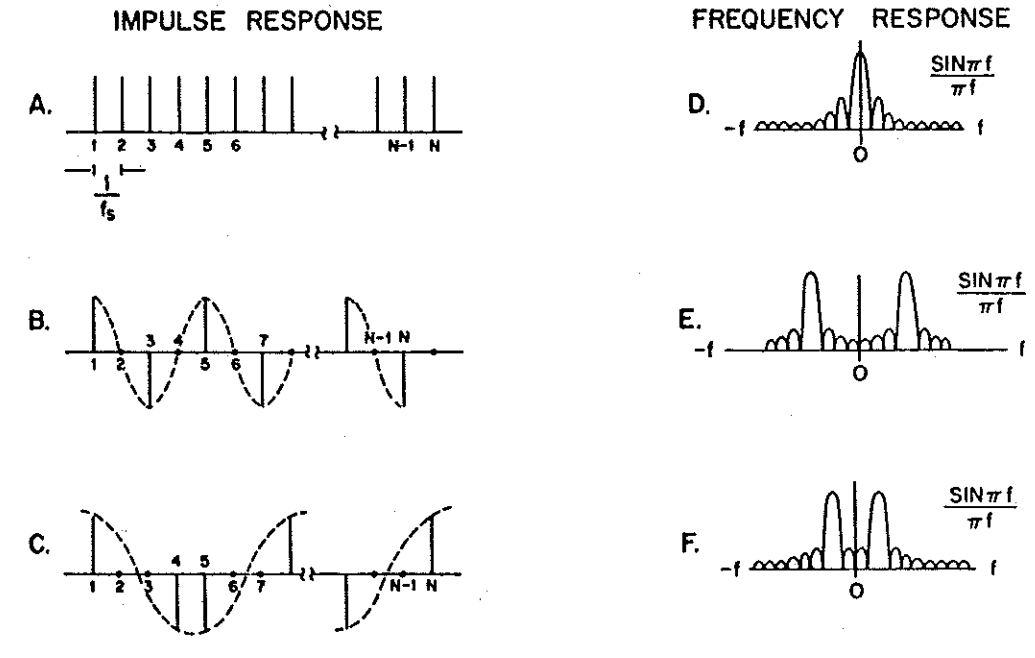

Figure 8. Three Simple Impulse Responses and the Resulting Frequency Response Produced by Each.

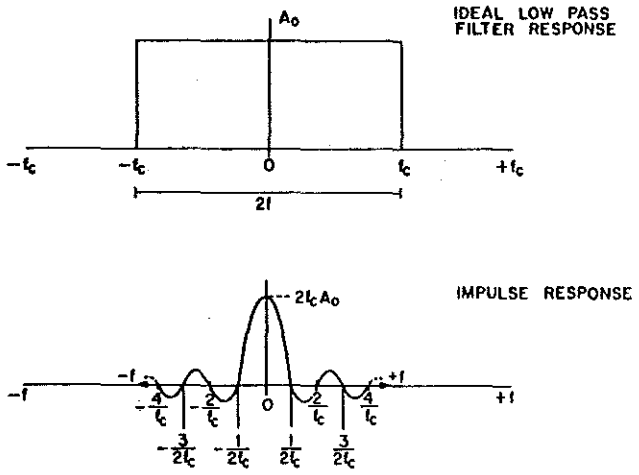

Figure 9. Impulse Response for an Ideal Low Pass Filter.

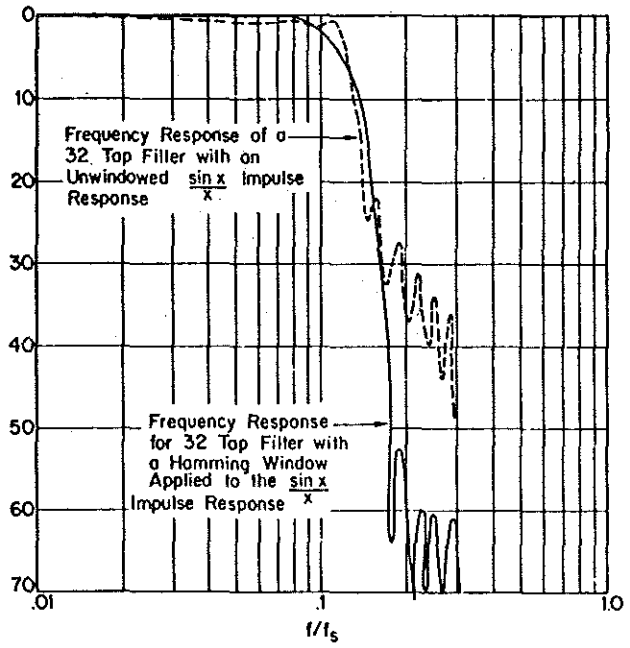

Figure 10. Comparison of Window and Unwindow Filter Response.

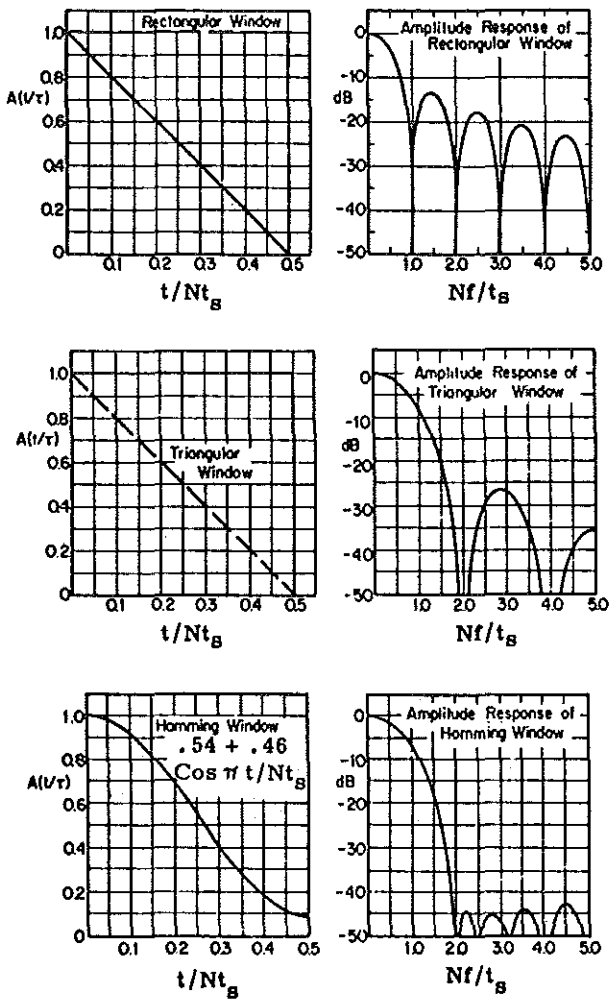

Table I. Comparison of Commonly Used Window Functions.

PART IIc

IMPLEMENTATION OF DISCRETE-TIME ANALOG FILTER AND PROCESSING SYSTEMS

R. R. Buss and S. C. Tanaka
Reticon Corporation
910 Benicia Avenue, Sunnyvale, California 94086

ABSTRACT

Sophisticated filter or processing systems may be built up from devices which delay sampled analog signals by multiple successive discrete-time periods. Thus, with the recent introduction of high-performance discrete-time sampled analog data devices, practical realizations are possible for a wide variety of discrete-time filters and processors.

A new integrated-circuit device, designated TAD-32, has 32 successive delay taps, each separated from the next by one sample period. Provision is also made for uninterrupted extension to a sequence of devices so that multi-section processors with tap sequences of arbitrary length may be used. The usable dynamic range normally exceeds 60 db and usable storage time up to hundreds of milliseconds is possible. The design techniques are reviewed, but emphasis is placed on the experimental results obtained for low pass and bandpass filters using various weighting criteria. Oscillograms and spectra are shown for transversal filters for uniform and for sin x/x tap weighting and for the above with Hamming windows. Swept response oscillograms are shown for Butterworth and for elliptic recursive filters.

INTRODUCTION

Until recently, signal processing involving successive time delays was implemented either by use of physical analog delay elements, such as acoustic or electric transmission-line delay elements, or by conversion to digital format for processing, then reconverting the processed results to an analog output. Wholly analog systems are cumbersome, expensive, and sensitive to environmental factors. On the other hand, conversion to wholly digital format is often unnecessary and penalizes the system in terms of cost, complexity, speed, and power.

A very attractive alternative is discrete-time processing of analog samples. Time is quantized, but relative amplitudes are preserved. Delay is accomplished by transferring samples from cell to cell in shift-register fashion, while preserving relative amplitudes. Discrete-time systems combine many of the best features of both digital and analog systems: the high speed and freedom from quantization effects of analog systems are combined with the time precision and flexibility of digital systems.

Tapped delay elements have applicability to a very wide range of processing functions. Two particular examples are FIR and IIR filters. FIR filters are those having finite impulse response; IIR filters are those having infinite impulse response. These two classes of filters are readily implemented with a Tapped Analog Delay (TAD). Such a device is the TAD-32, a new state-of-the-art bucket-brigade type of integrated tapped delay. A schematic circuit of the device is shown in Figure A. Information is read into the initial storage capacitor once per clock cycle during the period while ϕ_1 is at its high (positive) level. When ϕ_1 drops, the sample value is frozen and the simultaneous rise of ϕ_2 permits exchange of charge with the first tap-1 node, and similarly for other first nodes of the various taps. The sample values thus appear at the various nodes when ϕ_2 rises. When ϕ_2 falls and ϕ_1 rises, the charge state of each first node of a pair transfers to the second node of the pair for each tap, thus maintaining the output value for both halves of the clock period. The resulting output is designated full-wave (or full-period) output. Further, there is one sample time delay between the samples as they appear at the successive taps. The last node also supplies a feed-forward tap at the proper time to provide the set-up signal for another, series-connected TAD-32, so that multiple-section processors with more than 32 taps can be implemented. Clocking of the second device must be synchronous with the first, i.e. $\phi_{1A} = \phi_{1B}$, etc.

The device is capable of sampling at rates from 100 Hz to more than 5 MHz. This capability permits the translation in frequency of a given filter characteristic over a range of more than four decades simply by varying the clock rate. Simple two-phase complementary square-wave clock waveforms, of amplitude in the range 12 to 15 volts, are required to drive the device. These are positive waveforms, thus providing positive output with reference to

ground at each tap. No additional filtering is required at tap outputs before summing the desired (weighted) values. The summing amplifiers can provide the summing and filtering functions. A further general treatment of the device is given by Gene Weckler[1] and treatment of these analog delay circuits in various other processing forms may be found in a companion paper, this session[2].

FINITE IMPULSE RESPONSE (FIR) PROCESSOR

The Tapped Analog Delay is the basic building block of the transversal (FIR) filter. The transversal filter represents the most effective application of charge-transfer devices to sampled-data signal processing. The signals that appear at each tap of the TAD are weighted and summed. The ability to control externally the weight of each tap allows the user to design a wide variety of filter functions all based on the same basic component.

The general state diagram of a FIR filter or processor is shown in Figure 1. Each tap is weighted and their outputs then summed to give the filter output. The simultaneous availability of all signal taps enhances the processing gain by up to 20 log $\sqrt{N}$ db, where N is the number of available taps. This FIR type of filter is described in general terms in the companion paper. It is to be noted that we use the term "filter" in its broad sense inasmuch as correlation, convolution, and other such processes are a form of filtering. The FIR filter is unconditionally stable: the Z-plane contains only zeros (outside of the origin), no feedback is involved, and the influence of any signal segment is completely limited to times less than or equal to the maximum delay time of that segment; thereafter it passes out of the system and is lost. The general impulse response is as in Figure 2, where tap weights are given by the a_i. However, as Gene Weckler states in Reference 1, the limited or truncated impulse response of such a finite-duration device means that compromises must be made in the design. These compromises affect primarily the roll-off rate and the relative loss outside of the passband.

The simplest FIR filter has uniform weighting of all of the taps (the a_i of Figures 1 and 2 all are of unit amplitude). To show the impulse response, let a single pulse (sample) of unit amplitude be input. Later and earlier inputs are all zero. This pulse appears once only at any one tap; it then moves to the next successive tap where it again appears for one sample period. It moves in this manner until it appears at the last (N^{th}) tap, and then moves out of the system and is lost. The lowpass impulse response, which is the sum of all of the weighted tap outputs, is, thus, of uniform amplitude but limited by a rectangular "window" of width NT time periods, where N is the number of taps and T is the period separating the taps. This response is illustrated in Figure 3. The corresponding frequency response of this filter is easily found. It has a $(1/N)(\sin \omega N/2)/(\sin \omega/2)$ amplitude term (which for the range of N involved can be approximated by $(\sin \omega N/2)/(\omega N/2)$) and a linear-phase term $\exp(-j(N-1)\omega/2)$ which accounts for the delay through the system. Figure 4 shows the spectrum amplitude for this equal tap weighting, with a 300-Hz analysis bandwidth. The narrow bump at the origin is a combination of the zero-frequency response of the spectrum analyzer and a residual odd-even unbalance of the TAD-32, and is to be ignored. The nulls are partially masked by the relatively broad analysis bandwidth. A different spectrum analyzer, having a 3-Hz bandwidth, shows the null depth to be at least 60 db, as shown by Figure 5. Note that, to show capability, this particular spectrum was taken with a 5-MHz filter sample rate! All other FIR-filter spectra were obtained under conditions of an approximate 130-KHz sample rate.

The finite width and abrupt termination of the rectangular "window" of the impulse response (Figure 3) causes the broad high-amplitude side lobes of the spectrum of Figures 4 and 5. The key to practical design of discrete-time transversal (FIR) filters lies in making the appropriate compromises to bridge the gap between the ideal and the attainable, and to do it in some optimum sense. One such compromise is Hamming-window tapering of the tap weights to give balanced control over the rate of transition between pass and stop bands and of stop-band attenuation. An entirely analogous experience is the tapering of the illumination of an antenna reflector to control side lobes. For a window, the ideal, infinitely extended series of tap weights are multiplied by the appropriate Hamming factors, which terminate. The resultant calculated factors for "correcting" Figure 3 are shown by the oscilloscope overlay of Figure 6. Corresponding weights (resistance values) for the TAD-32 were then calculated and adjusted to one percent. The impulse response of the system was then observed, and slight trimming of the more significant weights

made to make the actual impulse response match the calculated response. This adjustment is very simple, almost noninteracting, and takes into account the nonzero output impedances of the buffers, as well as any slight irregularities in gain, etc.

The oscillogram of Figure 7 shows the actual measured impulse response, after trimming, and Figures 8 and 9 show the corresponding spectrum. There is a residual uncertainty in values of the order of one percent; with 32 taps, this one percent uncertainty leads to a maximum stop-band attenuation of the order of 40 db or less[3]. Figure 8 shows close-in stop-band attenuation of approximately 37 db or more. Figure 9 is an extended spectrum showing the first multiple response centered about the sampling frequency. Other responses center about integer multiples of the sampling frequency. Of interest in the spectrum is the rounded top of the passband. We will return to this point later

The time-domain and frequency-domain pairs shown in Figures 3-5 and 7-9 are examples of a general relationship between these two domains. That relationship is given by Fourier-transform pairs in the continuous domain, and by Z-transform pairs in the discrete-time domain.

To turn the problem backwards, suppose we desire a rectangular filter passband and start from that passband to determine its impulse response. We then find an impulse (time) response that has a sin x/x form which extends over all time, although with diminishing amplitude, as $x \rightarrow \infty$. The infinite time extension shows the practical impossibility of obtaining "ideal" rectangular passbands. Such an ideal is particularly elusive when the number of taps must be limited. Simple truncation of the "ideal" weighting is not optimum. However, let us once again modify the weighting by Hamming window factors so as to give a more tractable span of taps. Calculated impulse response, after such Hamming modification, are given as overlays in Figures 10 and 11 which show two different widths of the basic sin x/x response. The Hamming window is related to the number of taps and so constant. For the wide window of Figure 10, there are 16 sample times between the first sin x/x zero crossings; for the narrow window of Figure 11, there are only 8 sample times between the corresponding points. As before, calculated resistance values for the tap weights are trimmed to match the calculated impulse response. The corresponding measured impulse responses are shown in Figures 12 and 13. The performance of these windowed filters is shown in the spectra of Figures 14 and 15 for the wide window and Figures 16 and 17 for the narrow window. As before, these spectra show the passband and transition regions on an expanded scale to show detail (Figures 14 and 16) and then the whole spectrum observed out far enough to include the response around the sample frequency (Figures 15 and 17). Two features are particularly to be noticed: 1) a narrow impulse response corresponds to a wider frequency response, and 2) the attempt to match the ideal sin x/x impulse response, as opposed to the rectangular impulse response, gives rise to a much flatter passband in Figures 14 and 16 than was exhibited in the passband response of Figure 8.

So far, discussion has centered on the low-pass filter. A simple form of bandpass filter was chosen as illustrative of performance. To make the bandpass filter, pairs of taps were given alternate positive and negative weights: two positive followed by two negative, etc. Overall, the Hamming tapering was applied. The calculated impulse-response overlay is shown in Figure 18, and the actual response in Figure 19. Spectra, narrow scan and wide scan as before, are shown in Figures 20, 21 and 22. Figure 21 is a blowup of the central portion of Figure 20. In Figure 22, the narrow left peak is the spectrum analyzer's zero response, next comes the bandpass response, and the next three major peaks are, in order, the lower sideband, the sampling-rate carrier, and the upper sideband responses.

INFINITE IMPULSE RESPONSE (IIR) PROCESSORS

The state diagram for a general second-order recursive (IIR) filter processor is as in Figure 23. Filters of any order may be constructed; a second-order design is chosen as example. It is to be noted that, in general, implementation is possible using feedback loops, feedforward loops, a few delay elements, and the requisite weighting and summing functions. As in the transversal filters, multiplication is largely accomplished by selecting values of weighting resistors; addition is implemented easily by means of operational-amplifier summers, and throughout, amplitude remain as discrete (sampled) analog values which are held between sample times. Time is precisely quantized, with intervals determined by the sample frequency.

Because the recursive filter involves feedback, with near unity loop gain, precision and stable performance of the filter elements are of considerably greater importance, and aberrations are more damaging than in the comparable transversal filter. Further, because of the infinite extension of the impulse response, filter design differs considerably and filters may be constructed to have fewer elements and smaller overall time delay than for FIR filters. The choice of type and method of implementation of the filter, whether transversal or recursive, depends on the particular situation and the designer's engineering judgment and experience.

The TAD-32, while primarily designed to fit the needs of transversal filters, is also adaptable to use as the delay sections for recursive filters. It has a transmission factor, input to each tap output, that is near unity and primarily determined by a capacitance ratio. It thus has the requisite stability for IIR configurations. The multiple taps also give great flexibility to possible filter design. An experimental, flexible, second-order recursive filter was set up to show the general performance. Arrangements were such as to permit generation of a second-order Butterworth or of a second-order Chebyshev type of response[4]. A schematic diagram, showing the means of obtaining the pole pairs, is shown in block form in Figure 24 and in more detail in Figure 25.

A curious point arises with the recursive filter that is not met in the transversal filter. An analog input may be sampled properly by the device, and all internal combinations occur correctly, but there usually is also a direct (analog) path between the input and output (See Figure 23) that may permit between-sample analog values to change the output and so cause a type of quantizing error. It is thus evident that a sample-and-hold device optimally should be used, either at the input before the first summing point, or at the output after the last summing point. When used before the first summing point, the sample slice must be taken just after the sample has been selected by the TAD delay element, in order to insure proper delay, timing, and minimum disturbance. When the sample-and-hold is used after the output summing point, its sampling slice must be taken just before the end of a full clock period, after all data have settled. That is, when connected at the output, the S/H's sampler slice must occur just before the TAD freezes data; when connected at the input, the S/H's sampler slice must occur just after the TAD freezes data. In this way the analog input signal samples used are those values which occur at the proper point in time, and overall performance and accuracy is maximized.

In the circuits of Figures 24 and 25, a sample-and-hold was interposed in the output channel. In this location it has the added advantages that data have settled for the maximum time possible before reading, and further, that the maximum discrimination against clocking transients is obtained. The sampler slice was triggered by the ϕ_1 clock edge to give the desired timing, as discussed above. Although the TAD-32's output taps arise from internal source followers, additional buffer emitter-followers were used externally to avoid any reaction from adjustment of the tap weights.

The swept frequency response of the filters is indicated in Figures 26-31. A maximally-flat (Butterworth) two-pole bandpass response is shown in Figures 26 and 27. Only the first two taps of the TAD-32 were used. Sampling frequency is 900 KHz to give maximum passband response near 450 KHz. Qualitatively, the major feedback path is that from the first tap, giving an interface null near zero and integer multiples of the sampling frequency, and reinforcement (maximum response) for frequencies near odd multiples of half the sampling frequency. Figure 26 shows a frequency scan from 0 to 2 MHz to illustrate the multiple responses. Figure 27 shows the vicinity of 450 KHz, illustrating the flat-tapped bandpass.

A different Bufferworth filter is illustrated in Figures 28-30. For this filter, tap 6 and tap 12 were selected, with the result that minima occur at even multiples of $f_{sample}/12$, and bandpass responses at odd multiples of $f_{sample}/12$. Figure 28 shows the full frequency span out to the 900 KHz sampling frequency, Figure 29 shows the scan reduced to 450 KHz, and in Figure 30 the frequency sweep is reduced to approximately 80 KHz centered about 75 KHz to show the first of the bandpass responses in more detail. Figure 31 is the response of the same filter as Figure 30, except the weighting values have been readjusted to give a Chebyshev or elliptic response in place of the maximally flat choice.

Operational-amplifier and circuit phase shifts are evident in their effects on pass-band response flatness, and particularly noticeable

in Figure 28 at the higher-frequency maxima. This effect underscores the critical nature of the balance in the recursive filter.

In the recursive-filter examples, taps at KT and 2KT were chosen; other possibilities exist, in general, but require more complicated calculations to preselect desired weighting and are not as intuitively understandable as an illustration. For example, let a pair of adjacent taps, say at 16T and 17T, be fed back with equal weight, out of phase at zero signal frequency. Each will contribute to a maximum response near $f_{sample}/(2 \times 16\text{-}1/2)$. The response may be double peaked with a great deal of regeneration, or flattened to the desired extent by decreasing regeneration.

CONCLUSIONS

Bucket-brigade tapped analog delay lines are practical and economical discrete-time filter components. Tap weighting may be readily adjusted, either internally as part of the integrated-circuit design, or externally by means of weighting resistors, all with good stability. Filter performance ultimately becomes largely dependent on the precision with which tap weights may be adjusted. A single integrated circuit permits filters with passband to stopband ratios in excess of 35 db.

FIR (Transversal) filters are most readily implemented and give maximum processing gain; however, device stability is such that IIR (recursive) filters may likewise be implemented to take advantage of the longer-duration impulse responses possible and also to take advantage of the shorter group delay possible.

References

1. G. P. Weckler, "A Tapped Analog Delay for Sampled Data Signal Processing", Proceedings of the 19th Midwest Symposium on Circuits and Systems, August 16-17, 1976, (University of Wisconsin, Milwaukee).

2. U. J. Strasilla, "A Programmable Binary-Analog Correlator", (companion paper, this session).

3. R. D. Baertsch, W. E. Engeler, H. S. Goldberg, C. M. Puckette, IV, and J. J. Tiemann, "The Design and Operation of Practical Charge Transfer Transversal Filters", IEEE Transactions on Electron Devices, Volume ED-23, No. 2, February, 1976, p.p. 133-141.

4. D. A. Smith, W. J. Butler and C. M. Puckette, "Programmable Bandpass Filter and Tone Generator Using Bucket-Brigade Delay Lines", IEEE Transactions on Circuits and Systems, Volume CAS-21, No. 4, July, 1974, p.p. 497-501.

Fig. A. Tapped Analog Delay Line Mode Using Metal-Oxide-Silicon Integrated Circuit Technology

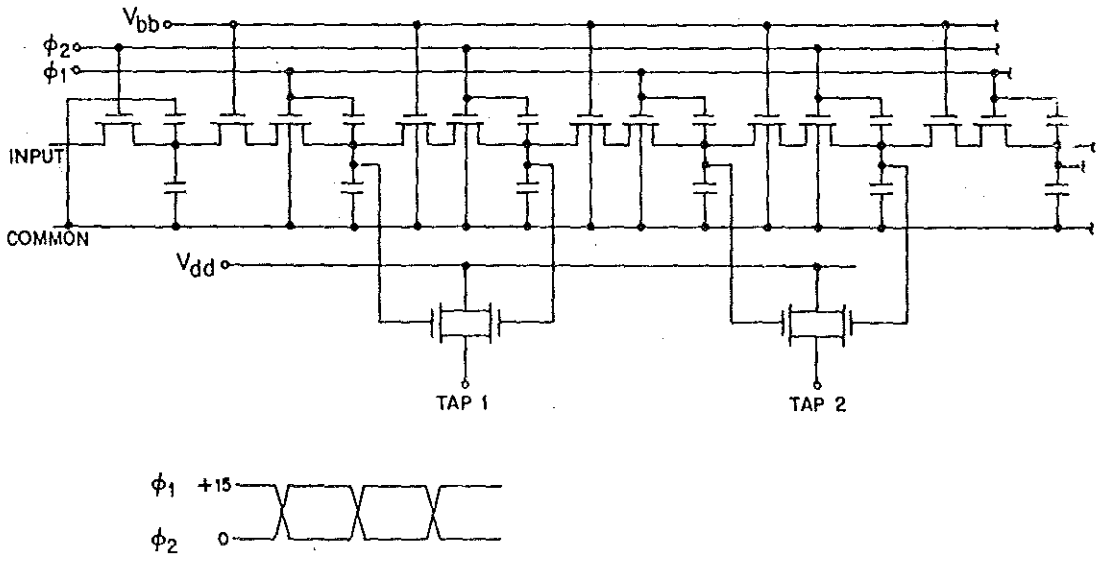

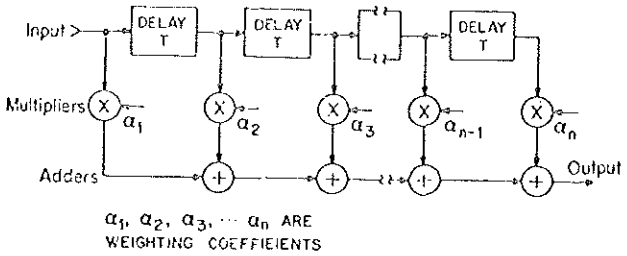

Fig. 1 General state diagram for transversal (FIR) filter.

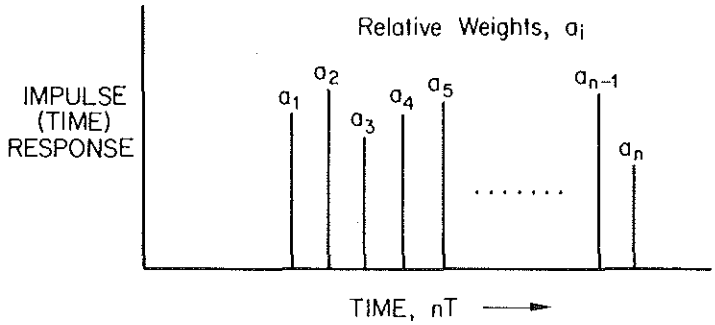

Fig. 2 Impulse response of FIR filter of Fig. 1. For uniform weighting, all $a_i = 1$.

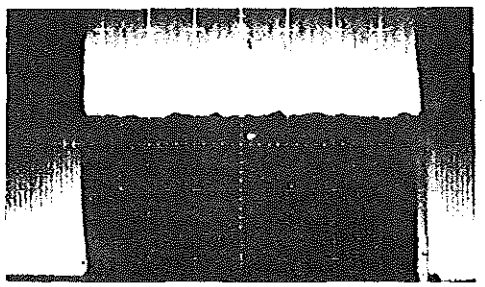

Fig. 3 Oscillogram of equal-weight impulse response.

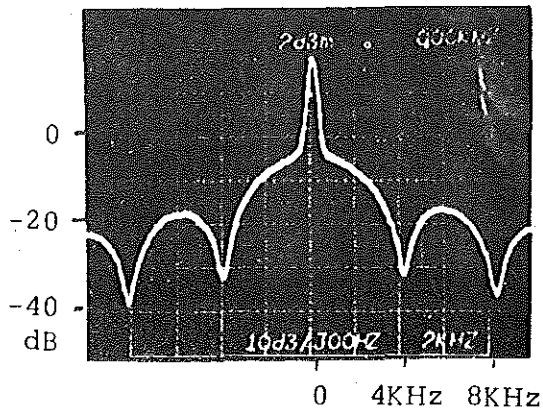

Fig. 4 Frequency spectrum for equal-weight FIR filter: 300 Hz resolution bandwidth, ±10 KHz scan.

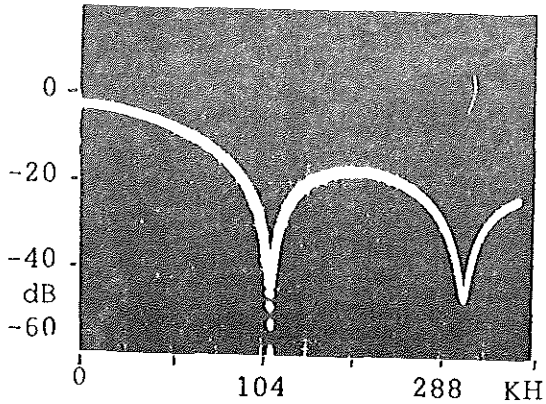

Fig. 5 Frequency spectrum for equal-weight FIR filter; 3 Hz resolution bandwidth, 360 KHz scan.

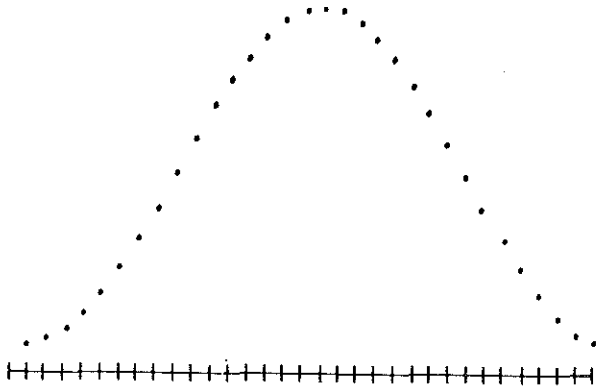

Fig. 6 Hamming window for 32-tap filter an oscilloscope overlay.

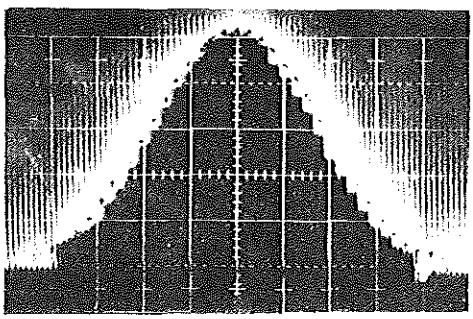

Fig. 7 Impulse response with equal weighting modified by Hamming window.

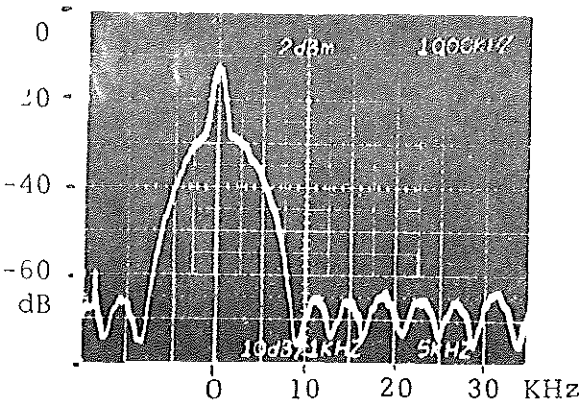

ig. 8 Spectral response with Hamming weighting.

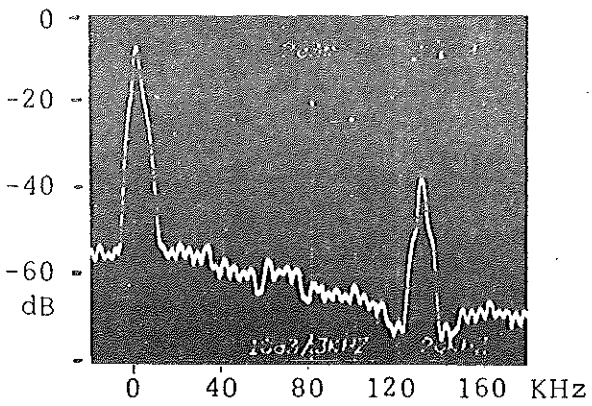

Fig. 9 Spectral response as in Figure 8, extended to show sampling-frequency area.

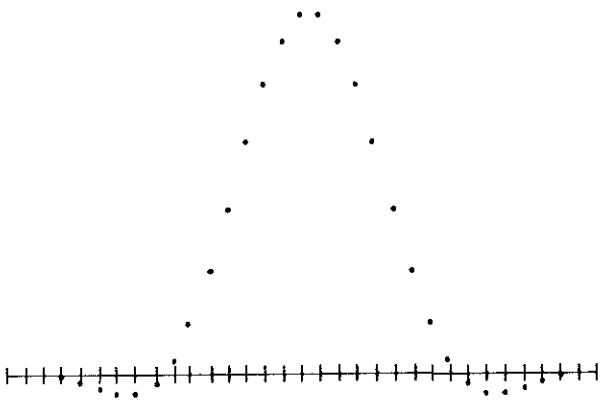

ig. 10 Oscilloscope overlay for Hamming-windowed sin x/x impulse response, 16 taps between zero crossings

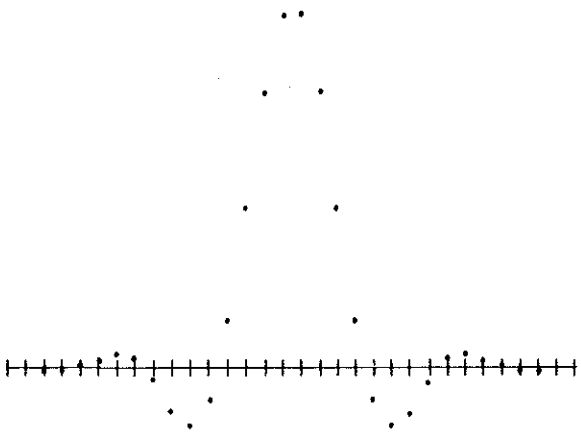

Fig. 11 Oscilloscope overlay for Hamming-windowed sin x/x impulse response, 8 taps between zero crossings.

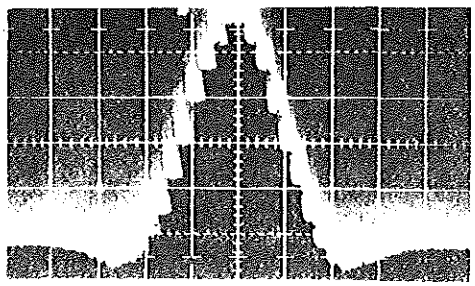

ig. 12 Actual impulse response matching Figure 10

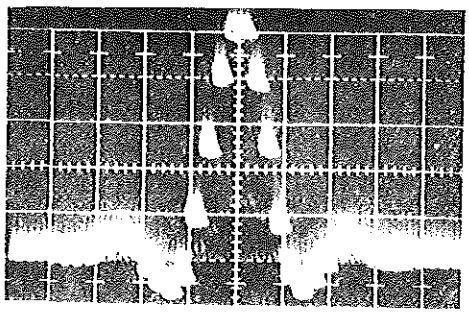

Fig. 13 Actual impulse response matching Figure 11.

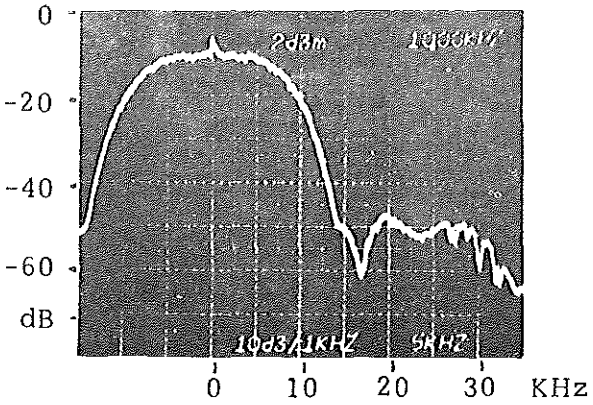

Fig. 14 Frequency spectrum, wide band, corresponding to impulse response of Figure 12.

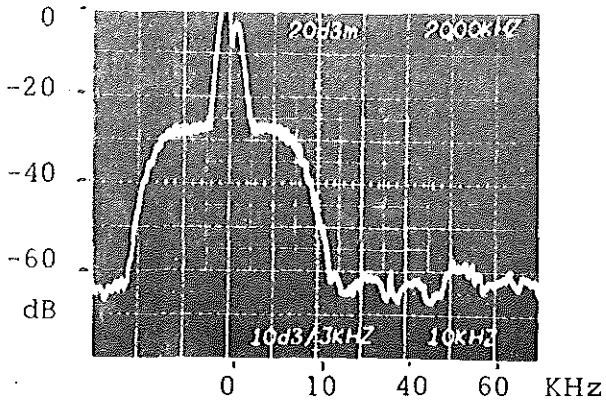

Fig. 16 Frequency spectrum, narrow band, corresponding to impulse response of Figure 13.

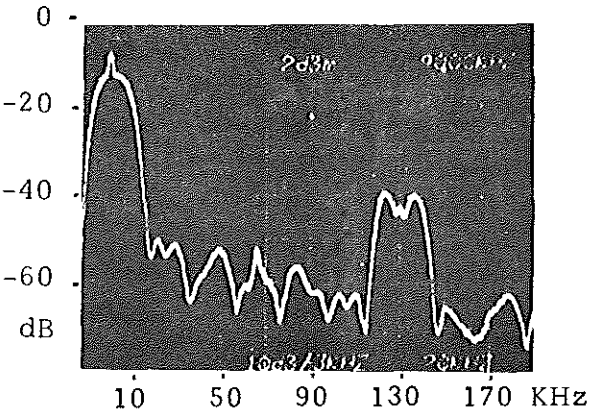

Fig. 15 Frequency spectrum, wide band, scan extended to show sampling-frequency rate.

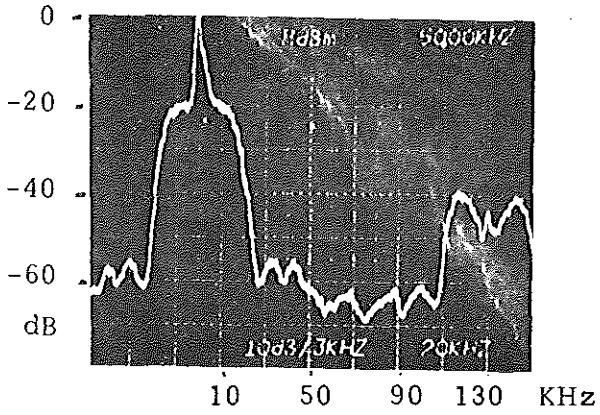

Fig. 17 Frequency spectrum, narrow band, scan extended to show sampling-frequency area.

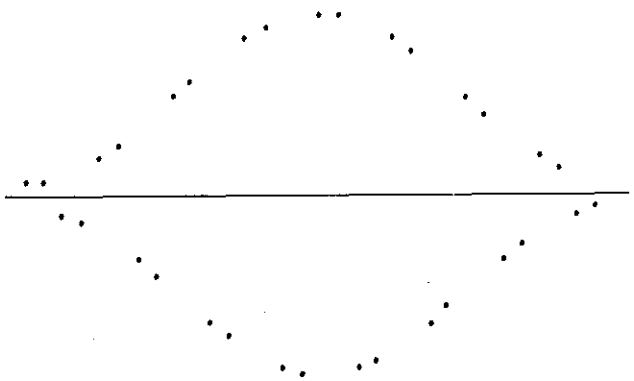

Fig. 18 Oscilloscope overlay for bandpass filter. Taps reversed in pairs, uniform weighting modified by Hamming window.

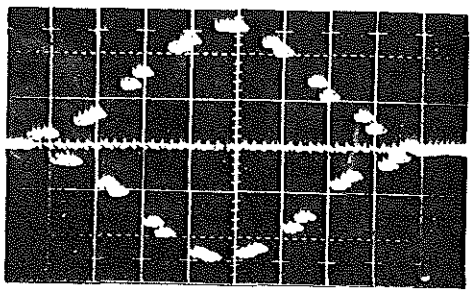

Fig. 19 Actual impulse response matc hg Figure 18.

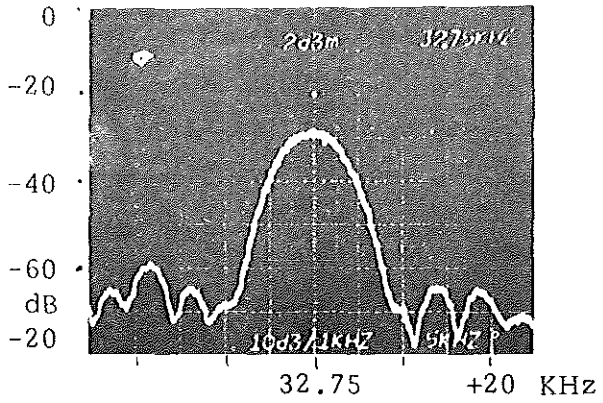

Fig. 20 Bandpass response corresponding to impulse response of Figure 19.

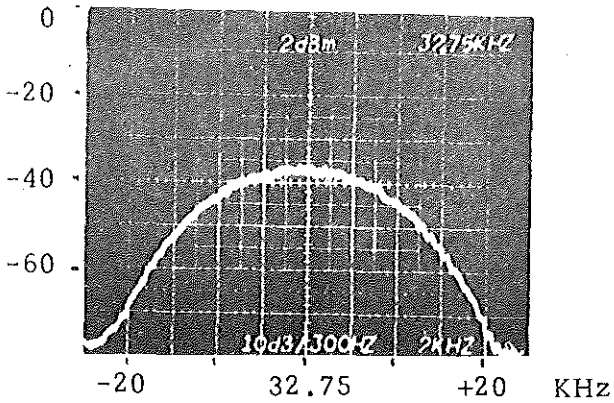

Fig. 21 Center section of Figure 20 expanded to show rounded passband shape.

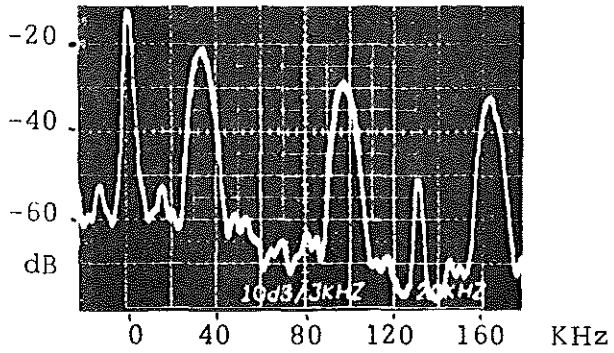

g. 22 Bandpass response corresponding to impulse response of Figure 19, scan extended to area of sampling frequency.

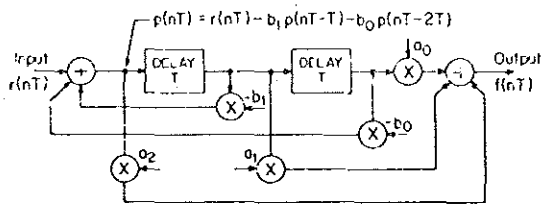

Fig. 23 General second-order recursive filter.

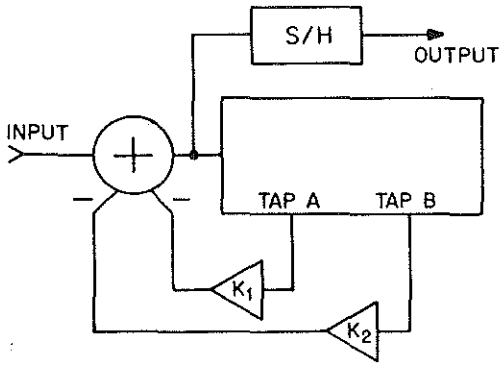

Fig. 24 Block diagram of experimental recursive filter.

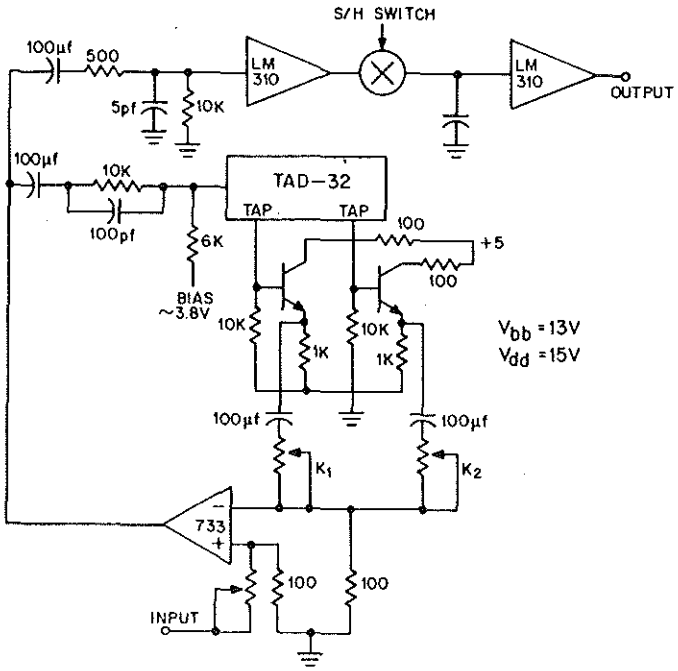

Fig. 25 Circuit diagram of experimental recursive filter.

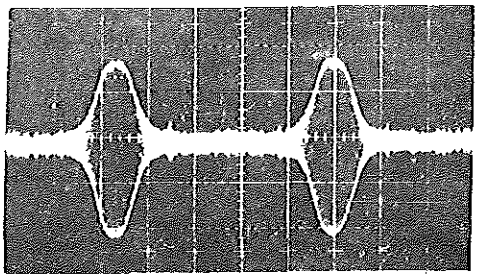

ig. 26 Swept frequency response, Butterworth filter, taps 1 and 2. f_s = 900 KHz, sweep 0 - 2 MHz.

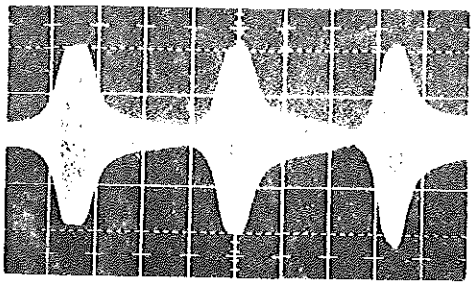

Fig. 29 Same as Figure 28, sweep 0 - 450 KHz, f_{center} = 225 KHz.

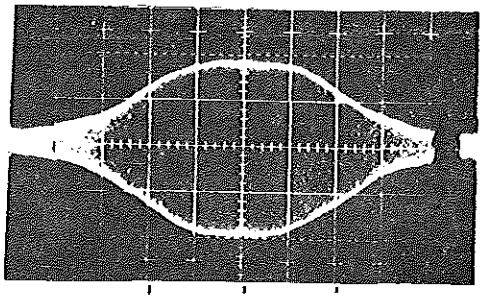

ig. 27 Same as Figure 26, sweep ± 100 KHz about 450 KHz.

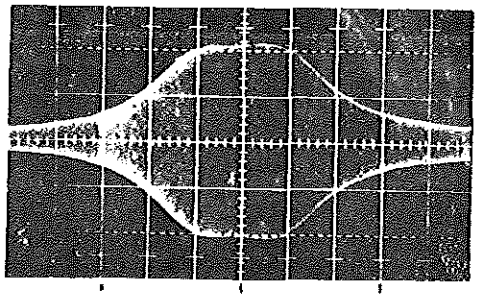

Fig. 30 Same as Figure 28, sweep ± 40 KHz about 75 KHz.

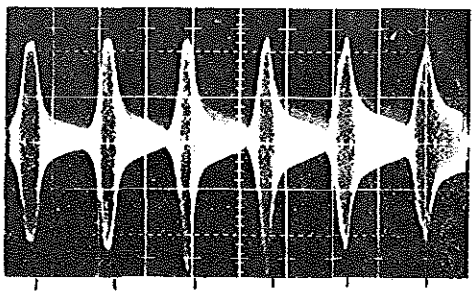

ig. 28 Swept frequency response, Butterworth filter, taps 6 and 12. f_s = 900 KHz.

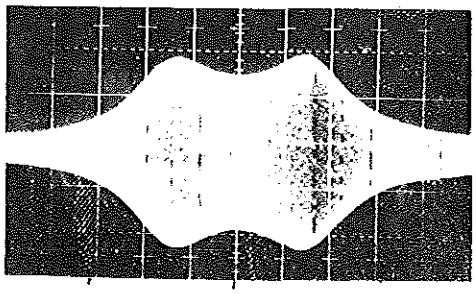

Fig. 31 Same as Figure 30, except weighting changed to Chebyshev values.

PART III A

ABSTRACT

A new large-scale integrated circuit device is discussed which may perform binary-analog correlation among other discrete-time analog signal processing functions.

The Binary Analog Correlator designated BAC-32, consists of a 32-stage tapped bucket-brigade delay line. The individual tapped analog samples are steered to either of two lines by switches which are controlled by the binary content of a static shift register. The possibility of entering and storing various patterns on the static shift register allows complex operations of the binary pattern on the analog voltage samples.

The function of the device is described. Its capability to perform various mathematical operations like convolution and correlation is explained and demonstrated. Various applications such as filtering, correlation, decoding, and chirp detection are shown.

INTRODUCTION

Advances in large-scale integrated circuit technology made it possible to create devices with signal-processing capabilities. These devices may perform tasks traditionally done by digital signal-processing algorithms in digital computers in such diverse areas as biomedical engineering, acoustics, sonar, radar, seismology, speech communication, data communication, nuclear science, image processing, and many others.

A new discrete-time analog device referred to as Binary Analog Correlator (BAC) will be described. This device is designed to perform correlation or convolution between an analog signal and a programmable binary function. The operation of the BAC duplicates the complex signal-processing task normally done by digital computers requiring D/A conversion, memory, a multitude of multiplications and D/A conversion and reduces it to a sequence of sample, store, shift, and multiply operations - all done on one chip. Discrete-time samples of the analog signal are shifted into an analog shift register at a clock rate of f_{c1}. After every clock period the temporarily stored analog samples are multiplied with a binary pattern residing in a static shift register. The feature that the binary pattern in the static shift register may be altered by shifting a new pattern into it makes this device extremely versatile.

It may be used in applications requiring correlation, convolution, code generation, decoding, filtering, or other types of signal processing where an analog signal operates on a variable binary pattern or where two continuous signals - one analog, the other binary - operate on each other.

GENERAL DESCRIPTION

The BAC-32 is a 32-stage charge-transfer storage device. The architecture is that of a tapped charge-transfer analog delay line in which each stage of the delay line has a pair of taps. These taps have switches in series with them which are controlled by the true and complement outputs of a static digital shift register. Thus, by loading a binary word into the static shift register, it will select the taps which are connected to two output lines; a zero at a shift-register cell will connect a tap to one output line, a 1 will connect a tap from the same stage to the other output line, thus providing the ability to do p-n correlation.

The analog input signal is sampled and the samples are moved into charge-transfer delay-line device. Sampling rates in the range from 5 KHz to 10 MHz are possible with this device. That means that an analog signal may be sampled at 10 MHz and may be transferred sequentially through the charge-transfer device. A given sample point on the analog signal will sequentially pass each tap as the signal moves past the taps. The output of the device will be the summed products of the signal values and the assigned binary weights and will be an indication of how well the analog signal correlates with the binary bit pattern placed in the static shift register. The static shift register may be rapidly reprogrammed; that is to say, a new word may be loaded into the static shift register at megacycle rates. Therefore, one can periodically

update the binary correlation code against which the analog signal is correlated. The outputs should be summed into a very low impedance or a virtual ground. Depending on the processing, one may want to use the two outputs individually or may want to take the difference between the two.

The analog delay line requires a two phase complementary square-wave clock. A sample is taken on each transition of this clock. The clock amplitude should be +15 volts with reference to ground. The static shift register requires a single TTL-level timing pulse to cause it to shift one stage. Data input to the static register is also at a TTL level. A shift-register output tap is provided to enable observation of the binary pattern previously stored.

The delay line characteristic of this device can be modeled by the series of sample-and-hold (S/H) circuits shown in Figure 1. Two-phase sampling is shown where the even numbered S/H's sample when the ϕ_2 switches are closed and the odd numbered S/H's sample when the ϕ_1 switches are closed. As a result, each input sample is sequentially moved from a given S/H to the adjacent S/H on each clock transition. For a particular input sample to reach the output of the fifth S/H requires five clock transitions, and for that same sample to reach the eleventh S/H requires six more clock transitions. In CTD terminology, each S/H is called a stage, and a given sample of information remains in a stage for one sample time. If desired, any stage could be non-destructively read out to obtain a delayed replica of the input signal. In sampled-data systems the delay between the taps is inversely proportional to the sampling frequency, thus providing flexibility and stability not available with a continuous time system. The sampled-data system has the flexibility of a digital system without the complexity, cost or power consumption.

The equivalent circuit of the left position of the BAC-32 is shown in Figure 2 in more detail. Samples are set up on the initial storage node during the period while the ϕ_1 clock waveform is at its high (positive) level. When ϕ_1 drops, the sample value is frozen and the simultaneous rise of ϕ_2 permits exchange of charge with the tapped node of stage 1; similarly for other tapped nodes. The sample values thus first appear at the various tapped nodes when ϕ_2 falls and ϕ_1 rises, the charge state is transferred to the non-tapped node of each stage and the tapped nodes are emptied. In order to avoid that the output signal carries no information while the ϕ_2 clock waveform is low, another complete set of BBD shift register, source followers, and tap switches controlled by the same static shift register is integrated on the same chip. At the other BBD shift register the clocks are interchanged causing the input waveform sample to be frozen when ϕ_2 drops.

Thus, since additional sample values appear at the tapped nodes of the second BBD while ϕ_2 is low, a full wave (or full period) output is generated by internally tying the + lines (and - lines) of both BBD's together. By this

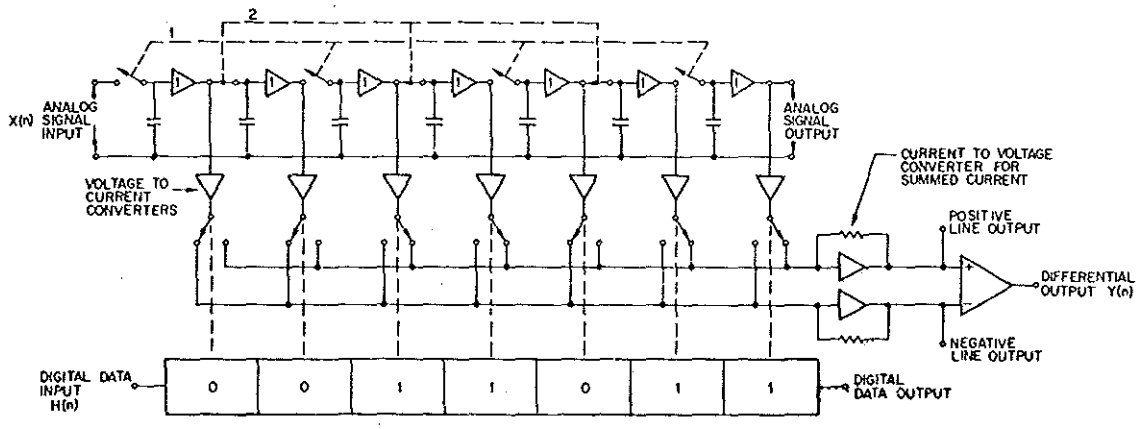

Fig. 1 A Binary Analog Correlator made with sample-and-holds and tapped-switches controlled by a static shift register.

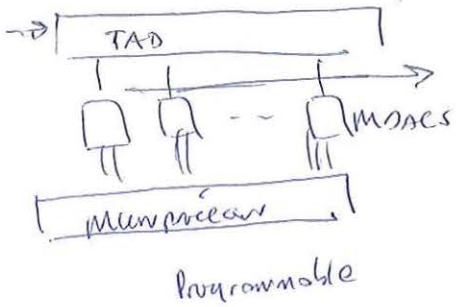

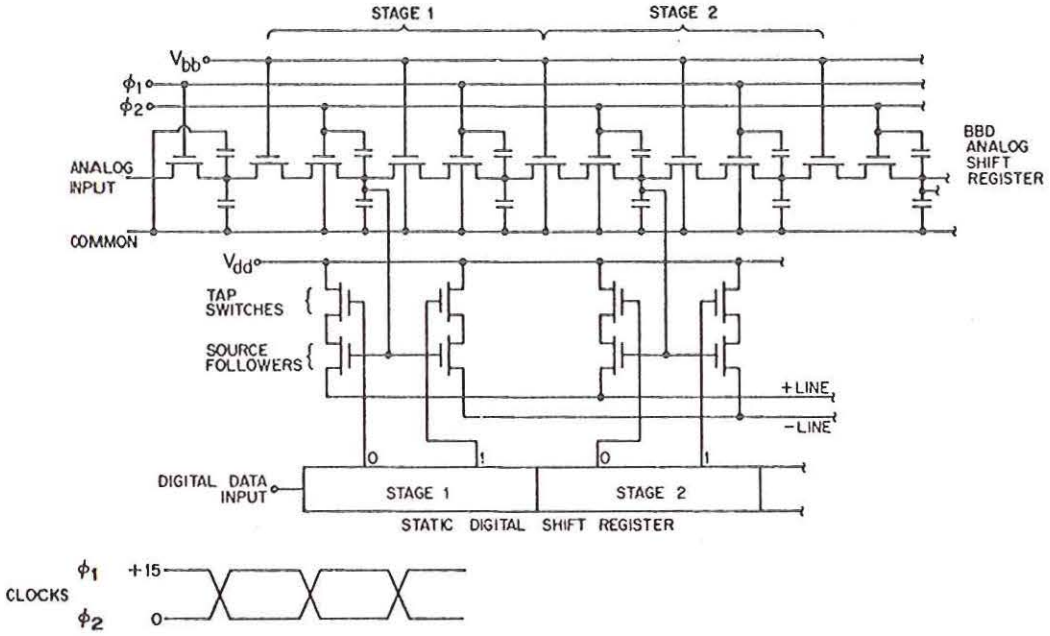

Fig. 2 The Binary Analog Correlator made using Metal-Oxide-Silicon Integrated Circuit Technology.

scheme we not only achieve full-wave output, but also a sample frequency twice that of the clock frequency, since at every clock transition a sample is taken. Clocking of the second device must be synchronous with the first, i.e., $\phi_{1A} = \phi_{1B}$.

Multiplication of the analog signal stored in the various stages with the binary pattern stored in the static shift register (SSR) is accomplished by either opening or closing the tap switches in Figures 1 and 2. Let us define the tap switch to be "open" when the static shift register stage controlling the switch contains a "0" and when the connection between the BBD stage and the + line is broken. In this case no current contribution on the + line is made by the analog sample of the corresponding BBD stage. The - line, however, receives a current proportional to the analog voltage sample. If the respective static shift register stage is in the "1" state, the + line receives a current proportional to the voltage sample. Depending on the status of the SSR, the resulting current on the + line will be proportional to the sum of the currents emanating from the BBD stage corresponding to the SSR stages containing a "1".

Conversion from a binary-analog correlator to an analog-analog correlator may be achieved, by operating several BAC's in parallel. In this case the analog signal inputs of the BBD's are tied together and the various SSR's may be loaded by the digital pattern obtained from the other analog signal by A/D conversion. When properly weighting and summing the various outputs, the final output waveform will correspond to the correlation of the two analog signals.

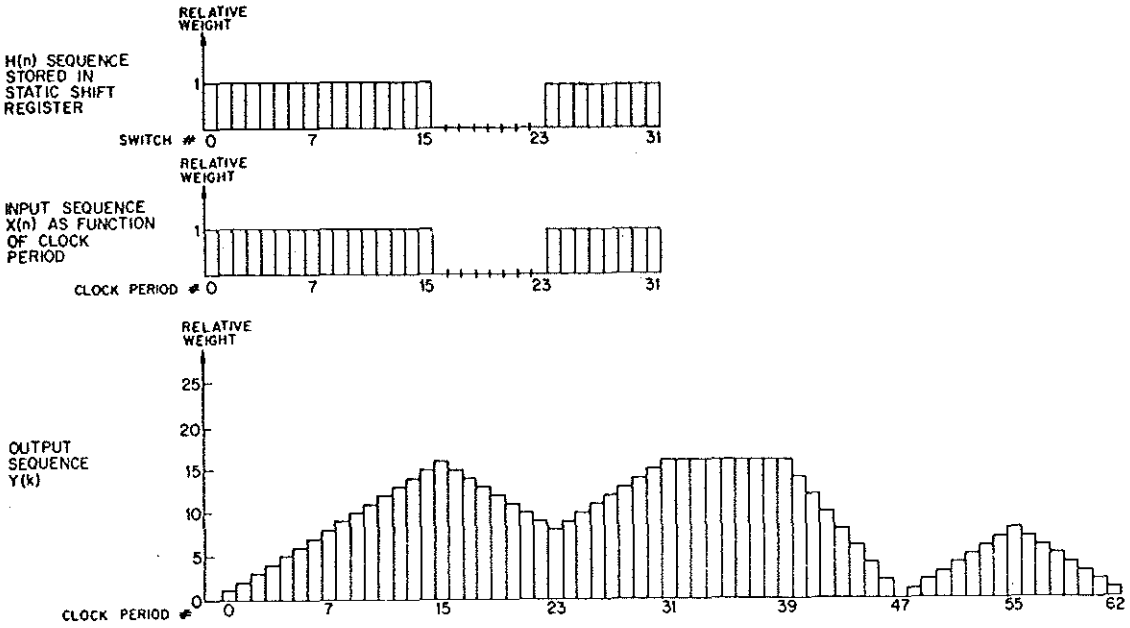

Fig. 3 Convolution of two-valued (bi-phase) sequences

CONVOLUTION

The basic operations that can be performed with the Binary Analog Correlator is that of convolution and correlation. Let us first consider the convolution of two-valued (bi-phase) sequences as depicted in Figure 3. To start off, we consider the output on the + line only. Sequence H(n) is used as a program word for the switches, i.e., a "1" in the sequence represents a closed switch, while a "0" represents an open switch. Sequence X(n) shown in the time domain in Figure 3 is sampled into the charge transfer delay line. The sample rate must, of course, be selected so that the delay through the line equals the period of the sequence, i.e., the sample rate must equal the data rate in the sequence. The output signal may be regarded as a super-position of consecutive delayed samples of H(n), where the weighting is determined by the height of the samples X(n). Figure 4 shows the window function, the signal and convolution of both, experimentally obtained with the BAC.

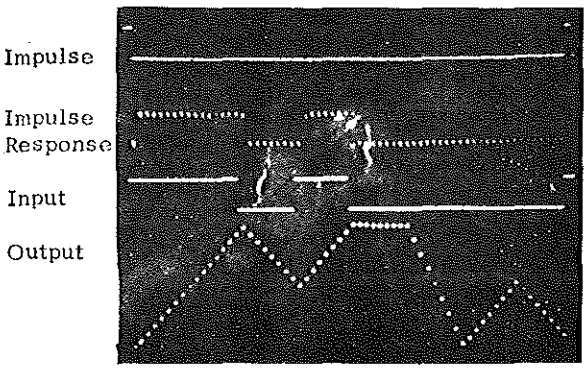

Fig. 4 Photo of window function (impulse response), input function and their convolution experimentally obtained with the Binary Analog Correlator

The process of convolution is better understood by considering Figure 5. The various components of the SSR sequence H(n) are designated H(0), H(1) ..... H(31). The input sequence X(n), represented in the time domain in

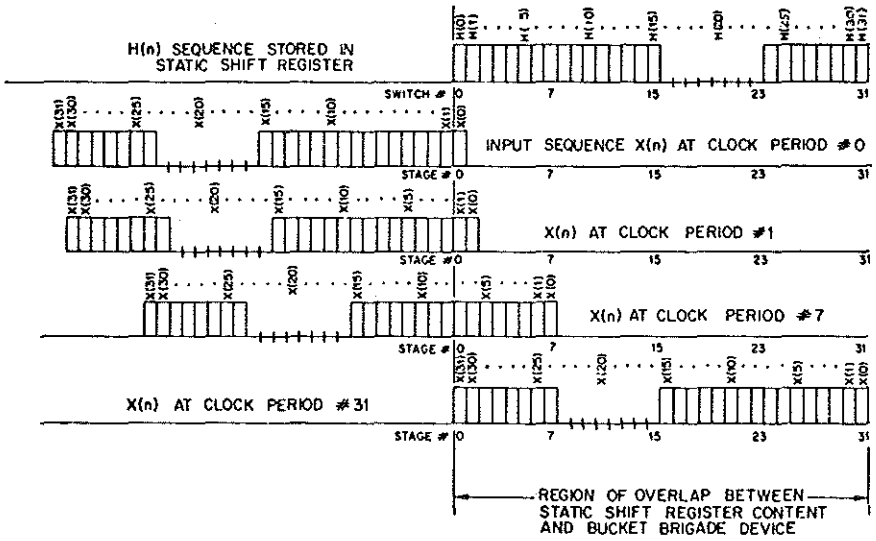

Fig. 5 Demonstration of the convolution operation (The output resulting from the convolution operation is given in Fig. 3)

Figure 3, is flipped around in Figure 5. Here it may be viewed as a geometrical sequence which is slid past the window function H(n) in steps - one position at every clock period.

In the example shown, there is an overlap of sample X(0) and H(0) at clock period #0, causing X(0) to appear at the output since H(0) = 1. At clock period #2, X(1) and X(0) overlap with H(0) and H(1), respectively. Thus, X(1) H(0) + X(0) H(1) = X(1) + X(0) (if H(0) = H(1) = 1) appears at the output at clock period #1.

More generally, the output at various clock periods correspond to:

Clock period #0 $Y(0) = H(0)\,X(0)$

Clock period #1 $Y(1) = H(0)\,X(1) + H(1)\,X(0)$

Clock period #7 $Y(7) = H(0)\,X(7) + H(1)\,X(6) + H(2)\,X(5) + \ldots\ldots H(7)\,X(0)$

Clock period #k $Y(k) = H(0)\,X(k) + H(1)\,X(k-1) + H(2)\,X(k-2) + \ldots\ldots H(k)\,X(0)$

The output at clock period #k may be expressed in a short form by using the summation sign, resulting in:

$$Y(k) = \sum_{n=0}^{N-1} H(n)\,X(k-n) \qquad (1)$$

This expression is referred to as the convolutional summation[1]. It can be shown to be the discrete-time or sampled-data equivalent to the convolutional integral of linear system theory. Though it was derived in our by-phase example, Equation 1 is also valid more generally, where H(n) and X(n) may be analog values, or where the sequence X(n) may be continuous, i.e., it is also valid for clock periods before clock period #0 or after clock period #31.

From signal and system theory we know that the convolution operation is a powerful concept for analog signal processing. If H(n) corresponds to the impulse response of a system, the system response to any signal is equal to the convolution of the impulse response H(n)

with the discrete-time samples of the input signal X(n). This follows from the fact that a linear system can be completely characterized by its impulse unit-sample response and that a linear system is defined by the principle of superposition. Thus, representing an arbitrary sequence X(n) as a sum of delayed and scaled unit samples, the composite system output may be viewed as the sum of the delayed and scaled impulse responses. Figure 6 demonstrates this concept with a square impulse response being convolved with an input sequence. The output corresponds to the sum of the delayed and scaled impulse responses.

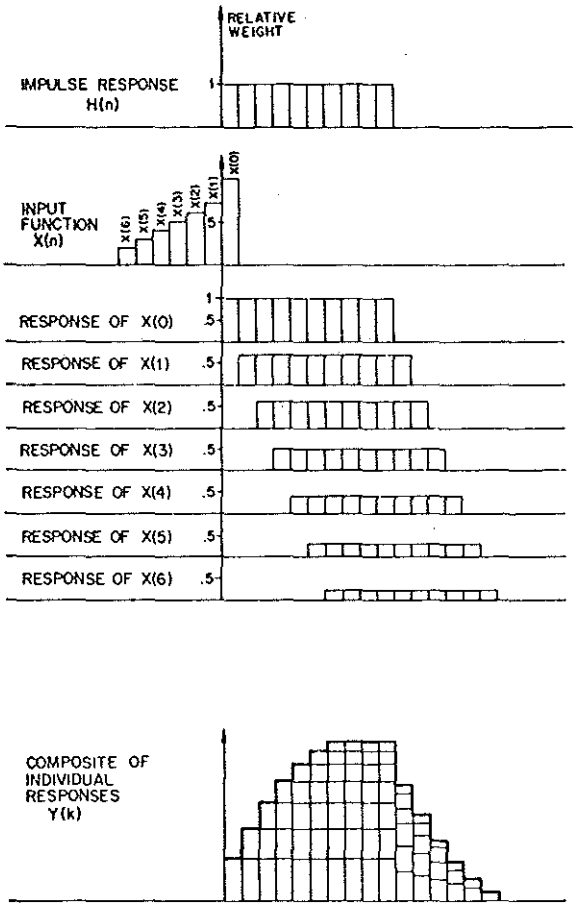

Fig. 6 Derivation of the system response from the superposition of delayed and scaled impulse responses.

Note that it takes N^2, or-in our N = 32 stage device-32^2 = 1024 multiplications to perform one convolution. Before the advent of discrete-time signal processing devices it was too time consuming and too costly to perform signal processing operations on digital computers by means of convolution. Thus, the concept of convolution remained in the area of theoretical mathematics for a long time. Even if one multiplication - considered to be a major computer operation - takes only 1usec, about 1msec would be required to calculate only one value of Y(k), thus considerably limiting the maximum permissible signal frequency in real time calculations. Also, performing the signal processing operation in the frequency domain by using the Direct Fourier Transform (DFT) did not speed up the process. Here also N^2 major operations are required for the N-point DFT. The introduction of the Fast Fourier Transform (FFT) algorithm in 1965 caused a tremendous upsurge in computerized digital signal processing[2]. The FFT cut down the major operations from N^2 to $N \log_2 N$. This results in 160 operations if N = 32, causing the operation in the frequency domain corresponding to our convolution to be performed in .16 msec.

Convolution in the time domain corresponds to multiplication in the frequency domain as follows:

$$\sum_{n=0}^{N-1} H(n)\, X(k-n) = H(n) * X(n) \Leftrightarrow \underline{H}(f)\, \underline{X}(f) \qquad (2)$$

where $\underline{X}(f)$ and $\underline{H}(f)$ are the Fourier Transform of X(n) and H(n), whereby $\underline{X}(f)$ is defined by:

$$\underline{X}(f) = \frac{1}{N} \sum_{n=0}^{N-1} X(n)\, e^{-j\,(2\pi/N)\,nf} \qquad (3)$$

The FFT algorithm was so efficient in comparison with the calculation by the convolution or DFT method, that in many cases calculations were performed by converting the signals first into the frequency domain and then back into the time domain, though the original signals and the desired result was in the time domain; for example the calculation of filtered signals or of the cross correlation (or covariance) function.

Discrete-time signal processing devices like the BAC now allow the direct calculation of filtered signals or of the correlation function in

the time domain. The great advantage of performing signal analysis this way is that the complex operation of Equation 1, involving N=32 multiplications for one data point is performed simultaneously during one clock period. Since the device may be operated at rates up to 10 MHz, one 32 point convolution or correlation may be performed in 64x.1 usec = 6.4 usec, giving us signal processing capabilities beyond the video frequency range. Not only the speed increase, but also the reduced complexity, and reduced power consumption make the BAC device look favorable when compared with a digital signal processor.

FILTERS

Let us look at the BAC's capability as a filter. If the SSR is filled by "1"'s only, the window function is rectangular. A rectangular impulse response corresponds to a $(\sin 2\pi f/2\pi f)^2$ characteristic in the frequency domain. Convolution of a signal by a rectangular window corresponds to the multiplication of the signal's spectral components by the $(\sin 2\pi f/2\pi f)^2$ envelope. This is the action of a filter, in which certain spectral components are passed while others are suppressed. The experimental power spectrum is shown in Figure 7. Experimentally the power spectrum was obtained by sweeping a sinusoidal input signal of constant amplitude from dc to 50 kHz, and by measuring and recording the corresponding power at the output. Due to its gradual roll-off and the high side lobes the filter characteristic of Figure 7 leaves much to be desired. This may be rectified by the choice of differently shaped windows [3,4].

For the time being we may use the BAC as a test vehicle to obtain a better feel for the overall concept. Due to the fact that different bi-polar window functions can quickly be generated simply by shifting a new pattern into the SSR, several filter configurations may be studied.

What is the relation of window width and the clock frequency f_{c1}, with the generated main

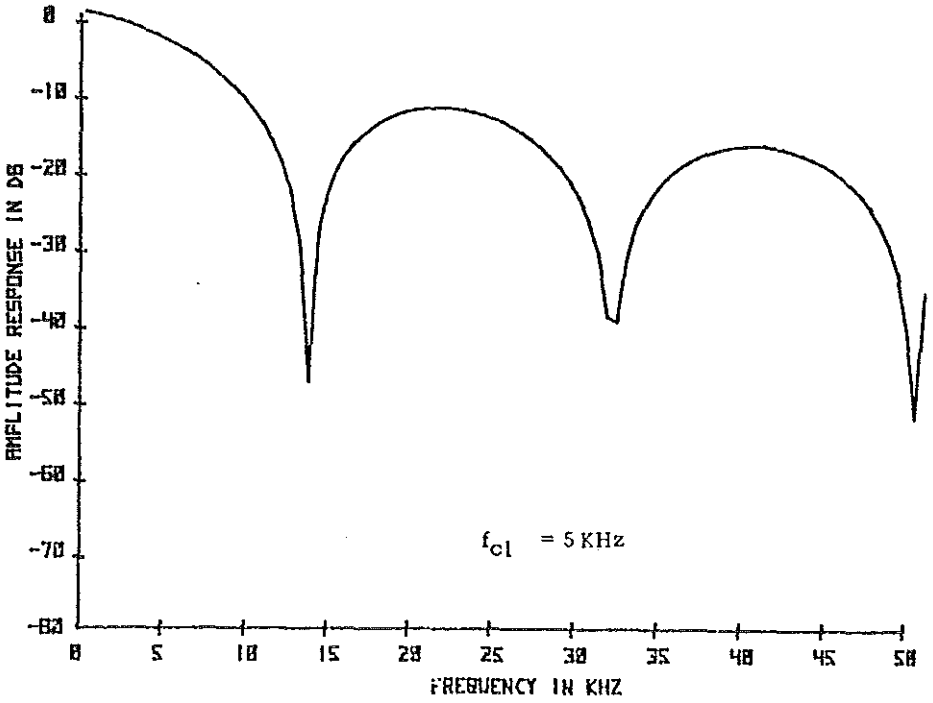

Fig. 7 Frequency spectrum of Binary Analog Correlator corresponding to a rectangular window of 32 taps.

and side lobes and the zero-frequencies, i.e., the frequencies at which the spectral response have minima? The rectangular window effectively integrates at every clock cycle the swept sine-wave in the BBD. At signal frequencies $f_s \ll f_{c1}/N$ the output signal is effectively enhanced by the summation effect of the device. When f_s approaches f_{c1}/N the output signal decreases due to the fact that more and more BBD samples have opposite polarity cancelling each other. No output signal results if one period of the input signal, $1/f_s$, equals exactly the time window in the BBD, N/f_{c1}, resulting in a zero (i.e., a minimum between the main lobe and the side lobes) in the frequency characteristic. Thus the first zero corresponds to:

$$f_s\Big|_0 = f_{c1}/N \qquad (4)$$

As the signal frequency is increased further, exact cancellation of the signal occurs at multiples of f_{c1}/N causing the other zeros. Equation (4) shows that the filter bandwidth may be altered by changing either f_{c1} or the number of on-taps N. By decreasing the number of on-taps the bandwidth is widened. This is experimentally demonstrated with the BAC in Figure 8, where the spectral characteristic corresponding to a window function of N = 32, 16 and 8 are plotted.

The filters discussed so far are low pass filters of varying bandwidth. How do we obtain bandpass filters? Signal processing theory will show us the way, taking advantage of the fact that there exists a similar correspondence as in Equation 2:

$$X(n)\ H(n) \langle = \rangle \underline{X}(f) * \underline{H}(f) \qquad (5)$$

Equation (5) states that multiplication in the time domain corresponds to convolution in the frequency domain. Particularly, the multiplication of the rectangular window function by a cosine-waveform results in the convolution of the rectangle's Fourier Transform with the delta function at f_0. In other words the convolution leads to a shifted version of the Fourier Transform function centered at f_0:

$$X(n) \cos 2\pi f_0 n \langle = \rangle \underline{X}(f) * 1/2 \left[u(f-f_0) + u(f+f_0)\right] = 1/2\ \underline{X}(-f_0) + 1/2\ \underline{X}(f_0) \qquad (6)$$

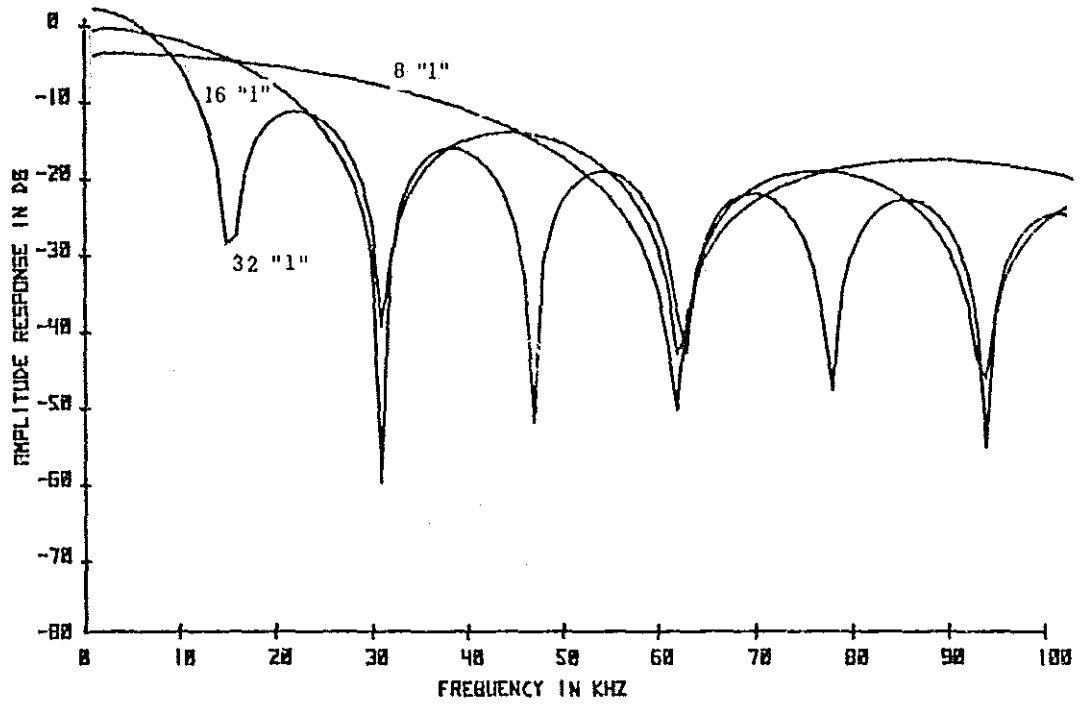

Fig. 8 Frequency spectrum of Binary Analog Correlator corresponding to windows of different widths.

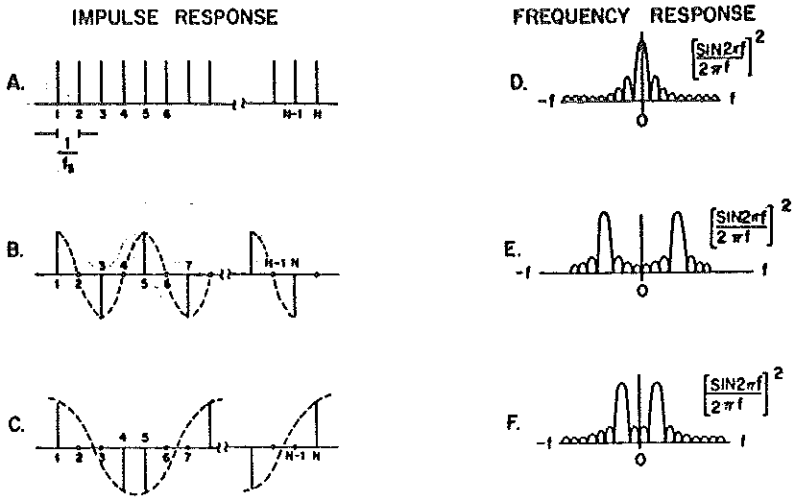

Fig. 9 Three simple impulse responses and the resulting frequency response produced by each.

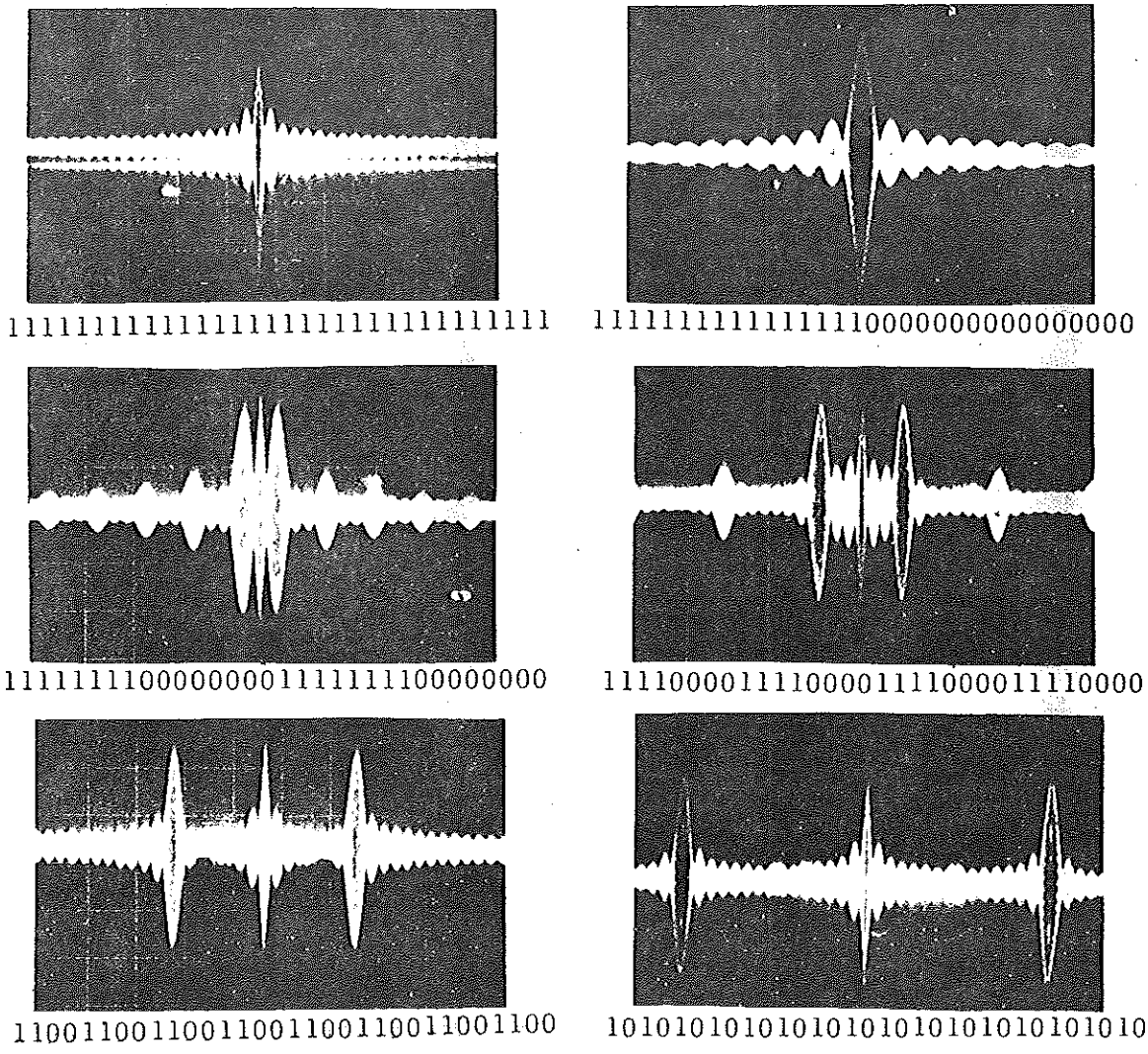

Fig. 10 Spectral linear response of Binary Analog Correlator when swept with constant amplitude input frequency from 300 KHz to 1 KHz to 300 KHz.

This is demonstrated in Figure 9 where the multiplication of the cos-wave times the rectangular window has been approximated by ternary levels[2]. Figure 10 shows experimental results obtained with the BAC for different SSR patterns. Experimentally, the output was taken from the + line only, resulting in a dc component plus the shifted component. The dc component would be nulled if the output were taken from a difference amplifier, causing the dc components on the + and - lines to null, and the shifted components to add. The poor filter characteristic due to the slow roll off and high side lobes is mainly due to the abrupt termination of the window function.

By using analog windows with a smooth transition to zero at the edges, much better filter characteristics may be obtained. Almost any filter characteristic may be achieved by proper selection of the window function. Analog windows may be approximated with the BAC by paralleling several BAC's and ending their digitally weighted outputs together. In this configuration the BAC is useful in filter applications demanding a frequent change of the filter characteristic. As the maximum clock rate for the SSR is 1 MHz, a new window pattern could be entered every 32 usec. Applications are envisioned where the BAC is ganged with a microprocessor, enabling the microprocessor to optimize the window for a certain desired result depending on the input signal. Also, corrections of signal deterioration due to a changing transmission medium may be performed with BAC devices. When, at intervals a known signal is sent through the transmission medium, the filter characteristic of the medium may be calculated. Application of a window function corresponding to the inverse of the characteristic of the medium causes a reconstruction of the original signal, since $Y(f) = M(f)\ M(f)^{-1}\ X(f) = M(f)\ H(f)\ X(f) = X(f)$ if $M(f)$ is the characteristics of the transmission medium, and $H(f) = M(f)^{-1}$. In those applications where a rapid computer generated analog window is not required, another analog device may be more suitable, such as the Tapped Analog Device discussed in Reference 3 and 4. This device allows one to change the tap weights over a wide range by adjusting potentiometers.

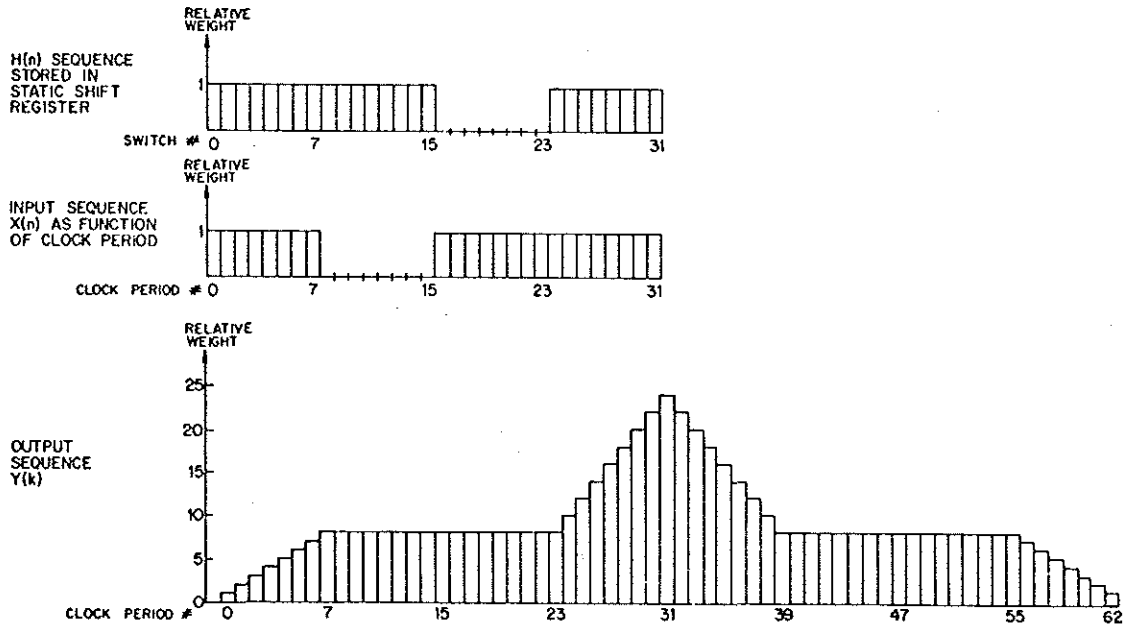

Fig. 11 Correlation of two-valued (bi-phase) sequences

CORRELATION

Correlation is the measure of similarity between two signals. In a way, the filter action discussed before is based on matching or correlating a signal sine-wave with a pattern in the SSR. At maximum overlap between the signal and the pattern, a maximum output resulted. The mechanism in determining the correlation function is similar to that of the convolution function in regard to the fact that two signal sequences are slid past each other, and at every clock cycle the output is computed from the summation of the multiplication of opposing pairs of coefficients. The main difference is, that in the resulting correlation sequence, k corresponds to the number of clock periods by which both signals are shifted from each other. With this concept in mind the correlation function may be determined, resulting in the expression:

$$Y(k) = \sum_{n=0}^{N-1} H(n)\, X(n-k) \qquad (7)$$

Figure 11 shows an example in which the correlation of two identical signals is demonstrated. Signal H(n) in the SSR represents a flipped over section of the time signal H(n). In the photo of Figure 12 the correlation example is demonstrated experimentally with the BAC. Similarly as in the case of convolution, the working of the BAC, as well as the derivation of Equation 7 can be visually understood by referring to Figure 13.

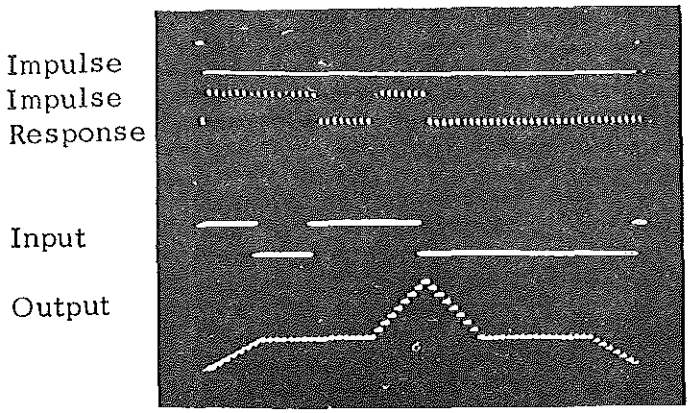

Fig. 12 Photo of window function, (impulse response), input function and their correlation experimentally obtained with the Binary Analog Correlator.

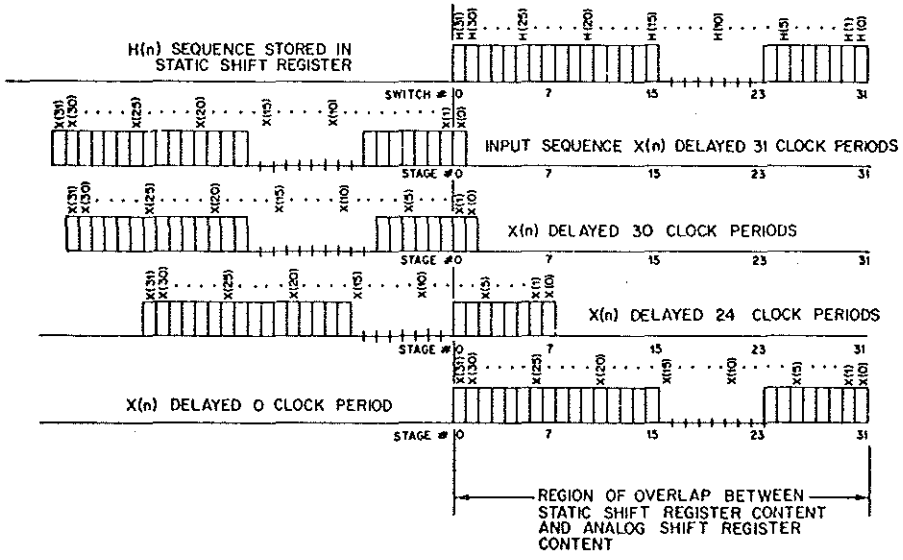

Fig. 13 Demonstration of correlation operation (The output resulting from the correlation operation is given in Fig. 11)

In such a case, where the multiplication of a signal with a time-delayed replica of itself is performed, the operation is defined as autocorrelation, expressed by:

$$Y(k) = X(n)\, X(n-k) \qquad (8)$$

The more general case, Equation 7, is called crosscorrelation, expressing the degree of agreement between two unlike signals. The cross-correlation differs from the convolution (Equation 1) only by the signs of n and k in X(n-k). Thus, for even functions correlation and convolution are equivalent.

CORRELATION APPLICATIONS

Aside from the filter applications, the BAC's ability to correlate opens a vast amount of applications. Autocorrelation allows the determination of the time-delay difference between two signal paths, such as in a telephone transmission network. In radar the range of a distant object may be determined by determining the time delay between the transmitted and received signal. Also the direction of the object is found by receiving the signal with two separate antennas. From the time delay of the received signals and the known antenna separation the angle of signal approach may be calculated by geometrical considerations.

With the test configuration shown in Figure 14, the mechanism of autocorrelation is simulated. A certain pattern is generated by transmitting the impulse response of a BAC, in the SSR of which a pattern has been loaded. The transmission line delay is simulated by another BAC, where the delay may be varied depending on the position of the "1" in the SSR. The preloaded SSR of the third BAC is then held stationary allowing the correlation operation with the delayed pattern as it is shifted through the BBD. The time at which maximum correlation occurs should coincide with the set delay.

The BAC is also useful for decoding a chirp signal in radar systems[5,6]. The chirp signal concept was developed in an effort to detect very small targets at a great range with a high angular resolution. In the design of a radar system using the pulse method the range and resolution was limited by these conflicting requirements: with a given transmitter tube power, the power of the signal could be increased only be extending the duration of the pulse. However, a long pulse limited the ability of the system to separate multiple targets clustered closely together. What was required was a transmitted signal that combined the large amplitude and long pulse width available with existing apparatus, but retained the range resolution capabilities inherent in a pulse of a much shorter duration. Using a burst of a frequency modulated signal was the answer to the above quest. By this method the frequency-spread characteristic of a short pulse within the envelope of a long duration signal allowing better resolution is accomplished. At the receiver the reflected-spread energy is bunched together by successively delaying the first portions of the signal until the last portion has arrived, and

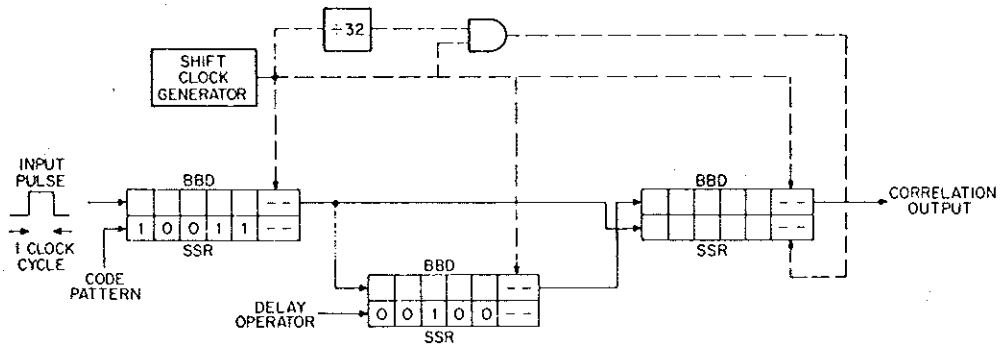

Fig. 14 Simulation of autocorrelation experiment using the Binary Analog Correlator as code generator, delay simulator and auto correlator.

the operator. Effectively, we have seen the device operating as an integrator during the discussion of the filter. When the window function was rectangular the output corresponded to that of a low-pass filter which principally is equivalent to an integrator. Since these operations may be performed in real time on signals exceeding the video frequency range, these may be used in image processing in conjunction with video cameras. The differentiator may bring out the edges in pictures having large equal-toned surfaces, while the integrator may be used for smoothening a picture in order to reduce its granularity. Experimental verification of the delay and integration operation using one BAC is presented in Figure 18.

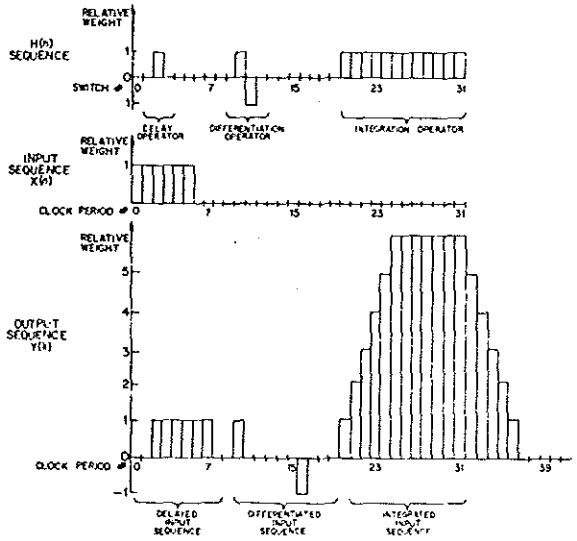

Fig. 17 Demonstration of delay, differentiation and integration operation performed by convolution.

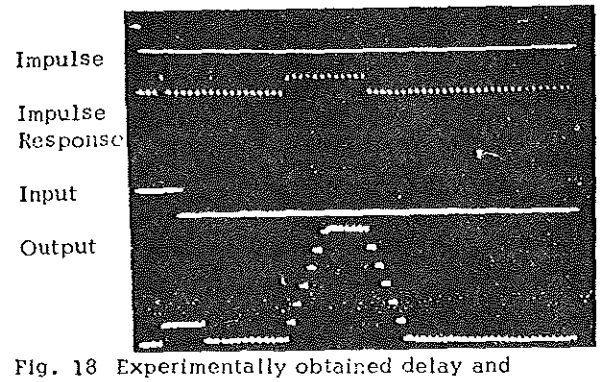

Fig. 18 Experimentally obtained delay and integration operation of a rectangular signal pulse.

CONCLUSION

In the discussion of the Binary Analog Correlator it was demonstrated how novel discrete-time analog signal devices of this type are opening new exciting possibilities in the area of signal processing. Complex tasks like convolution, matched filtering, correlation may be done with these large scale integrated devices at a high speed. Signal processors, so far only realizable with complex, power consuming digital computers, can now be built on one board. Thus, sophisticated equipment may be constructed with the new devices at reduced size and power consumption, leading to higher reliability. The low cost will also enable the hobbyist to realize many of his ideas with the novel approach.

Among other discrete time analog devices, the BAC is unique in the respect that its window function may be changed at a high rate. This makes it useful in adaptive type applications requiring real-time alteration of the window function. The device also allows one to experiment with different operations and patterns, making it useful as an educational tool. Concepts expressed with complicated formulas or simulated on, digital computers, may be demonstrated, requiring only the Binary Analog Correlator, some peripheral circuitry and one oscilloscope.

REFERENCES

1. W. D. Stanley, "Digital Signal Processing", Prentice Hall, 1975.
2. R. W. Ramirez, "The FFT: Fundamentals and Concepts", Tektronix, 1975.
3. G. P. Weckler, "A Tapped Analog Delay for Sampled Data Signal Processing", Proceedings of the 19th Midwest Symposium on Circuits and Systems, Aug., 1976.
4. R. R. Buss and S. C. Tanaka, "Implementation of Discrete-Time Analog Filter and Processing System", Wescon, 1976, Conference Proceedings.
5. R. C. Dixon, Spread Spectrum Systems, Wiley, 1976.
6. T. R. Klauder, A. C. Price, S. Darlington, and W. T. Albersheim, "The Theory and Design of Chirp Radar", Bell System Technical Journal, Vol. 39, No. 4, July, 1960.
7. C. E. Cook and M. Bernfeld, Radar Signals, Academic Press, 1967.

then releasing the energy in an output burst. This can be accomplished by the BAC in which the BBD is used for temporary storage of the incoming signal, and the chirp pattern in the SSR determines the moment of maximum correlation. Figure 15 in which a binary chirp in the SSR is correlated with a binary chirp signal, demonstrates this action. The output in Figure 15 is measured on the + line of the BAC.

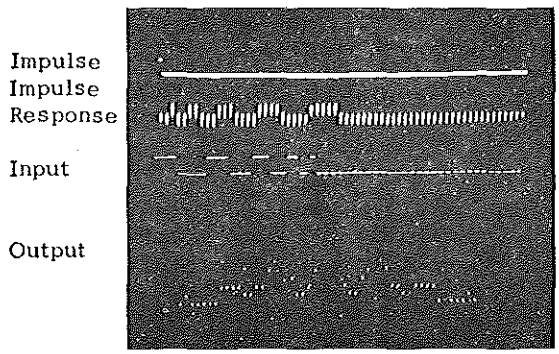

Fig. 15 Demonstration of correlation of simulated bi-phase chirp pattern with chirp pattern in static shift register.

The chirp also allows coding information to be buried in the signal. If the code does not have to follow a chirp pattern more than 4 billion code patterns may be realized with a 32 stage device[5]. Of course, for identifying codes using correlation not all codes are suitable. The figure of merit in selecting good codes is the index of discrimination, that is the separation between the maximum correlation peak and possible minor correlation peaks. An excellent code for maximum discrimination is the Barker Code, allowing detection of its presence in a noisy environment. Using this code, weak signals - for example in interplanetary space communication - may be detected. A 13-bit Barker Code has the sequence:

+ + + + + - - + + - + - +

Figure 16 shows the result obtained when the Barker Code loaded in the BAC SSR is correlated with the same code entered in the BBD. A high concentrated output burst indicates presence of the code. The trailing negative excursion is due to the fact that the SSR has 32 bi-level stages contributing false bits in the stages #13 to #31. The accomplished discrimination, however, is the same as that of a true Barker Code window pattern. A true Barker Code may be generated with 2 BAC's in parallel, allowing only the 13 stages to contribute to the output signal.

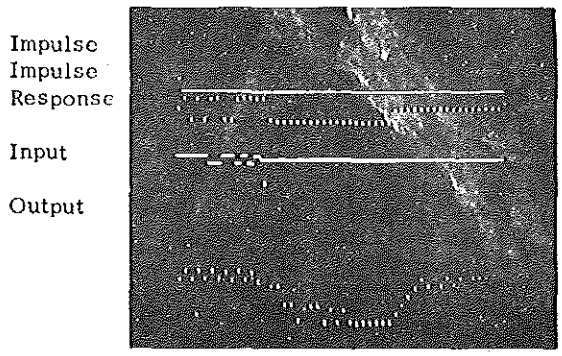

Fig. 16 Barker code signal being correlated with Barker code window producing concentrated output spike.

MATHEMATICAL OPERATIONS

It is seen that the list of applications for the BAC can be made large and that it is limited only by the imagination of the user. The BAC not only performs basic mathematical operations as delay, summation and multiplication but it may also differentiate or integrate an analog signal within limits defined by the window width. This is demonstrated in Figure 17 in which, for the purpose of saving space, the following operators have been entered in the same window function.

The delay operator consists of a single "1". The delay of the analog signal in terms of number of clock periods is determined by the number of positions of the "1" from the left of the SSR. An adjacent "+1" and "-1" in the SSR's, realizable if two BAC's are operated in parallel and the BBD inputs and line outputs are tied together, causes a differentiation of the input signal. The series of adjacent "1"'s are integration operators causing an integration of the input signal for the duration of the length of

PART III B

CHARGE TRANSFER DEVICES FOR SAMPLED-DATA PROCESSING

I. INTRODUCTION

Charge transfer devices (CTDs) make possible a new type of signal processing, simultaneously offering the characteristics of digital as well as conventional analog approaches. This type of processing is related to digital processing because the data are sampled and therefore are under the control of a master clock, resulting in the same advantages of temperature stability and flexibility of data handling which characterise digital systems. As the amplitude of the sampled data is retained in analog form, considerable reductions can be made in circuit complexity.

Recently, important advances have been made in digital signal processing. As digital signal processing theory relies mostly on the discrete time nature of the signal and not on the quantization of the signal amplitude, direct use can be made of digital signal processing techniques in designing systems using CTD technology. Thus, advantages of low cost, small size, reduced complexity, and low power consumption can be realized.

In this paper, a family of charge transfer devices is discussed. The common feature of this family is the capability to perform discrete-time signal processing. Basically, each device sums of the products of delayed samples of one signal either with samples of another signal or with a weighting function. This operation can be expressed as the discrete-time convolution which is the basis of signal processing. Complex operations such as correlation or filtering can now be done in real time at sample rates up to 10 MHz.

The common features of the devices are presented first -- the delay, multiplication and addition features. A universal signal processing device could be built using these basic building blocks, performing any conceivable operation between two signals -- either analog or digital -- either real time programmable or fixed. However, at the present state of the art, the construction of a universal LSI signal processing device would require giving up speed and power and increasing the complexity of the device. For this reason, we have chosen to create several devices which are application oriented, and which bring out the best features for particular applications. The class may be subdivided to distinguish among devices which perform convolution of a sampled-data analog signal with any of the following:

(1) A fixed binary signal;
(2) A fixed analog signal;
(3) A variable binary sequence; or
(4) A second sampled-data analog signal.

Another feature of the various devices is that each is programmable one way or another. A weighting function may be entered any of the following ways:

(1) Programming of binary or analog weights by setting a potentiometer;
(2) Real time programming of binary weights by entering a binary pattern into a digital shift register;
(3) Real time programming of an analog weighting function or entering an analog signal into a second analog shift register;
(4) Mask programming of a weighting function.

The following Reticon devices meet several of the above characteristics:

(1) Tapped Analog Delay
(2) Binary Analog Correlator
(3) Analog Analog Correlator
(4) 64-Stage Transversal Filter

The function of these devices and their applications are presented in Sections III and IV.

II. COMMON FEATURES OF THE CTD SIGNAL PROCESSING FAMILY

Why do the CTD devices give us such a powerful technique for discrete-time analog signal processing? After all, their basic capability is merely the ability to delay signal samples, to multiply, and to sum. The explanation is as follows:

The basic equation in discrete time signal processing is the convolutional summation (see Reference 1)

$$Y(k) = \sum_{n=0}^{N-1} H(n)\ X(k-n) \qquad \text{(Equation 1)}$$

where Y(k) is an output sample at the clock period k resulting from the summation of N products of weighting elements H(n) and of delayed samples of an input signal X(k). The convolution concept is appreciated if one realizes that the convolution of two signals in the time domain is the same as the multiplication of the Fourier transform of both signals X(f) and H(f) in the frequency domain.

$$\underbrace{H(n) * X(n)}_{\text{Convolution}} \longleftrightarrow \underbrace{H(f) \cdot X(f)}_{\text{Product}} \qquad \text{(Equation 2)}$$

Those familiar with the Fourier transform concept will recognize that the right side of Equation 2 describes the filter action where $\underline{H(f)}$ is a filter characteristic, and $\underline{X(f)}$ are frequency components of the input signal. Although the spectral filter characteristic $\underline{H(f)}$ is easily visualized, its counterpart in the time domain H(n) may be less known. The function H(n), however, is the inverse Fourier transform of $\underline{H(f)}$ which is equivalent to the impulse response of Equation 1. Thus any desired frequency response may be generated by determining the weighting coefficients H(n) in this manner.

This type of filter is called a transversal or finite impulse response (FIR) filter. In addition to the ease in determining their desired frequency response, there is an additional advantage to transversal filters. The phase characteristic of these filters can be designed to be linear over the entire frequency range of the filter, so that the time waveform of the input signal will not be distorted.

It would be prohibitively complex to attempt to make sophisticated filters the conventional way by using continuous analog devices. Before the availability of discrete-time signal processing devices, sophisticated filters were possible only by complex digital signal processing techniques, requiring A/D and D/A converters and computers capable of performing the Fourier and inverse Fourier Transform.

Transversal filters have a number of applications in addition to simple spectral filtering, such as matched filtering, single sideband modulation (Hilbert Transform), and spectral analysis.

Another wide area of applications may be addressed because convolution Equation 1 represents correlation if the input signal or the weighting function is reversed. Thus, an analog or binary signal may be correlated in sections with a signal pattern stored in the device, enabling the performance of pattern recognition or decoding. Two analog signals may be correlated if a section of one signal is held stationary temporarily until a section of the other signal is correlated with this section; the stationary signal portion is then replaced with a new signal section, and the correlation process is repeated. Correlation is applicable to the measurement of the degree of similarity of two signals. It is also used to extract signals buried in noise or to measure the delay of two similar signals carried on two different channels.

III. COMPARISON OF THE VARIOUS CTD SIGNAL PROCESSING DEVICES

As was previously mentioned, charge transfer devices can perform signal processing functions quite naturally. Charge transfer devices technology is available to create Bucket Brigade Devices (BBDs) or Charge Coupled Devices (CCDs). Bucket brigade devices are normally adequate for analog delay lines up to 256 stages; for longer delay lines, CCDs are preferred, because their stage/chip area density is about twice that of the BBDs. Only in the last few years has implementation of discrete-time analog signal processing devices been possible after improvements were made in the area of CTD technology. With present n-channel technology, charge transfer inefficiencies up to 5×10^{-5} are achieved, enabling high signal fidelity to be maintained when the signal passes through the delay stages.

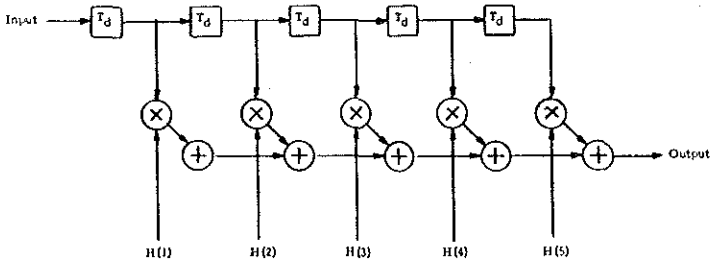

Figure 1. General Symbolic Representation of a Discrete-Time Signal Processing Device.

Figure 1 shows the general structure common to all of the devices of the family discussed. The figure is a symbolic representation of Equation 1. Every clock period a new input sample is taken. Input samples are delayed in a CTD, symbolized by delay elements T_d, where T_d is inversely proportional to the clock frequency. During every clock period, each delayed sample is multiplied by a weight H(1), H(2), etc, and the summation of the products appears at the output.

The main difference among the various devices discussed is the form of the weighting function or of the impulse response H(n) (binary or analog) and the way in which the impulse response is entered into the device (by real time entry or by presetting). Also, the multiplication and addition scheme varies from device to device. Figure 2 shows the various schemes that can be used for the convolution of the sampled-data analog signal with any of the following:

(1) A fixed binary signal -- switches selecting certain analog samples are set according to the binary sequence;
(2) A fixed analog signal -- multipliers a_1, a_2, etc. -- are set according to a weighting function;
(3) A variable binary sequence -- a static shift register controlling the tap switches is loaded with a binary sequence;
(4) A second sampled-data analog signal -- the second signal is temporarily stored in another CTD and its analog samples multiply the analog samples of the first signal.

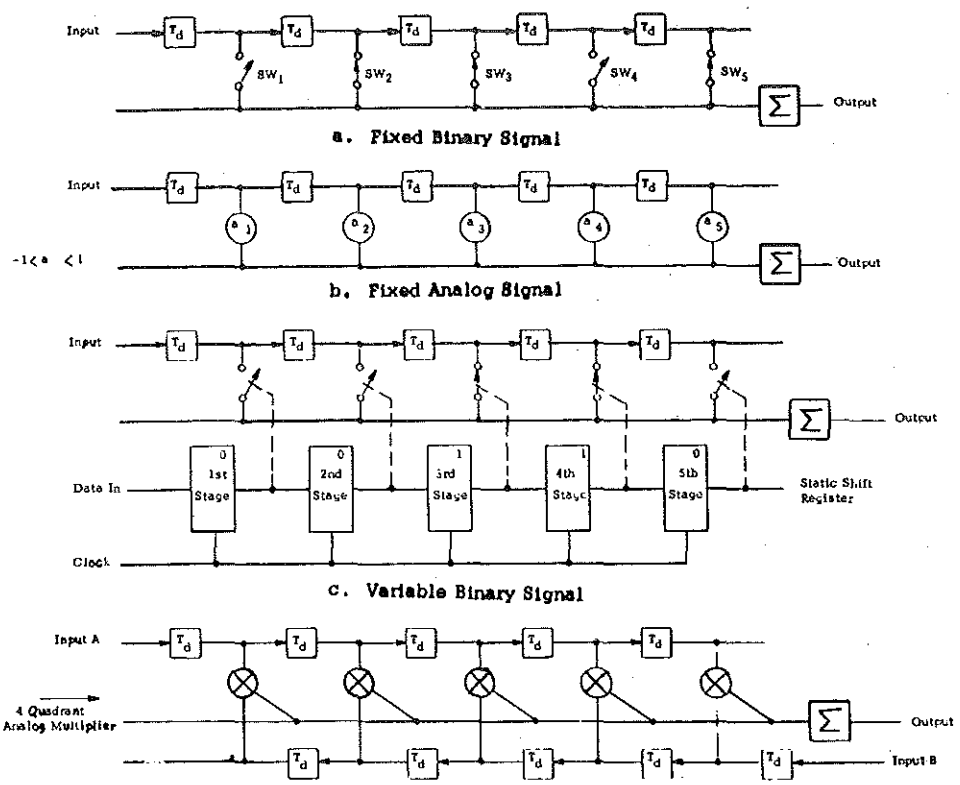

Figure 2. Comparison of Various CTD Structures.

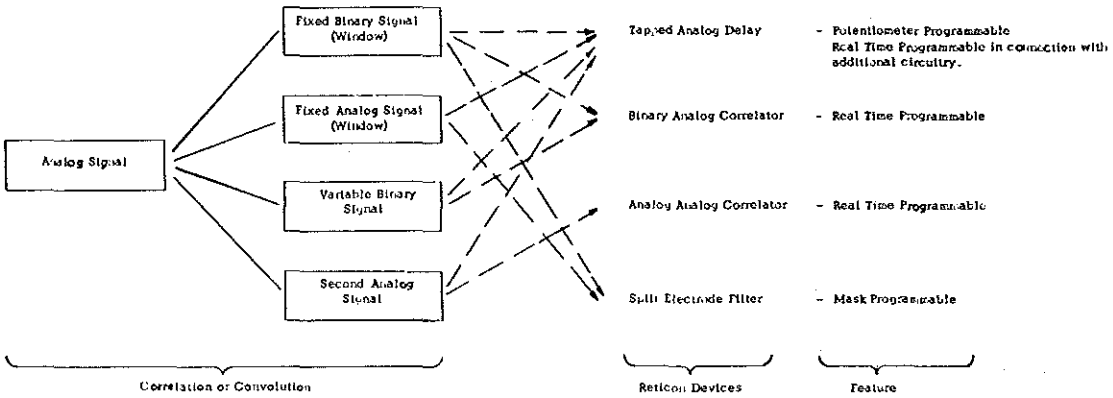

Figure 3. CTDs for Various Kinds of Analog Signal Processing.

In Figure 3 are those Reticon devices which fulfill the functions described above, as well as the extent to which the devices are programmable.

IV. DESCRIPTION AND APPLICATION OF THE CTD DEVICES

A. The Tapped Analog Delay

The Tapped Analog Delay (TAD-32) consists of a 32-stage CTD in which each stage is tapped to make it accessible at the device pins. The device is extremely versatile because it is left to the designer to choose and to implement a desired weighting function. The weighting function is implemented by choosing resistors corresponding to the weighting function, attaching these to the proper taps, and summing the resulting weighted analog-sample in an op amp. Positive and negative weights may be obtained by using a differential amplifier (see Figure 4).

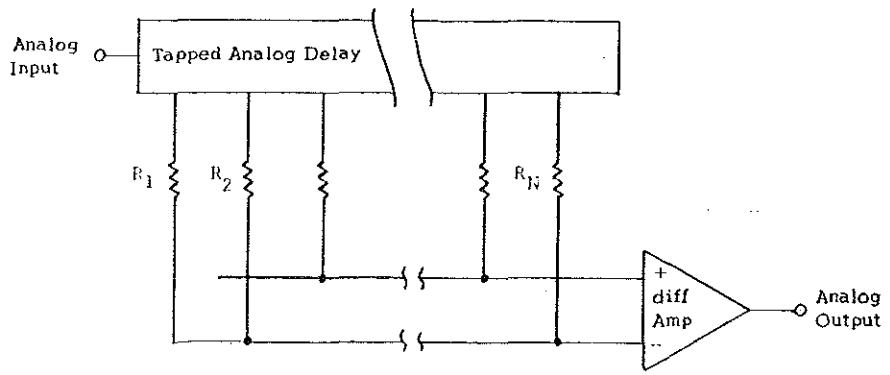

Figure 4. Tapped Analog Delay

The Tapped Analog Delay comes closest to the universal general purpose discrete-time processing device. It can have either a fixed or variable weighting function. Using external resistors, switches, and potentiometers, fixed coefficients can be established.

If it is used with an external digital shift register, or another Tapped Analog Delay, or with microprocessor controlled D/A converters, a system can be built to perform real-time signal processing. Thus, applications from filtering and coding to correlation may be realized with this device. Examples for some of the applications are given in References 2, 3, and 4.

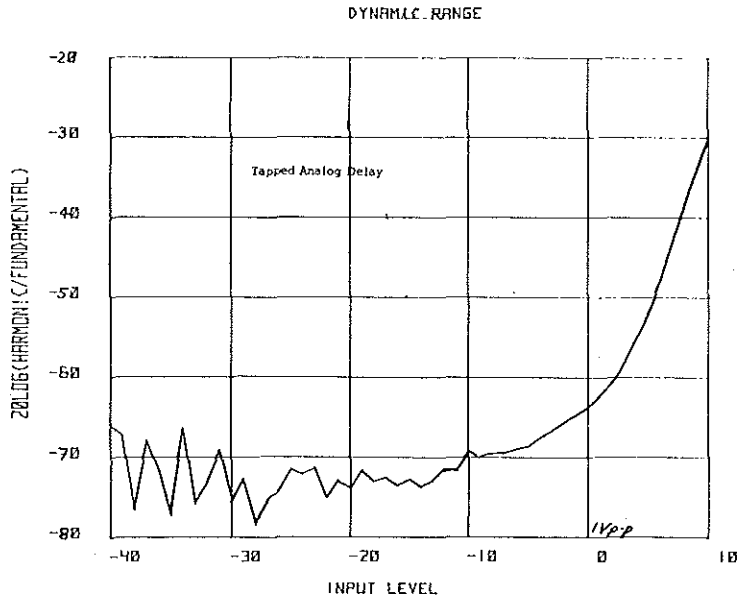

Figure 5. Harmonic Distortion of Tapped Analog Delay.

Linearity and noise set performance limits for the signal processing devices. Figure 5 shows the typical harmonic distortion for the Tapped Analog Delay as a function of input signal amplitude. Harmonic distortion is defined in this case as the ratio of the secondary harmonic to the fundamental, expressed in dB. The spectral noise is shown in Fig. 6 in comparison to the spectral response for a rectangular weighting function (all weighting resistors with the same value). The dynamic range was determined from this curve by calculating the ratio of maximum useable rms signal to the rms noise up to the Nyquist frequency expressed in dB. The relation of harmonic distortion and dynamic range is shown in Fig. 7.

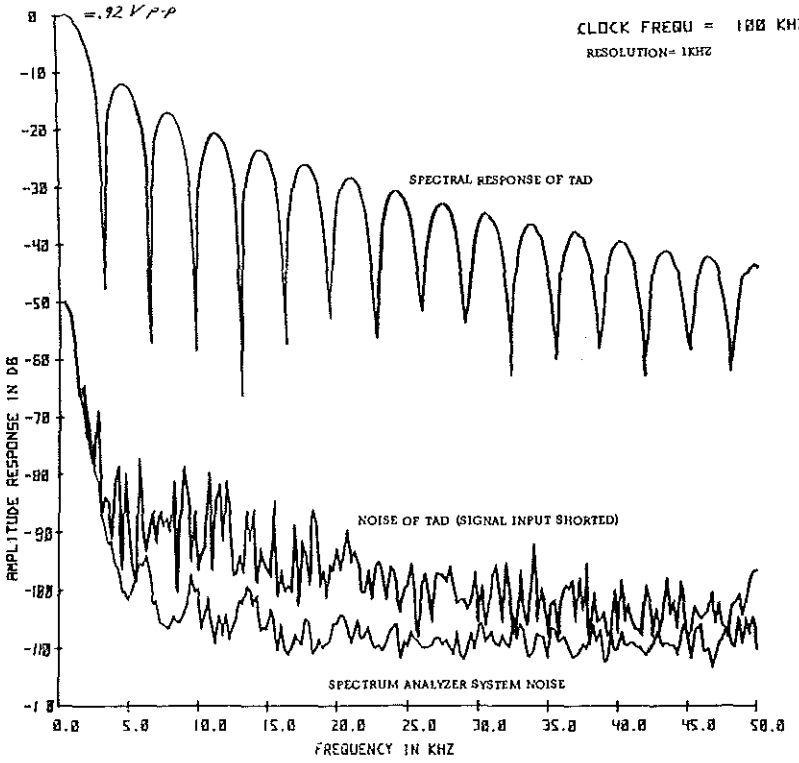

Figure 6. Spectral Response and Spectral Noise of Tapped Analog Delay with Rectangular Window.

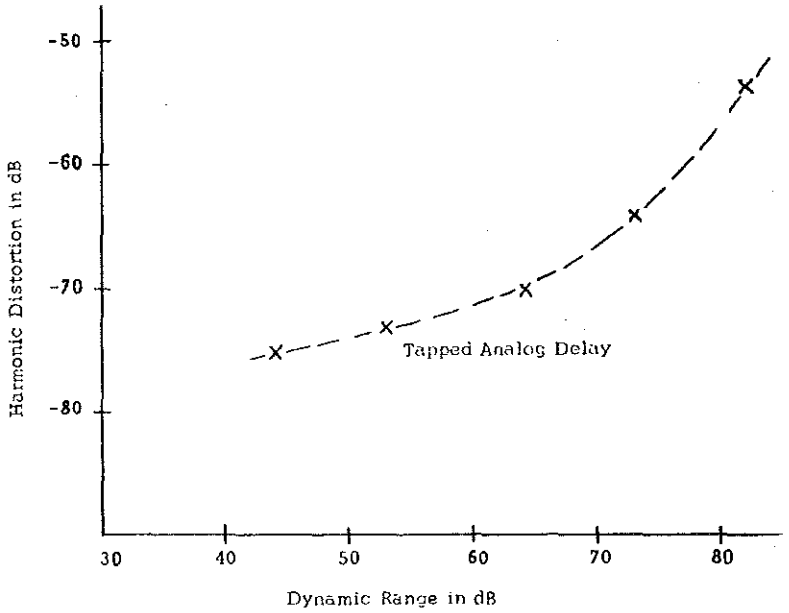

Figure 7. Harmonic Distortion as a Function of Dynamic Range in Tapped Analog Delay.

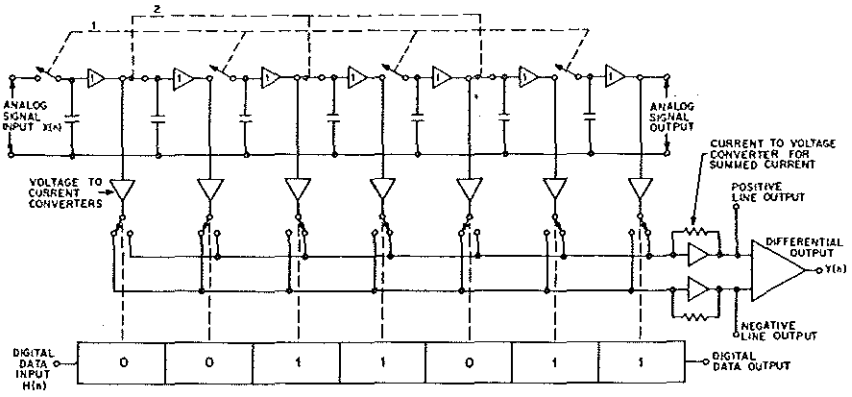

Figure 8. Binary Analog Correlator.

B. The Binary Analog Correlator

The Binary Analog Correlator is a 32-stage CTD in which analog samples are either added on a summing line or subtracted, depending on the position of the switches (see Ref. 5). The switch position is controlled by the outputs of a digital shift register (see Fig. 8). Thus a binary weighting function may be entered from the outside, making possible the real time correlation of an analog or binary signal and a binary signal.

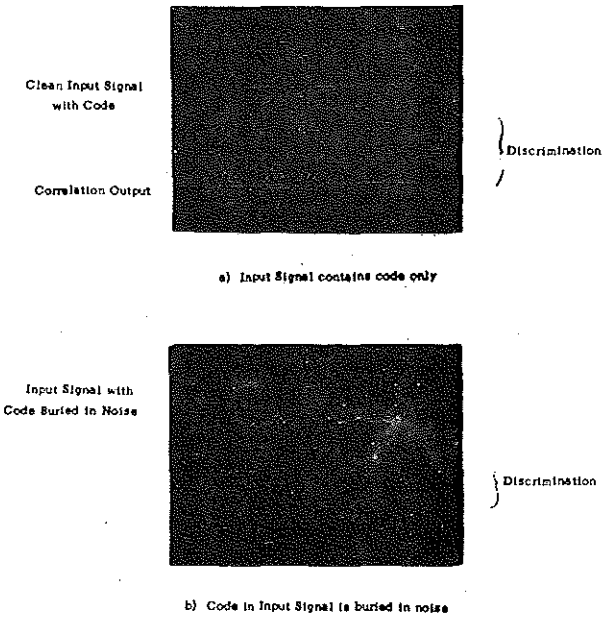

Figure 9. Correlation Output Obtained by Correlating Signal with High Discrimination Code with Same Code Stored in Digital Shift Register.

Figure 9 demonstrates the powerful capability of this device. How can a binary code such as that shown in the upper portion be detected when it is accompanied by a series of many other codes? To do this by hardware with discrete components is a cumbersome project. The task is made easy with the Binary Analog Correlator. The code to be detected is merely shifted into the binary shift register and is correlated against the incoming signal. The nature of correlation is such that when there is maximum agreement between the stored code and the binary signal, the output becomes maximum. If codes are transmitted--as is the case in radar or satellite applications -- the discrimination ratio (the ratio of the highest output signal to the next highest) must be very large. In the example of Fig. 9a, a code giving a large discrimination ratio is shown. Figure 9b demonstrates that the Binary Analog Correlator can still pick out the code buried in noise.

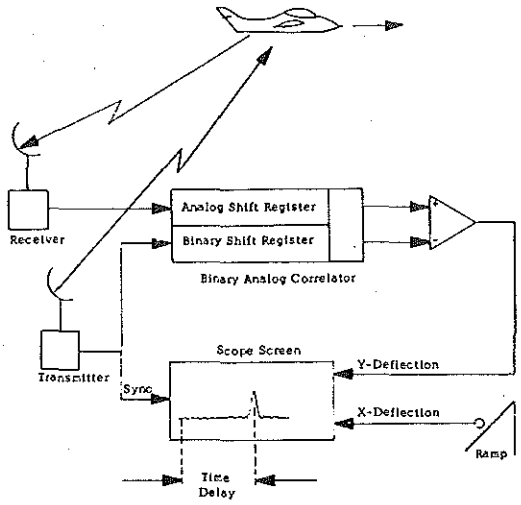

Figure 10. Radar Application for Binary Analog Correlator.

A typical application is shown in Fig. 10. Periodically, a code is transmitted and echos of the signal are received. The time delay at which correlation occurs between the transmitted signal and the received signal provides an indication of the distance of the object from which the signal was reflected. Coding may be used in a multitude of other applications, for example, in the addressing of various telephone receivers, where each station is assigned its own code.

Because there are 32 stages in the Binary Analog Correlator, 2^{32} or more than four trillion codes are possible. The device, therefore, can be used for decoding messages. It also has the capability to change the code key quickly.

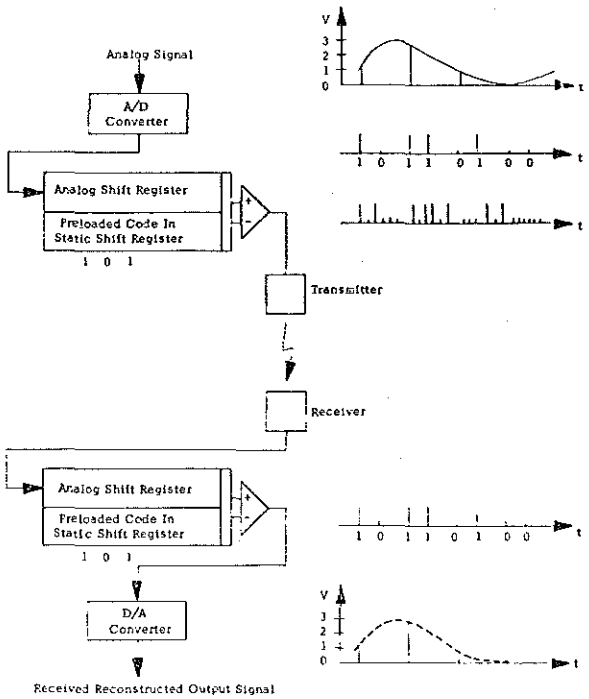

Figure 11. Binary Analog Correlator Used in Spread Spectrum Communication System.

Information coding is extensively used in spread spectrum communications, not for security but to overcome the power and noise constraints. In transmitting information, the information bits are spread out over time and frequency by coding each information bit. At the receiving station the spread information is recombined up again by correlation. The process of coding and decoding in a spread spectrum communication system is demonstrated in Fig. 11.

The ability of the Binary Analog Correlator to update the binary correlation word in real time also makes this device useful in combination with a microprocessor. Teaming up both devices, each may perform the task for which it is most suited. Correlation definitely comes more naturally to the discrete-time signal porcessing device. A 32-point correlation is completed in a BAC in 64 clock periods, or in 6.4 μsec; a microprocessor has to perform 2048 multiplications to do the same task, and also requires more memory. The correlation of an analog signal with another digitally coded analog signal may be performed by paralleling several BACs; each BAC processes a different binary weight. For the correlation of two signals, both in an analog form, the Analog Analog Correlator (see below) is best suited.

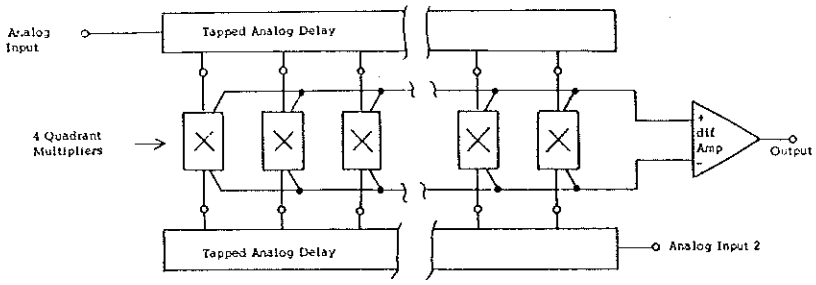

Figure 12. Analog Analog Correlator.

C. Analog Analog Correlator

Figure 12 shows the function of the 32-stage Analog Analog Correlator (AAC) in which two CTDs are used. The device contains 2 thirty-two stage analog delay lines. A different analog signal may be stored in each analog delay line. Each time a new sample is entered, all existing samples stored in the CTD are shifted one stage. At every clock period, the products of the opposing analog signal samples are summed, giving a measure of correlation at that point in time.

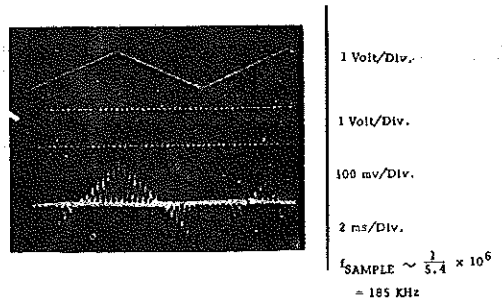

Figure 13. Demonstration of Convolution/Correlation Performed by Analog Analog Correlator.

A demonstration of the performance of the Analog Analog Correlator is shown in Fig. 13. A triangular waveform is correlated (convolved) with a square wave of higher frequency, resulting in the correlation (convolution) of both. In this case, correlation and convolution are the same because both signals are symmetrical functions. For unsymmetrical signals either correlation or convolution may be performed, because the second signal may be entered from either direction.

The AAC enables one to solve a large number of problems which so far can be handled only by complex equipment or with the aid of computers. For example, in medical research it may be used for the correlation of brain waves emanating from different portions of the brain. In ultrasonic imaging applications, it may be used to enhance the object of interest, for example a tumor, by ignoring the uncorrelated signals caused by the surrounding tissue when viewing the object from different viewpoints.

The ability of the AAC not only to correlate but also to convolve permits its use in filters. Its real time programmability enables its use in adaptive filtering. In telephone networks, a change in the transmission line characteristic may be equalized by altering the filter characteristic through an updating of the weighting function in the second CTD.

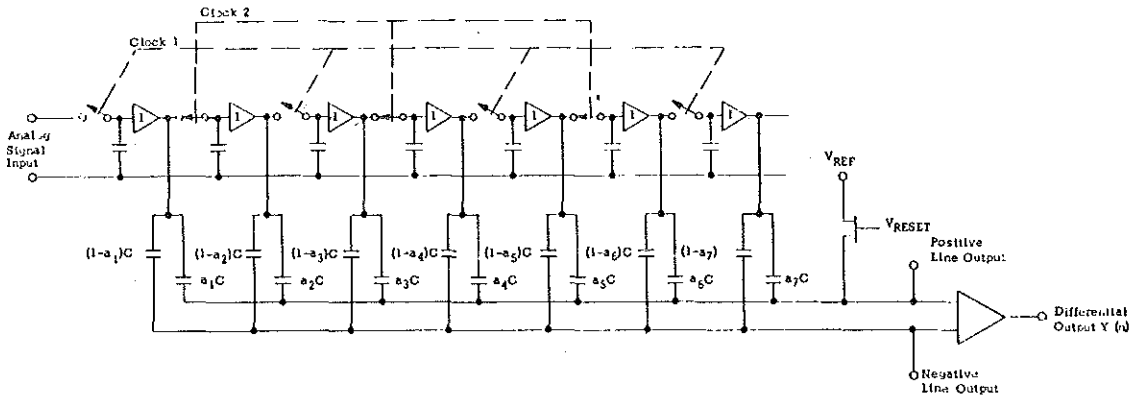

Figure 14. Transversal Filter with Split Electrode Structure.

D. Transversal Filter

In applications which require a large quantity of the same filter, the Transversal Filter is recommended. This filter has a split electrode structure as shown in Fig. 14. The weighting function is determined by the size of capacitors which sense the analog signal samples at the CTD taps. The weighting functions are mask-programmed similarly to the methods by which ROMs are programmed. Three types of filters were created by this technique which will cover another wide area of applications. These are 64-stage filters with a weighting coefficient accuracy of 1/2 percent. A FORTRAN computer program was used to determine the weighting coefficients. The program is capable of synthesizing optimal linear phase filters from an arbitrary frequency response (See Refs. 6 and 7).

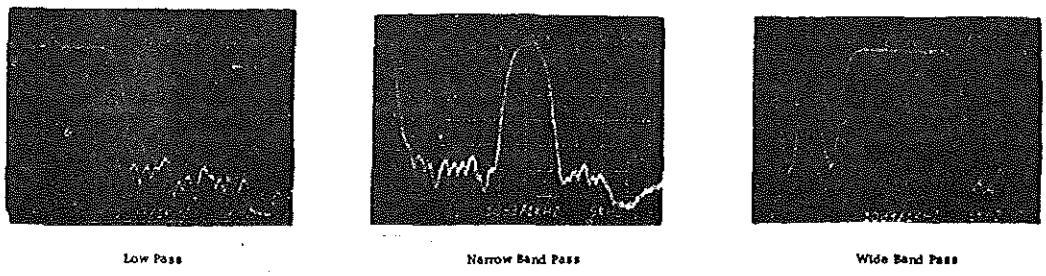

Figure 15. Spectral Response of Different Transversal Filters (Clock Frequency = 100 KHz). (High spikes are caused by Spectrum Analyzer d.c. Response.)

Figure 15 shows the frequency response of the filters which were designed for a minimum peak deviation from the desired response, an extremely high rolloff, and an out-of-band rejection of approximately 50 dB. One filter has a low pass, the others have narrow and broad band pass characteristics. The high spikes in the curves are caused by the dc response of the spectrum analyzer.

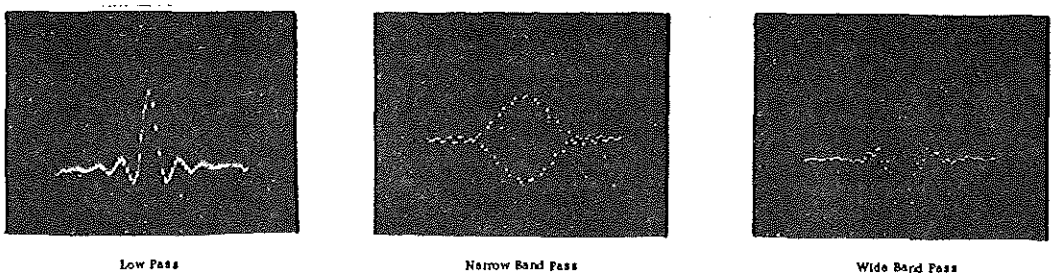

Figure 16. Impuse Response of Transversal Filters of Figure 15.

The filters show a rolloff greater than 100 dB/octave which, up to now, can be accomplished only by complex multi-stage circuits when using conventional analog devices. With the peripheral clock circuitry these filters can be built on a four square inch circuit board. The weighting function of the filters is evident by measuring the impulse response (See Fig. 16).

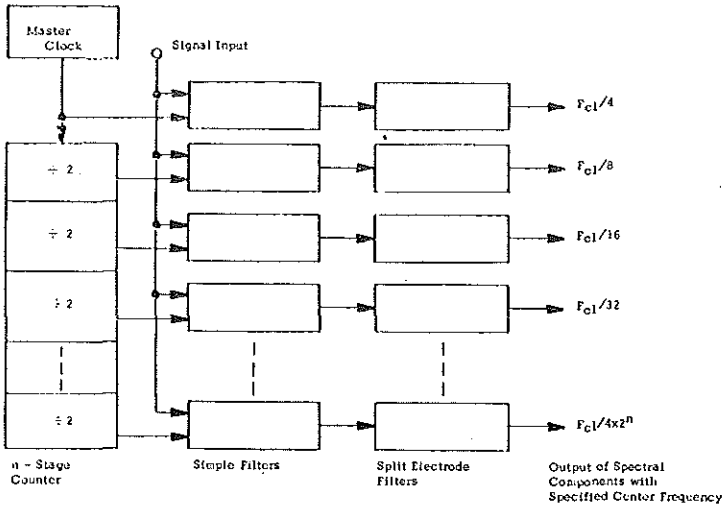

Figure 17. Spectrum Analyzer Using Transversal Filters.

The frequency characteristic of the mask-programmed discrete-time filter is not completely committed. The band edges and the bandwidth are functions of the clock frequency. Therefore, the spectral band to be filtered may be varied by adjusting the clock frequency to a filter-dependent multiple of the center frequency. An application taking advantage of this feature is a spectrum analyzer using several narrow band filters (See Fig. 17). Each successive filter is clocked by half of the clock frequency of the previous filters, thus covering a spectral range from $f_{cl}/4$ to $f_{cl}/4x2^n$ where f_{cl} is the frequency of the master clock and n is the number of $\div$ 2 stages in the counter. Simple filters have to be used ahead of the CTD filters to limit the signal up to the Nyquist frequency in order to avoid aliasing.

It appears that a simple filter using the transversal device will find applications in the touch tone system. The large quantity used in this field will certainly justify the cost of mask programming. The strong existing effort in making talking computers using vocoders in this area will also result in a demand for filters having unique frequency responses that can be implemented easily.

REFERENCES

1. A.V. Oppenheim, R.W. Schafer, Digital Signal Processing, Prentice-Hall, 1975, Englewood Cliffs, New Jersey.

2. S.C. Tanaka, R.R. Buss, G.P. Weckler, "The Tapped Analog Delay", IEEE trans on Parts, Hybrid and Packaging, Vol. PHP-12, No. 2, June 1976.

3. R.R. Buss, S.C. Tanaka, "Implementation of Discrete-Time Analog Filter and Processing Systems", 1976 Wescon.

4. G.P. Weckler, "Signal Processing with Charge Transfer Devices", 55th Convention of Audio Engineering Society, 1976.

5. U.J. Strasilla, "Binary Analog Correlator", 1976 Wescon.

6. R.W. Brodersen, "Introduction to Charge Transfer Devices - Discrete Time Processing", 1976 Wescon.

7. J.H. McClellan, T.W. Parks and L.R. Rabiner, "A Computer Program for Designing Optimum FIR Linear Phase Filters, IEEE Trans Audio Electroacoustics, Vol. AU-21, Dec. 1973, pp. 506-526.